UNIVERSIDADE FEDERAL DO RIO GRANDE DO SUL
INSTITUTO DE BIOCIÊNCIAS
PROGRAMA DE PÓS-GRADUAÇÃO EM GENÉTICA E BIOLOGIA MOLECULAR

Sobre embriões e borboletas: lições de *Heliconius erato phyllis* (Lepidoptera: Nymphalidae)

Ana Carolina Bahi Aymone

Tese de Doutorado submetida ao Programa de Pós-Graduação em Genética e Biologia Molecular da UFRGS como requisito parcial para obtenção do grau de Doutor em Ciências.

Orientador: Aldo Mellender de Araújo

Coorientadora: Vera Lúcia da Silva Valente

Porto Alegre, novembro de 2013.

Este trabalho foi realizado no laboratório de Genética Ecológica do Departamento de Genética, no laboratório de Histologia e Embriologia Comparadas do Departamento de Ciências Morfológicas, e no Centro de Microscopia Eletrônica - na Universidade Federal do Rio Grande do Sul, com auxílio de recursos do CNPq.

Agradecimentos

Seguindo a ordem embrionária, primeiramente agradeço aos meus pais, Margot e José Newton, por terem propiciado as condições iniciais para que eu chegasse até aqui. A eles, eu dedico essa tese!

Agradeço de forma especial ao Aldo e à Vera, por terem arriscado em me aceitar como orientada, mesmo não me conhecendo direito. Durante o desenvolvimento desse trabalho, eles me deixaram livre de restrições, permitindo com que eu traçasse minha própria ontogenia. Foi uma oportunidade imensa tê-los como orientadores - inspiradores!

Aos colegas do Laboratório de Genética Ecológica: André Klein, Bruna Missaggia, Janaína De Nardin, Luciana Oro, Marcelo Costa, Rosana Huff, e às ex-colegas: Ana Carolina Oro e Mariana Giozza, pela parceria nas coletas e criação de lagartas e borboletas. Além, claro, das nossas risadas e rodas de chimarrão. Em especial, agradeço à Bruna, pelas longas conversas sobre a "vida" (...) somos nós, Estamira! À Jana, pela amizade e por ser um exemplo de força e determinação, me incentivando sempre. E à Rosana, que sempre me deu o maior apoio pra seguir em frente.

À Nívia Lothhammer, por tudo que me ensinou sobre células, tecidos e técnicas histológicas de processamento de amostras, no Lab. de Histologia e Embriologia Comparadas (LABHEC), e por me ensinar a "olhar, ver e reparar" estruturas subcelulares.

Ao Diego de Oliveira, pelas dicas de digitalização de imagens no microscópio, e por encher o LABHEC de música, café e alegria! Ficar longas horas processando amostras não foi fácil, mas com o Diego, com certeza, o trabalho ficou mais leve...

À Daruzi Felippe, que me ajudou muito quando eu resolvia processar várias amostras no mesmo dia; se não fosse ela, eu não teria conseguido correr contra o tempo - foi uma ajuda heterocrônica. Valeu, flor de Lótus!

Ao pessoal do Centro de Microscopia Eletrônica, especialmente à Christiane Lopes, por ter me ensinado as técnicas de microscopia eletrônica de transmissão, com toda paciência que o mundo nanométrico exige.

Ao Elmo Cardoso, pelas incontáveis ajudas burocráticas; e principalmente por sempre me tranquilizar com seu otimismo contagiante!

Ao Prof. Frederik Nijhout (Duke University) e Arnaud Martin (University of California/Irvine) pelas valiosas informações além das referências bibliográficas.

Ao “poeta das borboletas”, Alexandre Ruszczyk, pelos vôos interplanetários.

Aos meus irmãos, Marco e Daniel, pelas coisas lindas que me ensinaram e pelo apoio constante!

Ao Nestor, por ter estado ao meu lado durante esse tempo todo, com paciência e compreensão, me dando a maior força, sempre! Obrigada por tudo!

Por fim, aos jardins que me inspiraram na infância, na ‘Rua Cecília Meireles’, pelas lagartas e borboletas, que sempre me fascinaram e me fascinam cada dia mais...

“No mistério do sem-fim
equilibra-se um planeta.

E, no planeta, um jardim,
e, no jardim, um canteiro;
no canteiro uma violeta,
e, sobre ela, o dia inteiro,

entre o planeta e o sem-fim,
a asa de uma borboleta.”
(Cecília Meireles).

É com muito carinho que agradeço a todas as pessoas que contribuíram de uma forma ou de outra para o desenvolvimento desta tese. A todos vocês, muito obrigada!!!

SUMÁRIO

Resumo

Os padrões de desenvolvimento são fundamentais para compreender a origem da diversidade fenotípica. Aqui, descrevemos pela primeira vez, a embriogênese de uma espécie de *Heliconius*. A análise do padrão embrionário de *Heliconius erato phyllis*, a partir da formação da blastoderme ao período pré-eclosão, revelou um padrão consistente com embriões de banda germinal longa, o que está filogeneticamente de acordo com a tendência evolutiva de Lepidoptera. O segundo objetivo desta tese consistiu em analisar o desenvolvimento do padrão de coloração das asas de *H. erato phyllis*. Descrevemos a ontogenia da pigmentação, a microestrutura, a morfogênese e as taxas de maturação das escamas pretas, amarelas, vermelhas, prateadas e marrons - ênfase foi dada às escamas prateadas e marrons, que até então não haviam sido consideradas na literatura. Enquanto as escamas de cor preta, amarela e vermelha apresentaram, cada uma, um único tipo de microestrutura, as escamas prateadas e marrons apresentaram diferentes tipos microestruturais. Isso é inconsistente com o modelo genético para o desenvolvimento da coloração em *Heliconius*, o qual assume uma correlação restrita entre microestrutura e pigmentação. Possivelmente, diferentes genes estão envolvidos em combinações alternativas entre microestrutura e pigmentação. Nosso terceiro objetivo consistiu em analisar, através de microscopia eletrônica de transmissão, a ultraestrutura dos discos imaginais das asas em lagartas de quinto instar. Verificamos que a formação da bicamada epitelial das asas, bem como a diferenciação das células precursoras das escamas, são pré-estabelecidas no estágio larval. Além disso, revelamos que a membrana peripodial, a qual reveste o disco larval da asa, desempenha um importante papel funcional no desenvolvimento das asas, o que muda a ideia de que o epitélio peripodial atua apenas como um simples revestimento. A análise ultraestrutural das asas de *H. erato phyllis* revelou importantes aspectos envolvidos na arquitetura desenvolvimental dos padrões de coloração em *Heliconius*.

Abstract

The patterns of development are key to understanding the origin of phenotypic diversity. Here, we described, for the first time, the embryogenesis of a *Heliconius* species. In *Heliconius erato phyllis*, the analysis of the embryonic pattern, from the blastoderm formation to the pre-hatching larva, was consistent with the long germ band embryos; which agrees with the phylogenetic trend of Lepidoptera. The second purpose of this thesis was to analyze the development of the color pattern in *H. erato phyllis* wings. We described the ontogeny of pigmentation, the microstructure, morphogenesis and maturation rates of the black, yellow, red, silvery and brownish scales - emphasis was given to the silvery and brownish scales, which were never taken into account in the literature. As for the black, yellow and red scales, they showed each a unique type of microstructure, while the silvery and brownish scales showed different microstructural types. This is inconsistent with the genetic model for the development of color patterns in *Heliconius*, which assumes a correlation between microstructure and pigmentation. Possibly, different genes are involved in alternative combinations between microstructure and pigmentation. Our third goal was to examine, by transmission electron microscopy, the ultrastructure of the fifth-instar larval wing discs. We showed that the formation of the epithelial bilayer of the wings, as well as the differentiation of the scale precursor cells occur already in the larval stage. Further, we reveal that the peripodial membrane plays an important functional role in the wing development, which challenges the traditional view of the peripodial epithelium as a simple surrounding membrane. The ultrastructural analysis of *H. erato phyllis* wings revealed important aspects involved in the developmental architecture of color patterns in *Heliconius*.

CAPÍTULO 1

Introdução geral

Cada organismo é resultado de dois processos: o desenvolvimento a partir de um embrião e a evolução a partir de seus ancestrais. Para compreendermos a origem da diversidade fenotípica, devemos entender esses dois mecanismos e a forte relação entre eles – é o objetivo da biologia evolutiva do desenvolvimento (evo-devo), a qual tem revelado muitos caminhos através dos quais o desenvolvimento pode conduzir à geração de novidades morfológicas.

Carroll (2008) propôs uma teoria genética da evolução morfológica com base em oito princípios derivados da evo-devo, os quais são: 1) Pleiotropia em mosaico: Muitas proteínas que regulam o desenvolvimento participam de múltiplos processos independentes e na formação de estruturas corporais distintas. Uma implicação desse fato é que tais proteínas estão sujeitas a fortes restrições evolutivas. Ainda, se a mesma proteína e, portanto, o mesmo gene, é capaz de moldar diversas estruturas, significa que para a função de um gene ser expandida não é necessária sua duplicação. 2) Ancestralidade da complexidade genética: Táxons animais distantes e morfologicamente distintos compartilham um kit de ferramentas, composto por genes responsáveis pela construção corporal com sequências similares. Isso enfatiza a idéia de que fortes restrições funcionais operaram sobre a evolução das proteínas. 3) Equivalência funcional de ortólogos e parálogos distantes: Muitas proteínas do kit, apesar de decorridos milhões de anos de evolução independente em diferentes linhagens, exercem a mesma função *in vivo* quando substituídas umas pelas outras. Isto indica que tais proteínas divergiram pouco em suas propriedades bioquímicas funcionais. 4) Homologia profunda: Estruturas anteriormente consideradas não homólogas (por exemplo, os olhos dos insetos e dos vertebrados) têm seu desenvolvimento governado por circuitos reguladores altamente

conservados. 5) Duplicação de genes do kit de ferramentas pouco frequente: A implicação disso é que a duplicação gênica não é necessária para a geração de novidades morfológicas. 6) Heterotopia e Heterocronia: Alterações espaço-temporais na regulação da expressão gênica são, por si só, capazes de gerar divergência morfológica. 7) Modularidade dos elementos *cis*-reguladores (ECR's): ECR's grandes, complexos e modulares são uma característica distintiva dos loci do kit de ferramentas. Isto oferece uma resposta para como as funções dos genes se diversificam sem duplicação das regiões codificadoras. 8) Vastas redes reguladoras: Proteínas reguladoras individuais controlam centenas de ECR's. A unidade estrutural básica do sistema de redes reguladoras genéticas (RRG's) é a ligação funcional entre um fator de transcrição e um ECR. A evolução das RRG's, portanto, afeta a evolução das ECR's, que por sua vez dirige a evolução do desenvolvimento.

Padrões embrionários de desenvolvimento

Análises comparativas entre diferentes filos animais evidenciam que embriões em estágios iniciais apresentam ampla diversidade morfológica e, no meio do desenvolvimento, convergem a uma forma notoriamente similar, antes de divergir novamente e gerar as "infinitas formas de grande beleza". Esse padrão de desenvolvimento constitui a chamada "ampulheta embrionária", onde o funil central corresponde ao estágio filotípico (Raff, 1996; Prud'homme & Gompel, 2010; Kalinka & Tomanck, 2012).

Em insetos, o estágio filotípico corresponde ao período onde ocorre a formação da banda germinal (Sander, 1984), sendo a embriogênese classificada basicamente em três tipos, classificados com base no padrão de formação da banda germinal: banda-curta, banda-intermediária e banda-longa. Embriões de banda-curta e -intermediária diferenciam

primeiramente a região cefálica, enquanto os demais segmentos permanecem indeterminados e vão se diferenciando progressivamente em direção aos últimos segmentos abdominais. Em contrapartida, embriões de banda-longa pré-determinam e/ou diferenciam todos os segmentos simultaneamente. De um modo geral, ordens ancestrais como Orthoptera e Odonata apresentam embriogênese de banda-curta, enquanto ordens derivadas como Diptera apresentam banda-longa. Lepidoptera, Coleoptera e Hymenoptera têm apresentado inconsistências a esse sistema de classificação, uma vez que vários tipos podem ser encontrados dentro de cada uma dessas ordens; além disso, a classificação de determinadas espécies tem sido complicada, devido a peculiaridades espécie-específicas, sendo muitas vezes consideradas “inclassificáveis” (Davis & Patel, 2002).

Em nível molecular, Kalinka et al. (2010) demonstraram que o estágio filotípico de *Drosophila* é marcado pela mínima divergência na expressão gênica observada ao longo do desenvolvimento e por fortes restrições seletivas sobre a regulação dos eventos ontogenéticos. Domazet-Loso & Tautz (2010) estabeleceram um índice filoestratigráfico com base no transcriptoma estágio-específico de *zebrafish*, em que o estágio filotípico caracterizou-se pelo transcriptoma mais ancestral, enquanto nos estágios anteriores e posteriores ao estágio filotípico o transcriptoma mostrou-se evolutivamente mais derivado.

Grande parte dos trabalhos sobre embriogênese em Lepidoptera não abrangem todo o período embrionário, sendo restritos a estágios específicos como blastoderme ou banda germinal (Kristensen, 2003). Dentre os lepidópteros, as espécies cuja embriogênese é mais bem elucidada, tanto em nível molecular quanto morfológico, são *Manduca sexta* e *Bombyx mori*, cujos embriões apresentam, respectivamente, características de banda-longa e banda-intermediária (Kraft & Jäckle, 1994; Nakao, 2010). No entanto, no gênero *Heliconius*, considerado um modelo emergente em estudos de evo-devo (Joron et al., 2006), aspectos da embriogênese são totalmente desconhecidos.

Desenvolvimento de padrões de coloração em asas de borboletas

Em Lepidoptera, o desenvolvimento das asas inicia com a diferenciação de “discos imaginais” - discos planos de células de origem ectodérmica, os quais crescem dentro da cavidade corporal das lagartas e sofrem evaginação durante a passagem para o estágio de pupa (Nijhout, 1991). Tais estruturas são de grande interesse para a evo-devo, que tem dado atenção especial à busca da origem e diversificação de padrões de coloração em asas de borboletas (Carroll, 2005; Carroll et al., 2005; Joron et al., 2006; Jenner & Wills, 2007).

Os pigmentos que compõem os padrões gráficos nas asas de borboletas começam a ser depositados no fim do estágio pupal. A deposição é feita na cutícula das escamas, que são estruturas extracelulares quitinosas produzidas por células epiteliais. Cada escama apresenta um único tipo de pigmento, e a posição relativa, na superfície da asa, de escamas de diferentes cores é o que determina o padrão final de coloração (Nijhout, 1991).

Os padrões de coloração em asas de borboletas são excelentes objetos de estudo para evo-devo, pois são estruturalmente simples, altamente variáveis e, em muitos casos, o significado evolutivo e ecológico dos diferentes padrões são bem conhecidos (Beldade & Brakefield, 2002; McMillan et al., 2002; Monteiro et al., 2006). Isto é particularmente verdadeiro para o gênero *Heliconius*, que combina uma ampla variação na coloração das asas com uma longa história de pesquisa nos campos da ecologia, evolução e comportamento (p.ex., Emsley, 1963; Benson, 1972; Gilbert, 1972, 2003; Brown, 1981; Mallet & Barton, 1989; Jiggins et al., 2001; Kapan, 2001; Langham, 2004; Finkbeiner et al., 2012).

Em grande parte dos casos a diversidade de *Heliconius* é dirigida pelo mimetismo Mülleriano, responsável pela convergência fenotípica de diferentes espécies culminando

na formação de raças geográficas, o que reforça a habilidade de educar predadores através da coloração aposemática compartilhada. As espécies *Heliconius erato e Heliconius melpomene* são um exemplo extremo de variação intraespecífica, exibindo mais de 20 padrões miméticos situados em diferentes áreas da região Neotropical (Brown, 1979).

Um progresso significante na compreensão da base genética responsável pela variação dos padrões de coloração em borboletas tem sido obtido recentemente. Em diversas espécies, tem sido constatado que a pré-determinação genética ocorre nos discos imaginais a partir do estágio larval (Reed & Serfas, 2004; Monteiro et al., 2006; Martin et al., 2012).

Em *Heliconius*, os mapeamentos genéticos têm evidenciado que três loci de grande efeito são responsáveis pelos principais padrões observados no gênero (Joron et al., 2006; Papa et al., 2008). Em *H. erato* e *H. melpomene*, esses três intervalos genômicos controlam vários padrões distintos, dentre eles a variação nas manchas e raios vermelhos situados respectivamente nas asas anteriores e posteriores, bem como a presença de uma barra amarela na asa posterior (Mallet, 1989; Naisbit et al., 2003; Jiggins et al., 2005; Kapan et al., 2006). Hines et al. (2012) analisaram temporalmente o transcriptoma nas asas de *H. erato* durante o estágio pupal e revelaram uma miríade de genes envolvidos na pigmentação e síntese de quitina e cutícula.

Do ponto de vista morfológico, escamas de diferentes cores - sejam elas cores químicas ou estruturais, apresentam diferenças microestruturais que se correlacionam à coloração (Ghiradella, 1984; Gilbert et al., 1988; Janssen et al., 2001; Prum et al., 2005). Gilbert et al. (1988) classificaram as escamas de *Heliconius* em três tipos, caracterizados com base na correlação entre microestrutura e tipo de pigmento presente. Escamas de tipo I (brancas ou amarelas) são caracterizadas pela presença de uma membrana obversa e ausência de vigas transversais. Escamas de tipo de II (pretas) não apresentam

membrana obversa e suas vigas transversais alinham-se paralelamente, enquanto que escamas de tipo III (alaranjadas e vermelhas) apresentam vigas transversais com um aspecto mais angular, devido à presença de membrana obversa adjacente às cristas longitudinais (Fig.1). Os pigmentos encontrados nas escamas de tipo I, II e III são, respectivamente: 3-hidroxiquinurenina (3-OHK, amarelo), melanina (preto) e xantomatina e dihidroxantomatina (alaranjado e vermelho, respectivamente).

Janssen et al. (2001) analisaram o quão ligados são os processos desenvolvimentais responsáveis pela pigmentação e pela microestrutura das escamas em *H. melpomene*. Através de microcauterizações sobre as asas no início do estágio pupal, foram induzidas mudanças ectópicas na coloração das escamas destinadas a se tornarem pretas ou vermelhas, i.e., escamas destinadas a se tornarem pretas foram induzidas a tornarem-se vermelhas e vice-versa. Tais alterações na pigmentação foram acompanhadas por alterações na microestrutura das escamas, sugerindo uma forte associação entre o desenvolvimento de ambas as caraterísticas.

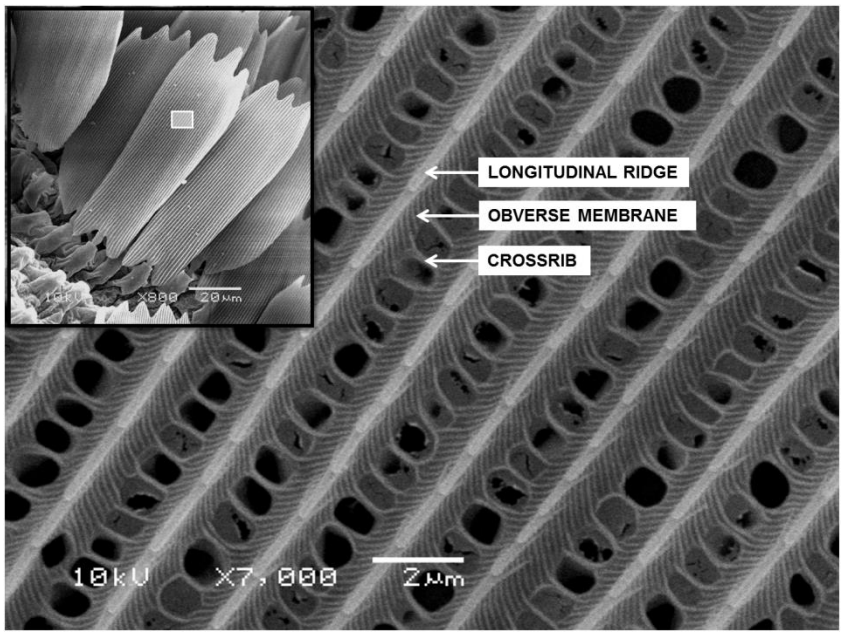

Fig. 1. Superfície de uma escama (tipo III - vermelha) de *H. erato phyllis* mostrando as caraterísticas microestruturais utilizadas na classificação das escamas de *Heliconius*.

Um importante aspecto do desenvolvimento da coloração em asas de borboletas diz respeito ao tempo de amadurecimento de escamas destinadas a diferentes cores. Koch et al. (2000) observaram através de microscopia eletrônica de varredura (MEV) que as escamas das asas de *Papilio glaucus* amadurecem em tempos diferentes, de acordo com a ordem de síntese dos pigmentos, que se depositam sequencialmente nas escamas. A taxa de maturação de escamas é possível observar em MEV, pois, após a desidratação em ponto crítico, as escamas imaturas colapsam, ao passo que as maduras permanecem íntegras, devido ao enrijecimento da cutícula. No tipo selvagem de *P. glaucus*, as escamas destinadas a serem amarelas amadurecem antes das escamas pretas - simultaneamente à síntese do pigmento amarelo (papiliocromo), que ocorre antes da síntese de melanina. Já nas fêmeas melânicas, que possivelmente mimetizam a espécie impalatável *Battus philenor*, há um atraso no amadurecimento das escamas que seriam amarelas no tipo selvagem, as quais amadurecem juntamente com as escamas pretas, consequentemente as asas se tornam inteiramente pretas.

A regulação coordenada dos tempos de maturação de escamas corresponde a um caso de heterocronia ontogenética, uma vez que *shifts* temporais resultam em diferentes fenótipos, no caso os padrões de coloração em asas de borboletas (Smith, 2003). Desse modo, através da redução ou aceleração das taxas de amadurecimento das escamas é possível alterar, acentuar, atenuar uma determinada cor, ou mesmo impedir a deposição de pigmento (ffrench-Constant, 2012).

Em *Heliconius*, a ontogenia da coloração foi descrita para *H. erato petiverana* (Reed et al., 2008) e *H. melpomene cythera* (Ferguson & Jiggins, 2009), entretanto, as taxas de maturação das escamas são desconhecidas em nível ultraestrutural. Além disso, apesar de serem conhecidos os padrões de expressão de determinados genes associados ao desenvolvimento das cores, nos discos imaginais larvais, os mecanismos de diferenciação celular e morfogênese do tecido epitelial das asas são desconhecidos, o

que é fundamental para compreender a evolução e o desenvolvimento dos padrões de coloração.

Heliconius erato phyllis (Fabricius, 1775)

Dentre as 23 subespécies de *Heliconius erato*, a extra-amazônica *Heliconius erato phyllis* apresenta a distribuição mais ampla, ocorrendo em vários biomas brasileiros (Holzinger & Holzinger, 1994). Pode ser encontrada em matas abertas ou perturbadas e, em florestas densas, ocorre em áreas de clareiras ou com grande incidência solar (Brown, 1981). Como as demais espécies de *Heliconius*, apresenta na fase adulta hábitos comportamentais complexos como a formação de dormitórios comunais, o que intensifica a detenção de predadores (Finkbeiner et al., 2012); alimentação a base de pólen, além de néctar, o que confere maior longevidade e ovogênese ao longo de toda a vida das fêmeas (Gilbert, 1972); alta capacidade de memória, orientação geográfica e inspeção acurada de plantas hospedeiras (Gilbert, 1982).

Em *H. erato phyllis* há um dimorfismo sexual na coloração das asas, presente também em outras espécies de *Heliconius*, o qual pode ser observado na parte inferior da superfície ventral da asa anterior e na parte superior da superfície dorsal da asa posterior. Nos machos, essas regiões são inteiramente prateadas; enquanto nas fêmeas, são prateadas apenas em parte da região proximal, sendo principalmente marrons. Embora as superfícies prateadas/marrons não tenham sido incluídas no estudo de Gilbert et al. (1988), elas podem ser importantes para compreender a relação entre as rotas ontogenéticas de microestrutura, maturação e pigmentação das escamas, que por sua vez são responsáveis pela diversificação dos padrões de coloração em *Heliconius*.

OBJETIVOS

→ Artigo 1

- Descrever os principais eventos embrionários, de importância filogenética, em *H. erato phyllis*, e comparar com outras espécies de lepidópteros documentadas na literatura.

→ Artigo 2

- Em adultos de *H. erato phyllis*, na superfície das asas, analisar a microestrutura das escamas amarelas, vermelhas, pretas, prateadas e marrons;

- No estágio pupal:

  - Descrever a ontogenia da pigmentação das escamas;

  - Analisar, através de microscopia eletrônica de varredura, o padrão heterocrônico do desenvolvimento das escamas destinadas a diferentes cores.

→ Artigo 3

- Em lagartas de quinto instar de *H. erato phyllis*, analisar a ultraestrutura dos diferentes tecidos que constituem os discos imaginais das asas, com base em microscopia eletrônica de varredura e transmissão.

CAPÍTULO 2

Embryogenesis of *Heliconius erato* (Lepidoptera, Nymphalidae) – A contribution to the anatomical development of an evo-devo model organism

Ana Carolina Bahi Aymone[1], Nívia Lothhammer[2], Vera Lúcia da Silva Valente[1,3], Aldo Mellender de Araújo[1,3]

[1] Post-Graduate Program of Genetics and Molecular Biology, Federal University of Rio Grande do Sul, Porto Alegre, Brazil. Av. Bento Gonçalves 9500, C.P. 15053, 91501-970, Porto Alegre, RS.

[2] Department of Morphological Sciences, Federal University of Rio Grande do Sul, Porto Alegre, Brazil. St. Sarmento Leite, 500, 90050-170, Porto Alegre, RS.

[3] Department of Genetics, Federal University of Rio Grande do Sul, Porto Alegre, Brazil. Av. Bento Gonçalves 9500, C.P. 15053, 91501-970, Porto Alegre, RS.

Manuscrito submetido à revista ***Development, Growth & Differentiation***

Abstract

The embryogenesis of a *Heliconius* species is documented for the first time. The period between blastoderm formation and pre-hatching larva was described in *Heliconius erato phyllis*. The syncytial blastoderm formation occurred approximately 2 h after egg laying (AEL); at about 4 h, the cellular blastoderm was formed. The germ band arise from the entire length of the blastoderm, and soon compacts occupying approximately two-thirds of the egg length. The protocephalon and protocorm differentiation occurs. Continued proliferation of the germ band is followed by its penetration into the yolk mass, forming a C-shaped embryo. Approximately 12 h AEL, the gnathal, thoracic and abdominal segments become visible. The primordium of the mouthparts and thoracic legs are formed as paired evaginations; while the prolegs, as paired lobes. At about 30 h, the embryo reverses dorsoventrally. The protocephalon and gnathal segments fuse, so that the relative position of the rudimentary appendages in this region shifts. The embryo assumes a U-shape in lateral view, and at about 56 h, the bristles begin the evagination from the larval cuticle. The larva hatches at about 72 h. We have seen that *H. erato phyllis* follows an embryonic pattern consistent with the long-germ embryogenesis, so we believe that *H. erato phyllis* could be classified as a long-germ lepidopteran. The study of the embryogenesis of *H. erato phyllis* provided a structural glimpse into the morphogenetic events which occur in the *Heliconius* egg period. Furthermore, the present study could help future molecular approaches to understand the evolution of *Heliconius* development.

Key words: blastoderm, butterfly development, embryo morphogenesis, germ band, *Heliconius*.

Introduction

The study of different models in development is the only way to understand how differences in the developmental program creates diversity, either in whole body plans or in structural details. In insects, segmentation mechanisms have been the most studied so far (Sander, 1984, 1988; Patel, 1994; Davis & Patel, 2002; Liu & Kaufman, 2005; Nakao, 2012). However, earlier key stages, such as blastoderm formation, are still poorly studied and are only recently beginning to be surveyed (Nagy *et al.*, 1994; Ho *et al.*, 1997; Masci & Monteiro, 2005). Data that can be obtained from embryological studies on insects are relevant not only for comparative embryogenesis but also to our understanding of insect body plan evolution.

As for segmentation, insect embryos have been classified as short-, intermediate- and long-germ embryos. In the short- and intermediate-germ embryos, the posterior segments are generated sequentially from an uncommitted growth zone; while in the long-germ embryos, all segments are specified simultaneously from cells covering the entire blastoderm. The difference between the short-, intermediate- and long-germ modes can be considered a case of developmental heterochrony, since timing shifts in the process of segmentation and patterning are involved in the generation of different phenotypes (Davis & Patel, 2002). In general, ancestral insects (e.g. grasshoppers) show short-germ embryogenesis; while the more derived insects (e.g. *Drosophila*) show long-germ embryogenesis. Historically, lepidopteran embryos were classified as intermediate-germ (Anderson, 1972); however, closer inspection in different species have shown that multiple germ types exist within this order (Kraft & Jäckle, 1994; Masci & Monteiro, 2005; Nakao, 2012). As for embryonic development, *Manduca sexta* and *Bombyx mori* are the most studied lepidopterans, which are representative of, respectively, intermediate- and long-germ embryos (Kraft & Jäckle, 1994; Nakao, 2010).

The Neotropical genus *Heliconius* has a long history of research in the fields of ecology, evolution and behavior (e.g., Benson, 1972; Mallet & Barton, 1989; Jiggins *et al.*, 2001). Diversification of the color patterns in the genus is well known for its intraspecific divergence and interspecific convergence, which in turn have been the focus of evo-devo studies (Joron *et al.*, 2006; Reed *et al.*, 2011; Hines *et al.*, 2012; Aymone *et al.*, 2013; Hill *et al.*, 2013).

Apart from their wing color pattern, *Heliconius* species show variation also in egg morphology (Dell'Erba *et al*., 2005), as well as in the oviposition modes, singly or in clusters (Brown, 1981). The *Heliconius* egg is subcylindrical, flattened at the base and the micropylar axis (imaginary line between the anterior and posterior poles) is located in a perpendicular position to the substrate (Beebe *et al.*, 1960). After oviposition, the anterior and posterior poles take the superior and inferior position, respectively (Hinton, 1981). The egg chorion is sculptured with longitudinal and transversal ribs, which delimit rectangular cells (Dell'Erba *et al*., 2005). Although the external morphology of *Heliconius* eggs is well known, aspects of embryo morphogenesis are totally unknown for this group of butterflies.

Here, we went for the first time into the egg of a *Heliconius* species. Our objective was to describe the embryogenesis of *Heliconius erato phyllis* (Fig.1A), from blastoderm formation to pre-hatching larva. Further, we described features of the yolk and serosa cells, which are functionally integrated into the egg structure as a whole. The analysis of *H. erato phyllis* embryogenesis is important not only for comparative studies within lepidopterans, but also for future molecular approaches to understand the evolution of *Heliconius* development.

Material and Methods

Egg-laying butterflies were captured in natural populations around the city of Porto Alegre (30º01'59"S, 51º13'48"W), State of Rio Grande do Sul, Southern Brazil, and transferred to open air insectaries at the Genetics Department of the Federal University of Rio Grande do Sul. Each unit of the insectaries measured 2 x 3 x 3 m with seminatural conditions and with hostplants (*Passiflora misera*, mainly). Butterflies were fed daily with a mixture of honey: water: pollen that was substituted every morning. After oviposition, eggs were collected and brought to the laboratory, where they were transferred to Petri dishes with humid filter paper, controlled temperature and photophase (25 ± 1ºC; 14 h/light/day).

To observe the blastoderm formation, we followed the protocol developed by Masci & Monteiro (2005) for the visualization of *Bicyclus anynana* embryos. So, eggs with time intervals of 1 h - including the moment of oviposition, until 10 h, were fixed in Carnoy (n=10/time). The egg chorion was removed and the dechorionated eggs were transferred to a 75% ethanol/25% PBS solution, rehydrated in ethanol series with PBS, stained with Hoechst 33258 (Molecular Probes) and observed under a spectral confocal microscope (Olympus FV1000®) with dye excitability in the spectral range of 405 nm.

Light microscopy and scanning electron microscopy (SEM) were used for to describe the embryogenesis as a whole. For light microscopy, eggs with time intervals of 1 h until the pre-hatching stage (n=20/time) were fixed in Bouin's solution. Due to the opaque and impermeable nature of the *H. erato phyllis* chorion, it was necessary to remove it to allow observation of the tissues within the egg. Previous attempts to make the chorion more permeable or translucent through chemical means were unsuccessful. Egg preparation was followed by dehydrating with ethanol series, diaphanizing, paraffin embedding, microtomy with 3 µm thick, and staining with hematoxylin and eosin, or with toluidine blue.

For the scanning electron microscopy, eggs (n=20/time) were fixed in glutaraldehyde. The embryos were isolated from the yolk mass, washed in PBS buffer,

dehydrated in a ketonic series, submitted to a critical point dryer (BALTEC®CPD-030), mounted on metal stubs with double-sided carbon tape, metalized with an approximately 15 nm gold layer (BAL-TEC ®SCD-050) and observed under a scanning electron microscope (JEOL®JSM-6060), at 10 kV.

The serosa cells and vitellophages were observed under a transmission electron microscope (JEM®1200EXII). Eggs were previously fixed in Karnowisky, postfixed in osmium tetroxide 2%, washed in PBS buffer, dehydrated in a ketonic series, embedded and included in resin (EMBED Epon 812). Ultramicrotomy was performed in LEICA®ULTRACUT UC7 ultramicrotome, with 100 nm sections, which were contrasted with uranyl acetate and lead citrate.

As we have given priority to the different developmental stages, their representation as figures at Results do not follow the usual increasing order, changing in accordance to the technique used.

Results

The egg period of *H. erato phyllis* was around 72 h under the controlled conditions. Below, we describe the main events that were observed throughout embryonic development in *H. erato phyllis*.

Blastoderm formation

The blastoderm was visualized by confocal microscopy in the periphery of eggs with approximately 2 h after egg laying (AEL); staining with Hoechst showed intense labeling in the cleavage nuclei (Fig.1B). We have seen that *H. erato phyllis* follows the same meroistic pattern found in the majority of the holometabolous insects; so, firstly, a syncytial blastoderm is formed. The syncytial blastoderm lacks membranes and all the

cleavage nuclei are contained within a common cytoplasm. Approximately 4 h AEL, the membranes started to develop around each of the nuclei creating individual cells which form the cellular blastoderm (Fig.1C).

Yolk and vitellophages

At the moment of the blastoderm formation, the cleavage nuclei that do not migrate to the periphery begin the cellularization of yolk forming the vitellophages (cf. Fig.2A-C), at about 4 h AEL. The vitellophages can show one or two nuclei, which are indented (Fig.2C, E). Some nuclei are densely involved by a mass of cytoplasm (Fig.2D) full of Golgi (Fig.2F), secretory vesicles (Fig.2G), glycogen granules (Fig.2H), and mitochondria (Fig.2I). The mass of cytoplasm, in turn, is surrounded by carbohydrates and lipid droplets.

Formation of the germ band

As the division of the blastoderm continues, the ventral region thickens and becomes the embryonic primordium (Fig.1D, cf. 4A-B), at about 5 h AEL. Cells fated to form the germ band arise from the entire length of the blastoderm (Fig.3A). Approximately 7 h AEL, the germ band compacts and occupies approximately two-thirds of the egg length. Further, the differentiation of the protocephalon and protocorm occurs. The protocephalon is the more prominent region at this stage, as it becomes large and bilobed (Fig.3B). Continued proliferation of the germ band (Fig.3C) is followed by its separation from the extraembryonic ectoderm and penetration into the interior of the yolk mass. The anterior and posterior ends of the germ band grow dorsally into the yolk and form, respectively, the stomodeum and proctodeum. The germ band becomes elongated antero-posteriorly, assuming a C-shape (Fig.4C), at about 10 h AEL.

After separation between germ band and extraembryonic ectoderm, this constitutes the serosa (Fig.4D). The serosa cells of *H. erato phyllis* are in most cases mononucleated and their cytoplasm are full of mitochondria, secretory vesicles, and prominent Golgi complexes, which are concentrically structured, indicating intense secretory activity (Fig.5A-C). At the moment of the serosa formation, the amnion is formed and it encloses the embryo in a fluid-filled amniotic cavity (Fig.4D). The formation of the amnion separates definitely the germ band from the extraembryonic ectoderm and it allows the embryo to engage in blastokinesis.

Segmentation

Approximately 12 h AEL, the segmental grooves become visible along the entire embryo, constituting the gnathal, thoracic, and abdominal segments (Fig.4C, E). The gnathal segments correspond to the labral, mandibular, maxillary and labial appendages (cf. Fig.7A, B). The abdominal region becomes divided into 10 segments (Fig.4E), the most posterior region of the embryo corresponds to the telson, a non-segmental terminal region (Fig.4E; cf. 7D, H). At about 16 h AEL, the primordium of the mouthparts and thoracic legs are formed as paired evaginations (Fig.7A, B), while the prolegs are formed in the abdominal segments as paired lobes (Fig.7A). At the moment of segmentation, the central nervous system (brain, suboesophageal, thoracic and abdominal ganglions) originates from the ectodermal cells of the ventral region of the embryo (Fig.6A-D).

Embryo revolution and dorsal closure

Approximately 30 h AEL, the embryo becomes wide and stout, and reverses dorsoventrally, changing the relative position of the yolk (Fig.3D, 4G-I). Earlier, the embryo was positioned within the yolk, but after its revolution, 42 h AEL, the yolk is contained

within the embryo. At first, the abdominal end turns ventrally, reaching the level of the ventral abdomen (Fig.7D); the embryo assumes a superficial position and it is J-shaped in lateral view. Finally, at about 48 h AEL, the abdominal end reaches the level of the thorax, and the cephalognathal region turns ventrally (Fig.7E). At the abdominal end, the 10^{th} abdominal segment and the telson fuse into one (Fig.7H). The embryo assumes nearly a U-shape in lateral view (Fig.7I). The yolk mass gradually decreases in volume owing to its increasing consumption by the embryo (Fig.4G-I).

After the embryo revolution, the lateral walls of the embryo grow dorsally replacing the amnion, which was provisionally covering the dorsal surface of the embryo. So, the dorsal closure occurs, and approximately 56 h AEL, the bristles begin the evagination from the larval cuticle (Fig.7I-J).

Formation of the gut

The development of the gut occurs throughout the embryo revolution (Fig.4G-J). Cells at the anterior and posterior ends of the C-shaped embryo migrate inward to form the foregut, hindgut, and midgut, approximately 32 h AEL. The foregut and hindgut arise from ectodermal cells of stomodeum and proctodeum, respectively. Endodermal cells derived from the stomodeum and proctodeum enclose the yolk in a tube creating the midgut (Fig.4G-J). Vitellophages enclosed by the midgut are integrated into the endoderm and form the midgut epithelium (Fig.4H-J). The elongating hindgut becomes subdivided into the small intestine, large intestine, and rectum, each containing cells of different size (Fig.4I). Shortly before hatching, at about 72 h AEL, the blind ends of the foregut and hindgut open out and the continuity of the digestive tract becomes established (not shown).

Formation of the head, thoracic and abdominal appendages

After embryos become wide and stout (Fig.4E, 7A), 30 h AEL, the protocephalon and gnathal segments begin to fuse, and the morphogenetic movement of these regions begins, so that the relative position of the rudimentary appendages in this region shifts to form the larval head. Approximately 32 h AEL, the labral rudiments fuse and the proximal part of each labial rudiment moves toward the median line and fuses to form a single structure (Fig.7C). The fused labial rudiment then further moves anteriorly between the maxillary rudiments (Fig.7F). At this stage, the thoracic legs become cylindrical and grow antero-posteriorly, but are not yet segmented (Fig.7G), as the prolegs on the 3^{th} to 6^{th} abdominal segments (Fig.7H).

At about 56 h AEL, the labrum and mandibles become thin and the incisor region of the mandibles are formed, while the labium and maxillas become sharp and segmented (Fig.7J). The antennas become segmented and project multiple sensilla. Six stemmata, beside each antenna, arise (Fig.7J). At this stage, the thoracic legs and prolegs are fully segmented; the tarsal claw on the leg tips shows its final shape (Fig.7K), as well as the crochets on the proleg plantae (Fig.7L).

Before hatching, at about 72 h AEL, the definite form of the head capsule and mouthparts are established (Fig.7M). At first, the mandibles become sclerotized and begin their abduction-adduction movements. Soon after, the embryo ingests the fragmented embryonic membranes. The anterior pole of the chorion is then ruptured by gnawing with mandibles and the larva hatches.

Discussion

The microscopy study of the embryogenesis of *H. erato phyllis* provided a structural glimpse of the morphogenetic changes which occur during its development.

Starting with the blastoderm formation, *H. erato phyllis* showed the same pattern observed in *Bombyx mori* (Nagy *et al.*, 1994) and *Bicyclus anynana* (Masci & Monteiro, 2005), which firstly form a syncytial blastoderm followed by the cellularization of the cleavage nuclei. In Lepidoptera, the blastoderm formation starts at the center of the egg cytoplasm, where the zygote nucleus undergoes meroblastic cleavages. After a series of mitosis, the nuclei migrate to the egg periphery with their cytoplasm islands and continue to divide there (Kobayashi *et al*., 2003). The cleavage nuclei that do not migrate to the periphery form the vitellophages, which can show one or two nuclei. Some nuclei are densely involved by a dense mass of cytoplasm, possibly due to high quantity of lipid droplets and carbohydrates from the yolk.

As for the germ band, we believe that *H. erato phyllis* could be classified as a long-germ lepidopteran. Taking into account the current insect embryology literature, there are three main types of embryos: those with long-, intermediate-, and short-germ bands. Characteristics of long-germ embryos include a large germ band within the egg, relatively short duration of embryogenesis, and inability to regulate embryogenesis in response to environmental perturbation (Davis & Patel, 2002). It has been observed that derived lepidopteran species, as *B. anynana* and *Manduca sexta*, follow this developmental pattern (Masci & Monteiro, 2005; Kraft & Jäckle, 1994). More ancestral lepidopteran species, however, have shorter germ bands, and a longer duration of embryogenesis with an ability to respond favorably to environmental changes during embryogenesis. It is believed that the fate of each cell in the short-germ embryos is determined later in the development, allowing for adjustments in cell fates (Nagy, 1995; Davis & Patel, 2002;). Indeed, another feature that discerns short- and long-germ embryos concerns the segmentation pattern. In many long-germ insects (e.g., *Drosophila*) all segments are specified almost simultaneously within the blastoderm. In short-germ insects only segments of the head are specified in the blastoderm, whereas the remaining segments of

the thorax and abdomen form progressively from a posterior growth zone (Davis & Patel, 2002). In spite of the complete segmentation of *H. erato phyllis* has not been visible in the blastoderm, soon after, at about 12 h AEL, the segmental grooves are present along the antero-posterior axis, which suggests a long-germ embryogenesis.

The size variation of *H. erato phyllis* germ band during the first 10 h of development were different from that in *B. mori*. In *B. mori*, the size of germ band is initially large and occupies most of the diameter and almost the entire length of the egg. However, this germ band soon contracts to occupy only half the egg length taking a short-germ appearance, and subsequently undergoes a phase of elongation (Nagy *et al.*, 1994), during which the segmental grooves are formed, first in the gnathal and thoracic regions and then sequentially in the abdomen. Due to this, together with molecular data, *B. mori* is considered an evolutionarily intermediate state in a transition from short- to long-germ type (Nakao, 2010). In *H. erato phyllis*, however, the early germ band is not so large in diameter as in *B. mori*, it is slender, but occupies the entire length of the egg, indicating that it arises from the entire length of the blastoderm. Further, following compaction, the germ band in *H. erato phyllis* occupies approximately two thirds of the egg length; thus, it does not reduce as much as *B. mori*.

The embryogenesis of *B. mori* resembles in some aspects the embryogenesis of *M. sexta*. In *M. sexta* the segmental grooves first appear in the gnathal-thoracic region, followed by the sequential appearance of abdominal segments (Broadie *et al.*, 1991). Despite of this intermediate-germ feature, molecular data for *M. sexta* show that a genetic prepattern exists simultaneously for all segments, such that *M. sexta* is considered a long-germ lepidopteran (Kraft & Jäckle, 1994). Both *M. sexta* and *H. erato phyllis* undergo a phase where only the head lobes plus a nonsegmented terminus are apparent; at this stage, there are no obvious signs of morphological segmentation.

As to the mode of formation of the embryonic membranes (serosa and amnion), in Lepidoptera, three types are known: the invaginate type, amnioserosal fold type, and fault type (Kobayashi *et al.*, 2003). The invaginate type is found in *Neomicropteryx* (Zeugloptera) and *Endoclyta* (Exoporia), and is thought to be the most ancestral type. In these genera, the relatively short germ band invaginates into the yolk forming a vesicular germ band, whereas the extraembryonic ectoderm closes above it, forming the serosa. Soon, one layer of the vesicular germ band differentiates into the germ band itself, and the other layer into the amnion. The vesicular lumen represents the amniotic cavity (Ando & Tanaka, 1980; Kobayashi & Ando, 1982). The amnioserosal fold type is found only in *Eriocrania* (Dacnonypha), whose embryonic membranes are formed by the invagination of the anterior and posterior regions of the germ band, forming folds which extend to the ventral midline and merge to form the amnion and serosa (Kobayashi & Ando, 1987). The fault type is known only in ditrysians and in the monotrysian *Stigmella*. In this type, the germ band is cut off from the extraembryonic ectoderm, and the serosa is formed by cell proliferation; the amnion is then formed independently by extension of the edges of the germ band. This mode of ontogeny of embryonic membranes is considered an apomorphic characteristic of Heteroneura (Kobayashi, 1996). In *H. erato phyllis*, the separation between germ band and extraembryonic ectoderm, and the consequent formation of the serosa and amnion, follows the same pattern observed in the fault type.

The serosa and amnion play a crucial role, respectively, in the secretion of the egg cuticle and in the dorsal closure of the embryo. It is generally assumed that the serosa cuticle, which is deposited beneath the chorion, is considered to be a protection for the embryo. This is plausible for cases where the chorion is thin or can even ruptures during embryogenesis. In Lepidoptera, however, the chorion is very sturdy and may not need the assistance of the relatively thin serosal cuticle (Larink, 1972). Despite of this, Lamer and Dorn (2001) studied the structure and function of the serosa throughout the embryonic

development of *M. sexta* by electron microscopy, revealing that the serosa cells in this species show intense cuticle secretion and might adopt several functions sequentially according to the changing needs of the embryo. Features of the cytoplasm of the serosa cells in *M. sexta* include the high quantity of Golgi complexes concentrically structured and secretory vesicles, which in turn were found in the serosa cells of *H. erato phyllis*. So, we can say that the serosa of *H. erato phyllis* is involved in cuticle secretion, despite the chorion stiffness of its eggs.

In addition, the serosal cells of the long-germ eggs tend to be mononucleated, in contrast to the short-germ species which are usually multinucleated (Wall, 1973; Kobayashi & Ando, 1984). The serosa cells of *H. erato phyllis* are mostly mononucleated, which suggests that it agree with the phylogenetic trend of the long-germ embryos.

As for the abdominal segmentation, the basic number of abdominal segments during embryonic development in Insecta is eleven, excluding the telson. The 11^{th} one has the tendency to be greatly reduced and is entirely lacking in some insects, especially in holometabolous. The absence of the 11^{th} abdominal segment is thus considered as an apomorphic character. In Lepidoptera larvae, this segment is absent. However, the embryos of *Neomicropteryx* and *Endoclyta* show temporarily the 11^{th} segment, which later disappears (Tanaka, 1993). In *H. erato phyllis* embryos, the 11^{th} segment do not appears, which is phylogenetically consistent with Heteroneura, that lacks this segment (Kobayashi, 1987).

As for the morphogenetic movements involved in the formation of the head, thoracic and abdominal appendages, *H. erato phyllis* follows the same pattern of formation observed in *M. sexta* appendages (Dow *et al.*, 1988).

In relation to the developmental time, *H. erato phyllis* develops relatively quick, as it completes embryogenesis at about 72 h AEL. To date, the developmental time of *B. anynana* is around 96-120 h (Masci & Monteiro, 2005), and *M. sexta* is around 100 h (Kraft

& Jäckle, 1994). As previously mentioned, the length of time of the egg stage is another distinguishing feature of the short- and long-germ insects (Davis & Patel, 2002).

As for the germ types, short- and intermediate-germ embryos are widely found among various insect orders, while the long-germ embryos are mostly restricted to those orders using nurse cells during oogenesis (e.g., Lepidoptera and Diptera). Nurse cells allow an increased and spatially polarized maternal contribution to the developing oocyte; this evolutionary innovation may have been an important precondition for rapid development, if not itself, a product of selection (Davis & Patel, 2002). So, the provisioning of maternal information by nurse cells might have been a precondition to the evolution of long-germ embryogenesis.

Closer inspection of the phylogenetic distribution of germ types reveals, however, that the long-germ type is more closely correlated to holometaboly, as the long-germ type is found in multiple clades within the Holometabola (Davis & Patel, 2002). This suggests that either long-germ embryogenesis has been secondarily lost in orders possessing representatives of multiple germ types, such as Lepidoptera, or it has evolved more than once.

This paper showed that *H. erato phyllis*, the more derived species whose embryogenesis was studied until now, conforms to a long-germ band lepidopteran. The analysis of *H. erato phyllis* embryonic development, from the blastoderm formation to the pre-hatching larva, provided a morphological glimpse into the *Heliconius* embryogenesis. Furthermore, the present study could help future molecular approaches to understand the evolution of *Heliconius* development.

Acknowledgements

We thank to our colleagues of the Ecological Genetics Laboratory for their help in collecting butterflies and daily feeding the caterpillars. Electron and confocal microscopy

were performed at the Electronic Microscopy Center from the Federal University of Rio Grande do Sul, Porto Alegre, Brazil. Thanks are also due to the Conselho Nacional de Desenvolvimento Científico e Tecnológico, CNPq, for financial support and for a doctoral scholarship to the first author.

References

Anderson, D. T. 1972. The development of holometabolous insects. In *Developmental Systems: Insects* (Eds. S. J. Counce & C. H. Waddington), pp. 165–242. Academic Press, London.

Ando, H. & Tanaka, M. 1980. Early embryonic development of the primitive moths *Endoclyta signifer* Walker and *E. excrescens* Butler (Lepidoptera: Hepialidae). *Int. J. Insect Morphol. Embryol.* **9**, 67–77.

Aymone, A. C. B., Valente, V. L. S. & Araújo, A. M. 2013. Ultrastructure and morphogenesis of the wing scales in *Heliconius erato phyllis* (Lepidoptera: Nymphalidae): What silvery/brownish surfaces can tell us about the development of color patterning? *Arth. Struct. & Dev.* **42**, 349-359.

Beebe, W., Crane, J. & Fleming, H. 1960. A comparison of eggs, larvae and pupae in fourteen species of heliconiine butterflies from Trinidad, W.I. *Zoologica* **45,** 111-154.

Benson, W. W. 1972. Natural selection for Müllerian mimicry in *Heliconius erato* in Costa Rica. *Science* **76**, 936-939.

Broadie, K. S., Bate, M. & Tublitz, N. J. 1991. Quantitative staging of embryonic development of the tobacco hawkmoth, *Manduca sexta*. *Roux's Arch. Dev. Biol.* **199**, 327–334.

Brown, K. S., JR. 1981. The biology of *Heliconius* and related genera. *Ann. Rev. Entomol.* **26**, 427-456.

Davis, G. K. & Patel, N. H. 2002. Short, long, and beyond: Molecular and embryological approaches to insect segmentation. *Ann. Rev. Entomol.* **47**, 669-699.

Dell'Erba, R. D., Kaminski, L. A. & Moreira, G. R. P. 2005. O estágio de ovo dos Heliconiini (Lepidoptera, Nymphalidae) do Rio Grande do Sul, Brasil. *Iheringia, Sér. Zool.* **95**, 29-46.

Dow, R. C., Carlson, S. D. & Goodman, W. G. 1988. A scanning electron microscope study of the developing embryo of *Manduca sexta* (L.) (Lepidoptera: Sphingidae). *Int. J. Insect Morphol. & Embryol.* **17**, 231-242.

Hill, R. I., Gilbert, L. E. & Kronforst, M. R. 2013. Cryptic genetic and wing pattern diversity in a mimetic Heliconius butterfly. *Mol Ecol.* **22**, 2760-2770.

Hines, H. M., Papa, R., Ruiz, M., Papanicolaou, A., Wang, C., Nijhout, H. F., McMillan, W. O. & Reed, R. D. 2012. Transcriptome analysis reveals novel patterning and pigmentation genes underlying *Heliconius* butterfly wing pattern variation. *BMC Genomics* **13**, 288.

Hinton, H. E. 1981. *Biology of insect eggs*, V.1. Pergamon, London.

Ho, K., Dunin-Borkowski, O. M. & Akam M. 1997. Cellularization in locust embryos occurs before blastoderm formation. *Development* **124**, 2761–2768.

Jiggins, C. D., Naisbit, R. E., Coe, R. L. & Mallet, J. 2001. Reproductive isolation caused by colour pattern mimicry. *Nature* **411**, 302-305.

Joron, M., Jiggins, C. D., Papanicolaou, A. & McMillan, W. O. 2006. *Heliconius* wing patterns: an evo-devo model for understanding phenotypic diversity. *Heredity* **97**, 157-167.

Kobayashi, Y. 1996. Gross embryology of a monotrysian heteroneuran moth *Stigmella castanopsiella* Kuroko (Nepticulidae, Lepidoptera), and its phylogenetic significance. *Trans. Lepid. Soc. Japan* **47**, 194-200.

Kobayashi Y. & Ando H. 1982. Phylogenetic relationships among the lepidopteran and trichopteran suborders (Insecta) from the embryological standpoint. *Z. Zool. Syst. Evolutionsforsch.* **26**, 186–210.

Kobayashi, Y. & Ando, H. 1984. Mesodermal organogenesis in the embryo of the primitive moth, *Neomicropteryx nipponensis* Issiki (Lepidoptera, Micropterygidae*). J. Morphol.* **181**, 29–47.

Kobayashi Y. & Ando H. 1987. Early embryonic development and external features of developing embryos in the primitive moth, *Eriocrania* sp. (Lepidoptera, Eriocraniidae). In *Recent Advances in Insect Embryology in Japan and Poland* (Eds. H. Ando & C. Jura), pp. 159–194. ISEBU, Japan.

Kobayashi, Y., Tanaka, M. & Ando, H. 2003. Embriology. In *Lepidoptera, moths and butterflies,* Vol. 2 (Ed. N. P. Kristensen), pp. 495-544. Walter de Gruyter, Berlin.

Kraft, R. & Jäckle, H. 1994. *Drosophila* mode of metamerization in the embryogenesis of the lepidopteran insect *Manduca sexta*. *Proc. Natl. Acad. Sci. USA* **91**,6634–6638.

Lamer, A. & Dorn, A. 2001. The serosa of *Manduca sexta* (Insecta, Lepidoptera): ontogeny, secretory activity, structural changes, and functional considerations. *Tissue & Cell* **33**, 580-595.

Larink, O. 1972. Zur Struktur der Blastodermcuticula von Petrobius brevistylis und *P. maritimus* (Thysanura, Insecta). *Cytobiologie* **5**, 422-426.

Liu, P.Z. & Kaufman, T.C. 2005. Even skipped is not a pair-rule gene but has segmental and gap-like functions in *Oncopeltus fasciatus*, an intermediate germ band insect. *Development* **132**, 2081–2092.

Mallet, J. & Barton, N.H. 1989. Strong natural selection in a warning colour hybrid zone. *Evolution* **43**, 421-431.

Masci, J. & Monteiro, A. 2005. Visualization of early embryos of the butterfly *Bicyclus anynana*. *Zygote* **13**, 139-144.

Nagy, L. M. 1995. A summary of lepidopteran embryogenesis and experimental embryology. In *Molecular Model Systems in the Lepidoptera* (Eds. M. R. Goldsmith & A. S. Wilkins), pp. 139-164. Cambridge University Press, Cambridge.

Nagy, L. M., Riddiford L. M. & Kiguchi K. 1994. Morphogenesis in the early embryo of the lepidopteran *Bombyx mori*. *Dev. Biol.* **165**, 137–51.

Nakao, H. 2010. Characterization of *Bombyx* embryo segmentation process: expression profiles of engrailed, even-skipped, caudal, and wnt1/wingless homologues. *J. Exp. Zool.* **314**, 224–231.

Nakao, H. 2012. Anterior and posterior centers jointly regulate *Bombyx* embryo body segmentation. *Dev. Biol.* **371**, 293-301.

Patel, N. H. 1994. Developmental evolution: insights from studies of insect segmentation. *Science* **266**, 581–90.

Reed, D., Papa, R., Martin, A., Hines, H. M., Counterman B. A., Pardo-Diaz, C., Jiggins, C. D., Chamberlain, N. L., Kronforst, M. R., Chen, R., Halder, G., Nijhout, H. F., McMillan, W. O. 2011. *optix* drives the repeated convergent evolution of butterfly wing pattern mimicry. *Science* **333**, 1137-1141.

Sander, K. 1984. Embryonic pattern formation in insects: Basic concepts and their experimental foundations. In *Pattern formation: A primer in developmental biology* (Eds. G. M. Malacinski & S. V. Bryant), pp. 245-268. Macmillan, New York.

Sander, K. 1988. Studies in insect segmentation: from teratology to phenogenetics. *Development* **104**, 112-121.

Tanaka, M. 1993. Mesoblastic somites in the embryos of primitive moths, *Endoclita sinensis* (Moore) and *E. excrescens* Butler (Lepidoptera: Hepialidae). *New Entomologist* **42**, 16-25.

Wall, C. 1973. Embryonic development in two species of *Chesias* (Lepidoptera: Geometridae). *J. Zool.* **169**, 65–84.

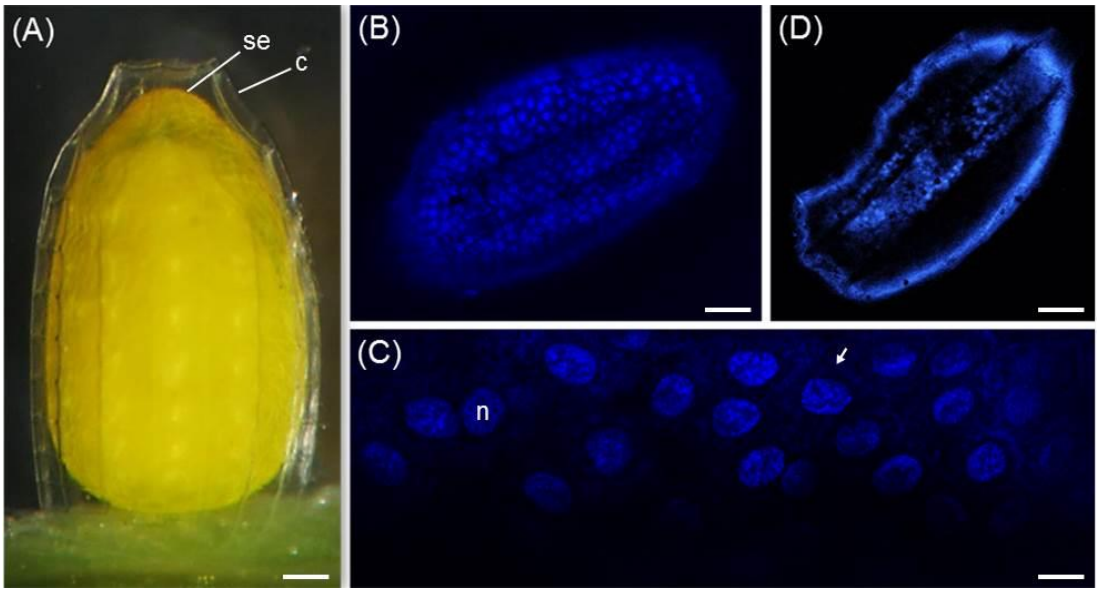

Fig. 1. Egg and the blastoderm formation in *H. erato phyllis*. (A) Egg and some of its components. (B-D) Confocal micrographs. (B) Syncytial blastoderm formation stained with Hoechst, nuclei in blue. The nuclei are uniformly distributed along the egg periphery. (C) Cellular blastoderm formation begins when the nuclei delimitation occurs by surrounding membranes (arrow). (D) Germ band differentiation at the superficial midline of the egg. c (chorion), n (nuclei), se (serosa). Bars: 100 µm, 100 µm, 25 µm, 100 µm, respectively.

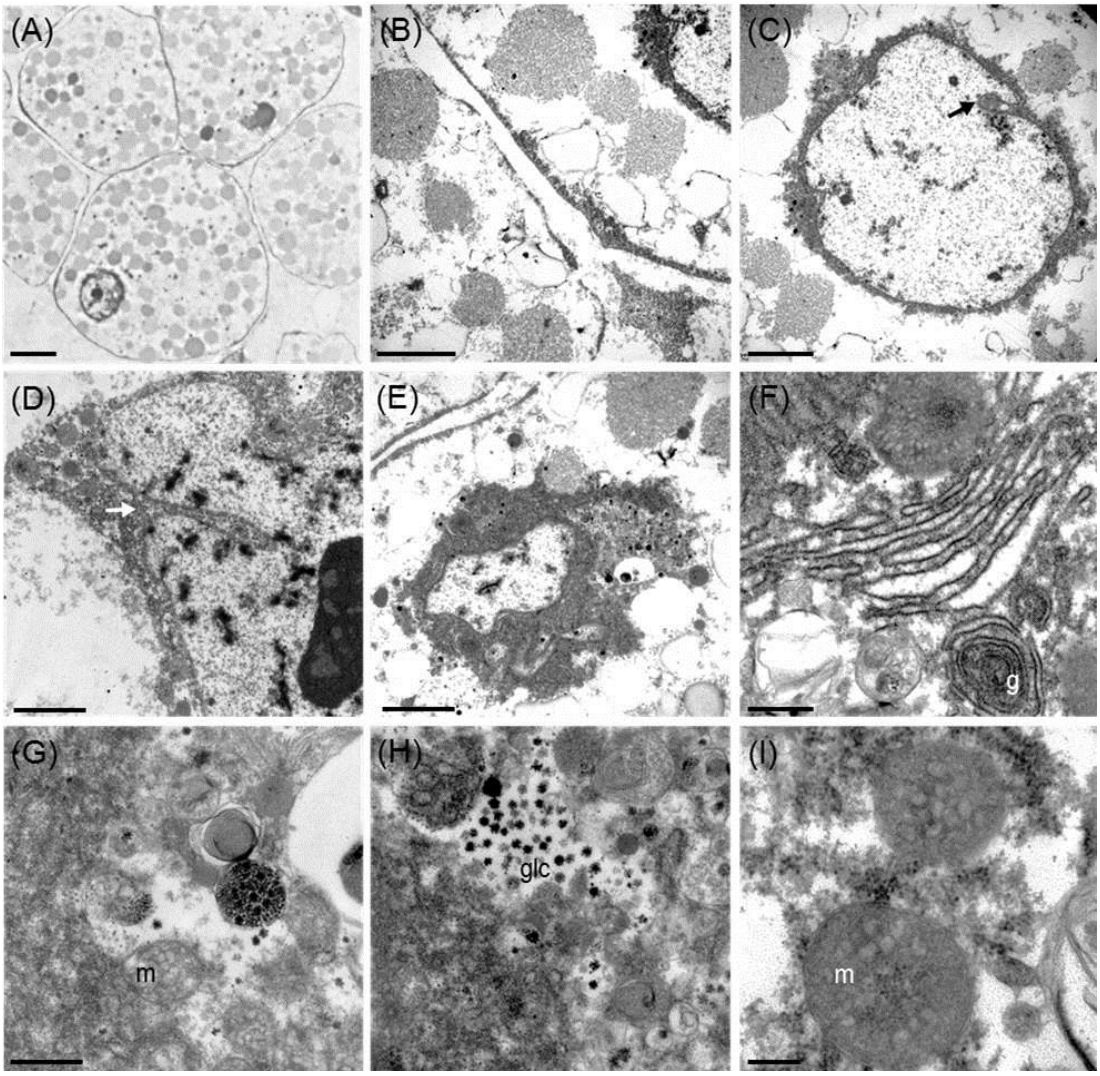

Fig. 2. Yolk of *H. erato phyllis* embryo visualized by TEM. (A) Vitellophages showing high quantity of carbohydrates (light grey circles). (B) Interface between two vitellophages and detail of the carbohydrates. (C) Euchromatic nucleus with an indentation (arrow). (D) Detail of a nuclear indentation (arrow) occupied by cytoplasm. (E) Euchromatic nucleus surrounded by a dense mass of cytoplasm, which is surrounded by the lipids (white circles) and carbohydrates. (F) Detail of a cytoplasmic region near the nucleus showing granular endoplasmic reticulum associated with Golgi. (G) Secretory vesicle full of protein (electron-dense regions). (H) Free glycogen granules. (I) Mithochondria on transversal section. g (Golgi), glc (glycogen granules), m (mitochondrion). Bars: 2.5 µm, 0.5 µm, 0.5 µm, 1 µm, 0.5 µm, 0.5 µm, 0.5 µm, 0.5 µm, 0.2 µm, respectively.

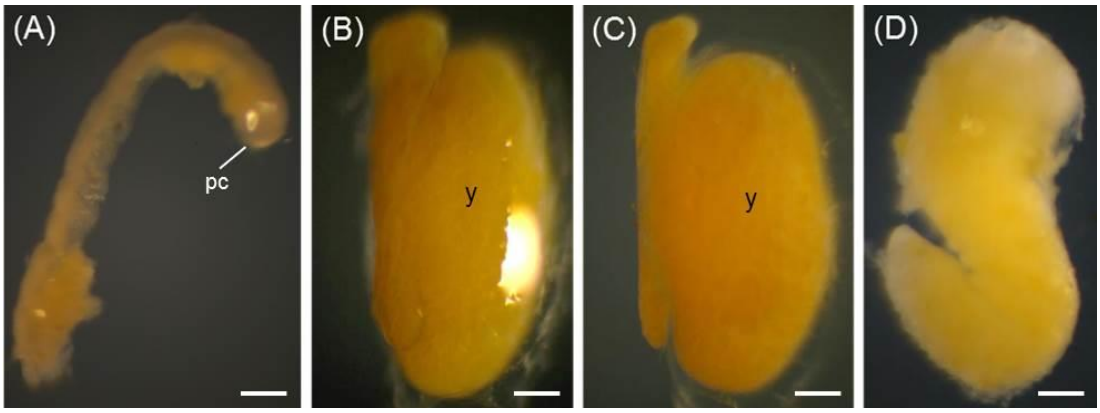

Fig. 3. The germ band and the embryo after blastokinesis of *H. erato phyllis* (dechorionated eggs), under stereomicroscopy. The dorsal region of the germ band (A-C) and of the embryo (D) is at the right in all pictures. (A) Initially, the germ band (isolated of the egg) is slender and occupies approximately half of the longitudinal circumference of the egg. (B) The germ band reduces in length becoming wider, mostly at the anterior region (on the top). (C) The germ band elongates again. Further, after proliferation, the germ band penetrates into the yolk mass, where it engages in blastokinesis. (D) Revolution of the embryo (isolated of the yolk mass). Note that the abdominal end turns ventrally, reaching the level of the ventral abdomen. pc (protocephalon), y (yolk). Bars: 100 µm.

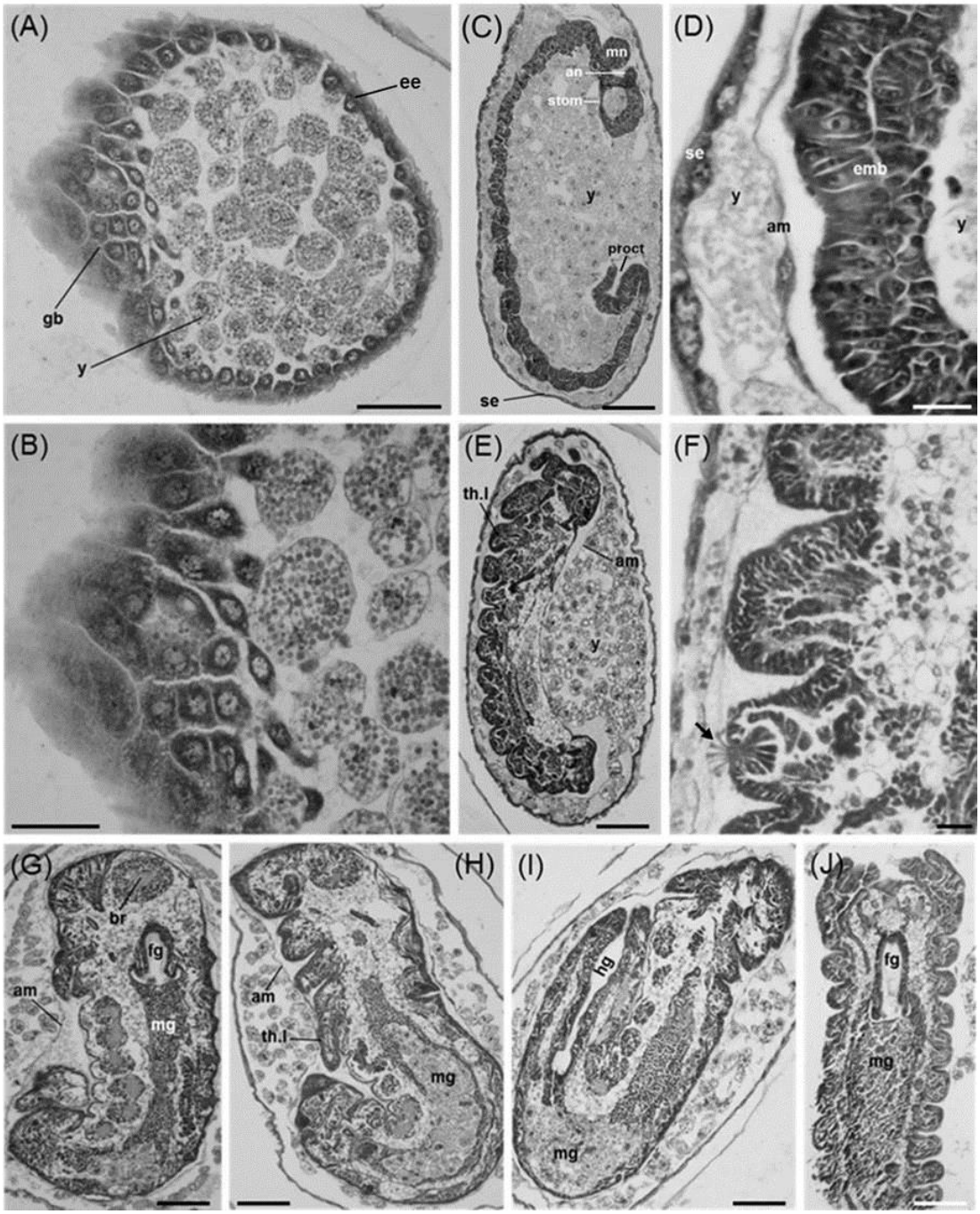
(A)
ee
gb
y
(C)
mn
an
stom
y
proct
se
(D)
se
emb
y
am
y
(B)
(E)
th.l
am
y
(F)
(G)
br
fg
am
mg
(H)
am
th.l
mg
(I)
hg
mg
(J)
fg
mg

Fig. 4. Formation of the germ band and segmentation in *H. erato phyllis* (light microscopy). (A, B) Transversal section of the egg showing cell proliferation originating the germ band. (C) Lateral view of the C-shaped embryo, already detached from the extraembryonic ectoderm, showing segmentation. (D) Detail of the interface between serosa, yolk, amnion, amniotic cavity and embryo, which is now definitely isolated from the egg periphery. (E) The embryo becomes larger and stout. The appendages of the head, thorax and abdomen arise as evaginations on the ventral region. (F) Detail of the developing prolegs showing the formation of the crochets (arrow), while they are not yet everted. (G-J) Embryos after revolution showing the intestine in different angles. (G) Dorsolateral view, showing the foregut and midgut. (H) Lateral view, showing the interior of the midgut full of vitellophages. (I) Lateral view, showing the midgut and the hindgut. (J) Ventral view, showing the foregut and midgut. ab1-11 (abdominal segments 1-11), am (amnion), an (antenna), br (brain), emb (embryo), ee (extraembryonic ectoderm), fg (foregut), gb (germ band), hg (hindgut), mn (mandible), proct (proctodeum), se (serosa), stom (stomodeum), th1-3 (thoracic segments 1-3), th.l (thoracic leg), y (yolk). Bars: 50 µm, 25 µm, 100 µm, 20 µm, 100 µm, 10 µm, 100 µm, 100 µm, 100 µm, 100 µm, respectively.

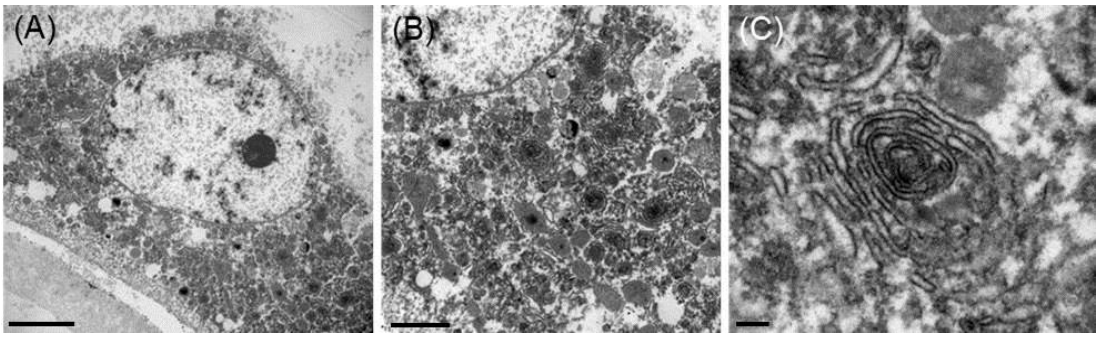

Fig. 5. The serosa of *H. erato phyllis* egg visualized by TEM. (A) Mononucleated serosa cell. (B) Cytoplasm of the serosa cell showing high density of Golgi, mitochondria and secretory vesicles. (C) Zoom area showing the Golgi circular cisterns. Bars: 5 µm, 2 µm, 1 µm.

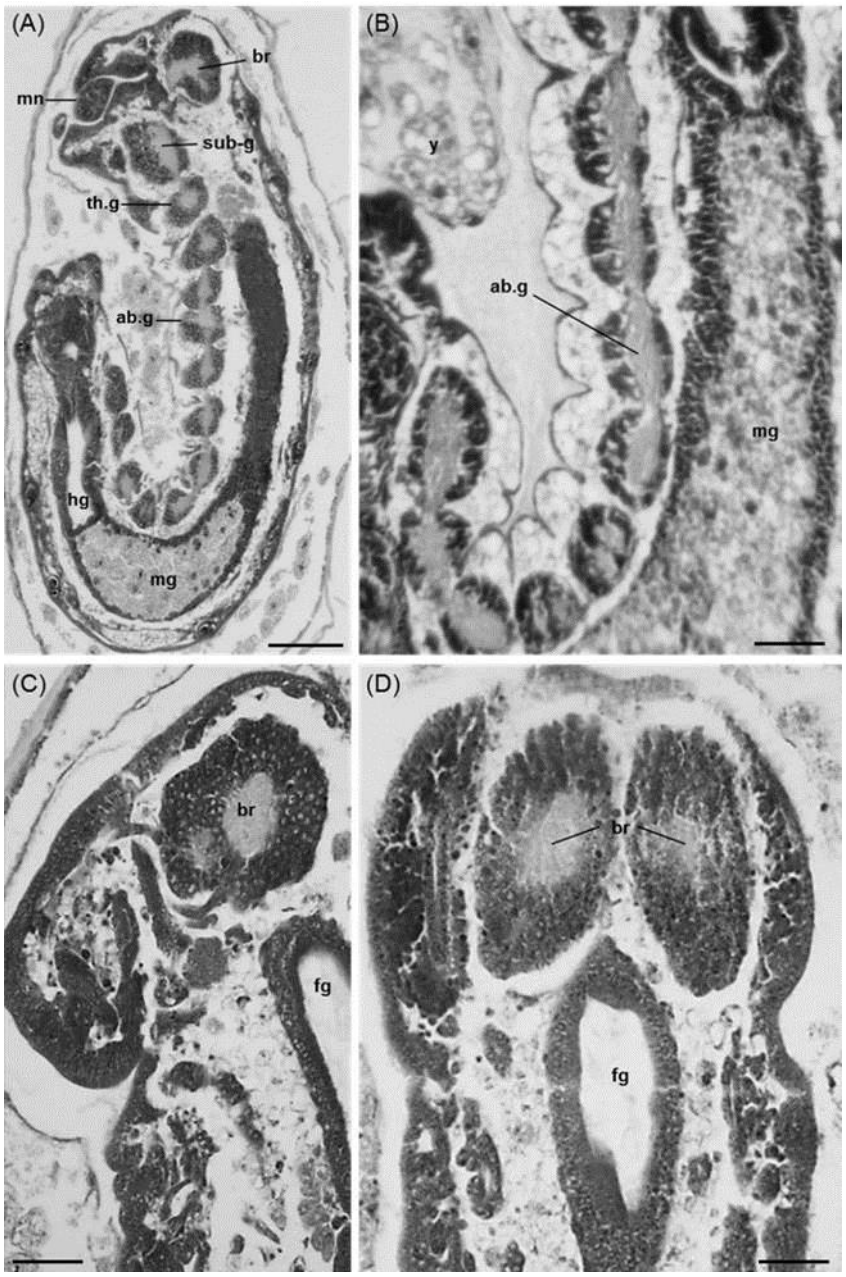

Fig. 6. The central nervous system in *H. erato phyllis* embryos (light microscopy). (A) Lateral view, showing the brain followed by the suboesophageal ganglion, and the thoracic and abdominal ganglia. (B) Enlarged vision of the abdominal ganglia. (C) The brain in lateral and (D) dorsal view. ab.g (abdominal ganglion), br (brain), fg (foregut), hg (hindgut), mg (midgut), mn (mandible), sub.g (suboesophageal ganglion) th.g (thoracic ganglion), y (yolk). Bars: 100 µm, 50 µm, 50 µm, 50 µm, respectively.

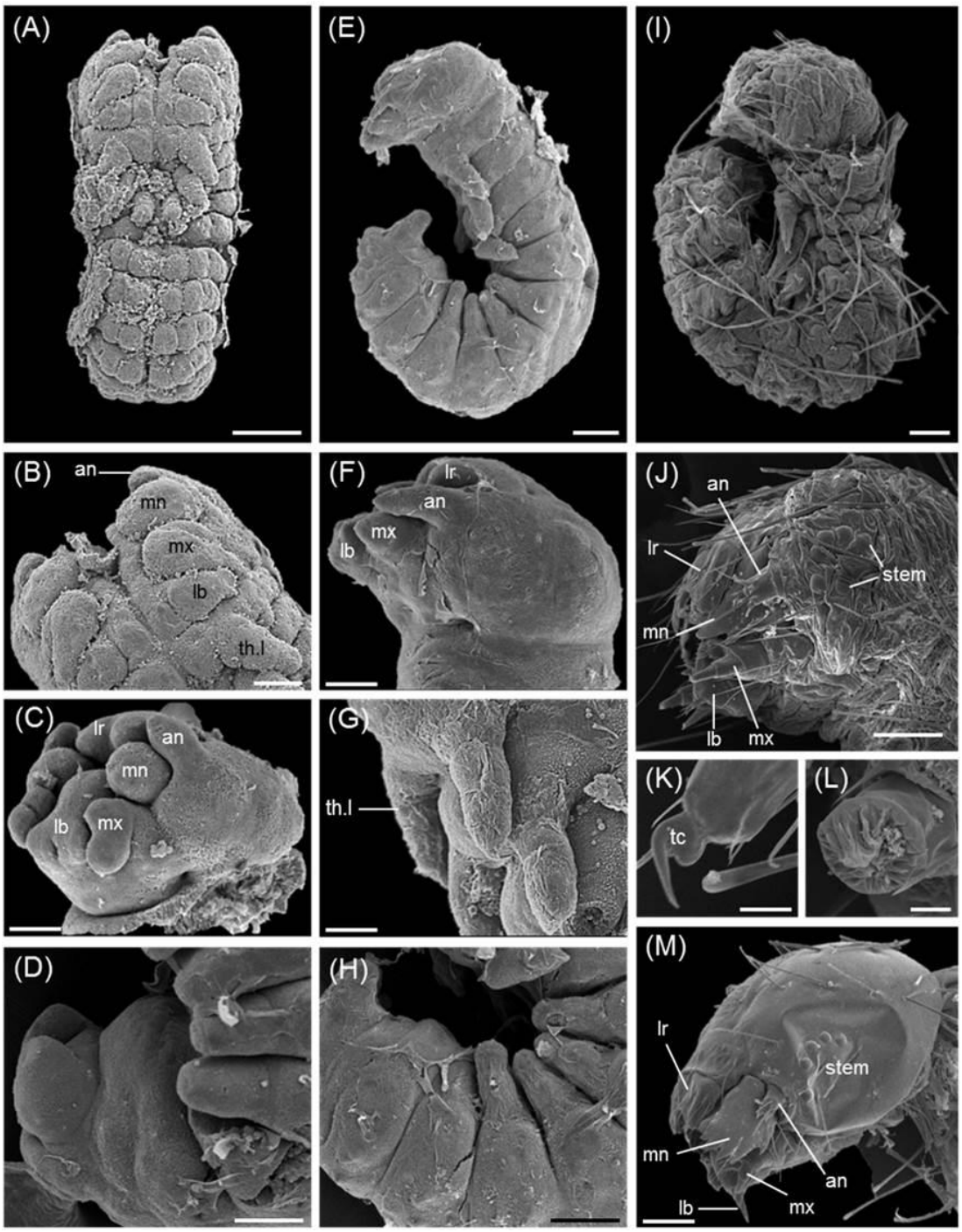
(A)
(E)
(I)
(B)
an
mn
mx
lb
th.I
(F)
lr
an
mx
lb
(J)
an
lr
stem
mn
lb
mx
(C)
lr
an
mn
lb
mx
(G)
th.I
(K)
tc
(L)
(D)
(H)
(M)
lr
stem
mn
an
lb
mx

Fig. 7. Formation of the appendages in *H. erato phyllis* embryo visualized by SEM. (A) Ventral view of the germ band at about 16 h AEL; (B) Zoom area showing the primordium of the antenna, mandible, maxilla, labium and first thoracic leg. (C) Head segments fused, after embryo revolution; note the changed shape and position of the head appendages. At this stage, the abdominal end (D) becomes differentiated and turns ventrally. (E) Embryo at about 48 h, showing the segmentation pattern of the thoracic and abdominal regions; (F) Zoom area showing the shape change of the head appendages; (G) Zoom area of the developing thoracic legs; (H) Zoom area showing the posterior abdominal segments, note the fusion at the abdominal end. (I) Embryo at about 56 h, showing the final position of the embryo into the egg; (J) Zoom area showing the shape change of the head appendages; stemmata arising. Note the rugged appearance of the head capsule. (K-L) Zoom area showing the thoracic legs and prolegs fully developed; note the tarsal claw on the leg tip (K), and the evagination of the crochets in a proleg (L). (M) Final shape of the head capsule. an (antenna), lb (labium), lr (labrum), mn (mandible), mx (maxilla), stem (stemmata), tc (tarsal claw), th.l (thoracic leg). Bars: 100 µm, 50 µm, 50 µm, 50 µm, 100 µm, 50 µm, 50 µm, 100 µm, 100 µm, 100 µm, 20 µm, 20 µm, 100 µm, respectively.

CAPÍTULO 3

Ultrastructure and morphogenesis of the wing scales in *Heliconius erato phyllis* (Lepidoptera: Nymphalidae): What silvery/brownish surfaces can tell us about the development of color patterning?

Ana Carolina Bahi Aymone[1], Vera Lúcia da Silva Valente[1,2], Aldo Mellender de Araújo[1,2]

[1] Post-Graduate Program of Genetics and Molecular Biology, Federal University of Rio Grande do Sul, Porto Alegre, Brazil. Av. Bento Gonçalves 9500, C.P. 15053, 91501-970, Porto Alegre, RS.

[2] Department of Genetics, Federal University of Rio Grande do Sul, Porto Alegre, Brazil. Av. Bento Gonçalves 9500, C.P. 15053, 91501-970, Porto Alegre, RS.

***Arthropod Structure & Development* 42: 349-359**

DOI: 10.1016/j.asd.2013.06.001

Abstract

Usually the literature on *Heliconius* show three types of scales, classified based on the correlation between color and ultrastructure: type I – white and yellow, type II – black, and type III – orange and red. The ultrastructure of the scales located at the silvery/brownish surfaces of males/females is for the first time described in this paper. Besides, we describe the ontogeny of pigmentation, the scale morphogenesis and the maturation timing of scales fated to different colors in *H. erato phyllis*. The silvery/brownish surfaces showed ultrastructurally similar scales to the type I, II and III. The ontogeny of pigmentation follows the sequence red, black, silvery/brownish and yellow. The maturation of yellow-fated scales, however, occurred simultaneously with the red-fated scales, before the pigmentation becomes visible. In spite of the scales at the silvery/brownish surfaces being ultrastructurally similar to the yellow, red and black scales, they mature after them; this suggests that the maturation timing do not show a relationship with the scale ultrastructure, with the deposition timing of the yellow pigment. The analysis of *H. erato phyllis* scale morphogenesis, as well as the scales ultrastructure and maturation timing, provided new findings into the developmental architecture of color pattern in *Heliconius*.

Key words: butterfly scales, color x ultrastructure correlation, development.

Introduction

The butterfly wing patterns are excellent objects of study for evo-devo, because they are structurally simple, highly variable, and, in many cases, the evolutionary and ecological significance of the different patterns are well known (Beldade and Brakefield, 2002; McMillan *et al.*, 2002; Monteiro *et al*., 2006). This is particularly true for genus *Heliconius*, which combines a broad variation of color patterns with a long history of research in the fields of ecology, evolution and behavior (e.g., Benson, 1972; Mallet and Barton, 1989; Jiggins *et al.*, 2001; Kapan, 2001). In most cases the diversity of *Heliconius* is guided by Müllerian mimicry, which is responsible for the phenotypic convergence of different species, culminating in the formation of geographic races, which enhance the ability to educate predators by shared aposematic coloration (Langham, 2004). The species *Heliconius erato* and *Heliconius melpomene* are an extreme example of intraspecific variation, exhibiting over 20 mimetic patterns situated in different areas of the Neotropical region (Brown, 1979).

Significant progress has been made recently in understanding the genetic base responsible for the variation of color patterns in *Heliconius*. Genetic mapping has shown that three loci with a great effect are responsible for the main patterns observed in the genus (Joron *et al.*, 2006; Papa *et al.*, 2008). In *H. erato* and *H. melpomene*, these loci control several distinct patterns, including the variation of the red forewing patches and the presence of a yellow hindwing bar (Mallet, 1989; Naisbit *et al.*, 2003; Jiggins *et al.*, 2005; Kapan *et al.*, 2006). Hines *et al.* (2012) studied the transcriptome in *Heliconius erato* wings throughout pupal development and revealed a myriad of genes involved in the cuticle formation and pigmentation of scales, providing a network-level glimpse into the genetic architecture of intraspecific phenotypic variation in *Heliconius*.

A major aspect of the development of color patterns in butterfly wings concerns the rates of scale maturation (ffrench-Constant, 2012). Koch *et al.* (2000) using scanning electron microscopy (SEM) found that scales fated to different colors in *Papillo glaucus* mature at different times, this because the maturation state may allow or not the access of pigments, which are sequentially synthetized in the scale cells. By air-drying pupal wings, the rate of scale maturation can be readily observed using SEM, since scales that had finished sclerotization remain erect, whereas the immature scales collapse. Smith (2003) applied the concept of 'developmental heterochrony' to the regulation of maturation timing in butterfly scales, since the timing shifts may result in different color patterns, as in the case of *P. glaucus* polymorphism. In *Heliconius*, the ontogeny of pigmentation was described for *H. erato petiverana* (Reed *et al.*, 2008) and *H. melpomene cythera* (Ferguson and Jiggins, 2009), however, the maturation timing of scales is unknown at the ultrastructural level.

From the morphological standpoint, scales of different colors show ultrastructural differences which are correlated with the pigmentation (Ghiradella, 1984; Gilbert *et al.*, 1988; Janssen *et al.,* 2001; Prum *et al.*, 2005). Gilbert *et al.* (1988) classified the scales of *Heliconius* as three types, based on the correlation between ultrastructure and type of pigment present. Type I-scales (white or yellow) (Fig.3A) are characterized by the presence of an obverse membrane and the absence of crossribs. Type II-scales (black) (Fig.3B) do not show an obverse membrane and their longitudinal ridges are connected by ladder-like crossribs, while type III-scales (orange and red) (Fig.3C) show an obverse membrane retained immediately adjacent to longitudinal ridges and over each crossrib. The pigments responsible for the yellow, black, orange and red colors are, respectively: 3-hydroxykynurenine (3-OHK), melanin, xanthommatine and dihydroxanthommatine. The white color is structural and does not show pigmentation.

In *Heliconius erato phyllis* males, a red-banded race of *H. erato*, beyond yellow, red and black patterns, occurs two silvery surfaces (“silvery friction surfaces”, after Crane 1955), one located on the inferior part of ventral forewing (Fig.1C) and the other in the superior part of dorsal hindwing (Fig.1D). In females, these regions are silvery only in part of the proximal region (Fig.1A-B), being mostly brownish, constituting a sexual dimorphism easily seen. Although the silvery/brownish surfaces were not included in the study by Gilbert *et al.* (1988), they could be important for understanding the relationship between the pathways of microstructure, maturation timing and pigmentation of scales, which in turn are involved in the developmental architecture of color patterns.

Our first objective was to confirm the ultrastructural types of yellow, black and red scales in the adult wings of *H. erato phyllis,* since it was not included in the study by Gilbert *et al.* (1988), and to analyze the ultrastructure of the scales located on the silvery and brownish surfaces (males and females, respectively) (Fig.1), which were, to our knowledge, never taken into account in the literature.

Another purpose was to describe the ontogeny of pigmentation and, at the ultrastructural level, to describe the morphogenesis and the maturation timing of phenotypically different scales as regards ultrastructure and color, including the scales situated on the silvery and brownish surfaces, throughout the pupal development. With this we intend to understand the interaction between the ontogenetic pathways responsible for the maturation timing, microstructure and pigmentation in the wing scales of *H. erato phyllis*. Are maturation rates related to the pigmentation or to the microstructure pathways?

Material and Methods

Object of study, collection and breeding

Egg-laying butterflies were captured in natural populations around the city of Porto Alegre (30°01’59’’S, 51°13’48’’W), State of Rio Grande do Sul, Southern Brazil, and transferred to open air insectaries at the Genetics Deparment from the Federal University of Rio Grande do Sul. Each unit of the insectaries measured 2 x 3 x 3 m with seminatural conditions and with hostplants (*Passiflora suberosa*, mainly). Butterflies were fed daily with a mixture of honey : water : pollen that were substituted every morning.

Eggs were collected daily and brought to the laboratory, where they were individually in plastic vials with humid filter paper and kept under controlled temperature and photophase (25 ± 1°C; 14 h / light / day). The caterpillars received a daily diet of *Passiflora suberosa* leaves – a natural host for *H. erato phyllis* in the outskirts of Porto Alegre.

Scales ultrastructure

After emerging, butterflies (males and females) were left resting to complete the extension of wings; afterwards they were refrigerated for 1 h. Fore and hindwings were removed, mounted on metal stubs with double-sided carbon tape, kept in a desiccator for 24 h, metalized with a layer of approximately 10 nm of gold (BAL-TEC® SCD-050) and finally observed under a JEOL® JSM-6060 scanning electron microscope, at 5 kV.

Scale morphogenesis and maturation

Pupae at different stages of development were fixed in Dietrich (Kahle) fluid for at least one week. As pupal developmental time is variable among individuals, we followed Ferguson and Jiggins (2009) classification for the pupal wing stages in *Heliconius melpomene*, which are: *Early Pupa* (EP), *Pre-ommochrome* (PO), *Ommochrome Only* (OO), *Early Melanin* (EM), *Mid Melanin* (MM) and *Late Melanin* (LM).

The pupal wings were isolated, washed in PBS buffer, dehydrated in a ketonic series, submitted to a critical point in (BAL-TEC® CPD-030), mounted on metal stubs with double-sided carbon tape, metalized with an approximately 15 nm gold layer (BAL-TEC® SCD-050) and observed under a scanning electron microscope (JEOL® JSM-6060), at 10 kV. At least 10 males and 10 females of each stage were submitted to ultrastructural analysis.

Although males and females were studied, the figures enclosed illustrates only males (the exception is Fig.1 which shows both sexes), since there were no differences between them in the structure and development of the scales.

Results and Discussion

Ontogeny of the pigmentation

In *Early Pupa* stage (Fig.2A), the wing consists of a thin epidermal bilayer of semitransparent tissue, while in early *Pre-ommochrome* stage, the wing has an opaque cream color and does not show pigmentation. In late *Pre-ommochrome* stage (Fig.2B), the red-fated scales on the dorsal surface of the forewing appear slightly more clear than the cream color, while the yellow-fated scales on the hindwing become white (Fig.2C).

In *Ommochrome Only* stage (Fig.2D-F), the red-fated scales on the dorsal surface of the forewing become progressively dark from a pale orange to a deep red (Fig.2D). On its ventral surface (Fig.2E), the red scales appear clearer than the dorsal red patch. In the hindwing (Fig.2F), the yellow-fated scales remain unpigmented.

In the *Melanin* stages (Fig.2G-I), black scales become pigmented, as well as the scales situated on the silvery/brownish surfaces (Fig.2H-I). The pigmentation of the yellow-fated scales occurs within a few hours before adult emergence, after the complete melanin deposition. The final color pattern of the adult after emergence is shown in figure1.

As in *H. melpomene cythera* (Ferguson and Jiggins, 2009), *H. erato petiverana*, *H. erato cyrbia* and *H. himera* (Reed *et al.*, 2008), in *H. erato phyllis* the yellow-fated scales become pigmented lastly, in spite of which they mature before the black and silvery/brownish-fated scales, which become pigmented before the yellow scales. This suggests that the maturation state is not determinant for the yellow scales pigmentation, since there was no relationship between the yellow-fated scales maturation and 3-OHK deposition timing. On the other hand, the fact that the melanin did not deposit in the mature yellow-fated scales shows that possibly the particular biochemistry of the yellow-fated scales impedes the melanin deposition.

Reed *et al.* (2008) observed that the pigmentation time of the red and black scales are spatially associated with the expression of the *vermilion* gene, but not the white and yellow scales. The fact that *vermilion* is needed to synthetize 3-OHK, which in turn is the precursor of dihydroxanthommatine, made it clear that the synthesis of 3-OHK of the yellow scales does not occur *in situ*. By marking 3-OHK with C^{14}, the authors observed that the 3-OHK molecules which are deposited on the yellow-fated scales come directly from the hemolymph, and that their synthesis possibly occurs in the fat bodies, given that the amount of 3-OHK in these structures was greater at the time of the greatest concentration of 3-OHK in hemolymph.

The relationship between the expression of *vermilion* and the pigmentation of the red and black scales, however, does not occur in *H. melpomene cythera* (Ferguson and Jiggins, 2009), in which *vermilion* is expressed over the entire surface of the wing throughout pupal development. The authors suggested that this difference in the transcriptional pattern of *vermilion* is possibly associated with the “imperfect” mimicry of *H. melpomene* in relation to *H. erato.* A subtle distinction between these two species corresponds to the marginal limit of the red patch, which is clearly demarcated in *H. erato* and “blurred” in *H. melpomene*.

Scales ultrastructure

The ultrastructure of the yellow (Fig.3A), black (Fig.3B) and red (Fig.3C) scales on the dorsal surfaces of the wings is in accordance with the types classified by Gilbert *et al.* (1988).

At silvery surfaces of males, as well as at silvery-brownish surfaces of females, scales were found whose upper surfaces are undistinguishable to the three types characterized by Gilbert *et al.* (1988). Their main difference is located at the brownish area of females, where only types II and III were found (males showed the three types). The proximal area of the silvery surfaces, in both sexes, contain acute scales of type I only (Fig.4). However, the scales whose upper surfaces are undistinguishable to the types I (except acute scales) and III on the silvery/brownish surfaces, show differences in the trabeculae location in relation to the types I and III characterized by Gilbert *et al.* (1988).

In what follows we characterize the scales located at the silvery/brownish surfaces. In the scales that are similar to type I-scales (Fig.3D) there is an obverse membrane between the longitudinal ridges. Windows of different sizes occur in the obverse membrane, especially in the central region of the scales. On the surface of the obverse membrane, there are transverse flutes (=microribs of Ghiradella, 1985) perpendicular to the longitudinal ridges. Except in the acute scales (Fig.4D), the obverse membrane is supported by trabeculae (connections of the upper and lower scale surfaces). The type II-scales (Fig.3E) do not show obverse membrane and exhibit ladder-like crossribs, which are narrower than the longitudinal ridges and are supported by trabeculae. Finally, the scales that are similar to type III-scales (Fig.3F) show an obverse membrane retained immediately adjacent to longitudinal ridges and over each crossrib. For this reason, the crossribs appear thicker and show a more angular aspect than the crossribs of type II-

scales. The crossribs are supported by trabeculae. We kept the three original types and stressed the ultrastructural differences in Table 1.

Gilbert *et al.* (1988) observed that the trabeculae support the crossribs only in type II-scale. In type I and III-scales, the trabeculae basically support the longitudinal ridges, but not the obverse membrane in type I neither the crossribs in type III-scale. However, in the scales from the silvery/brownish surfaces similar to type I (except acute scales) and III-scales, trabeculae were found supporting, respectively, the obverse membrane and the crossribs, which is a distinctive feature from the usual type I and III proposed by Gilbert *et al.* (1988) for the white/yellow and red scales.

The pigmentation of the silvery and brownish surfaces is due possibly to different melanin concentration and oxidation level. The ultrastructural variability of the scales in the silvery surfaces of males may be responsible for the different levels of reflectance that can be viewed from different angles, causing a structural effect in these regions. The region of the acute scales (Fig.1, 4A) shows a more brilliant and iridescent grey color, due probably to the structural effect provided by the obverse membrane.

Scale morphogenesis and maturation

In *Early Pupa* stage (Fig.2A), approximately 6 h after pupation, the wing surface shows a polygonal pattern consisting of penta- to heptagonal cells of equivalent size (Fig.5A). The apical surface of these cells is full of microvillosities (Fig.5B). Both the polygonal pattern and the presence of microvillosities on the apical surfaces agree with what was observed in *Pieris rapae* (Honda *et al*., 2000).

After 24 h, the scale precursor cells (SPCs) (Fig.5C) begin the differentiation process. The apical surface of the SPCs is circular with a diameter approximately twice as big as that of the general epithelial cells (GECs), and does not show microvillosities.

In early *Pre-ommochrome* stage, after 48 h, the apical surfaces of the SPCs (Fig.5D) have become higher than those of the GECs, which in turn increased in number, allowing greater spacing between the parallel lines of SPCs. These extend along the anteroposterior axis of the wing, corresponding to the lines of scales that will later appear on the wing surface. Bifurcations and points of anastomosis between the SPCs lines become more evident.

The beginning of the SPCs differentiation process is similar to that in *P. rapae* (Yoshida e Aoki, 1989), however, during the differentiation, the shape of apical surface of the SPCs from *P. rapae* (Yoshida e Aoki, 1989) and *Manduca sexta* (Nardi e Magee-Adams, 1986) become proximodistally elongated, while those of *H. erato phyllis* remain circular.

At the molecular level, Reed (2004) analyzed the role of Notch, a family of transmembrane proteins, in adjusting parallel lines of SPCs in *H. erato petiverana.* The high concentration of Notch in the GECs membranes confers anti-adhesive properties between GECs and SPCs, so that the SPCs never come into contact with each other, and are kept aligned by the surrounding GECs.

In Lepidoptera, the parallel arrangement of scales is considered a derived trait, basically present in butterflies and skippers. In lower moths the SPCs are distributed randomly (Nijhout, 1991), which suggests that the evolution of the cellular organization played a major role in the divergence of color patterns in lepidopterans. Furthermore, there is a cryptic variation in the way by which the SPCs of different species are arranged in lines. In *H. erato phyllis* (Fig.5D)*, H. erato petiverana* (Reed, 2004) and *Junonia coenia* (Nijhout, 1991), lines are already specified at the beginning of the SPCs differentiation, which occurs *in situ*. In *P. rapae*, however, the SPCs differentiation takes place in a disordered manner and hours later they are organized in lines (Honda *et al*., 2000). In

Manduca sexta, Nardi and Magee-Adams (1986) observed that the SPCs initially randomly distributed are aligned by cell migration.

Approximately 60 h, the sockets, structures that support the scales, arise oriented in the proximodistal direction (Fig.5E). About 72 h, the finger-like processes (“protoscales”) appear asynchronically and soon flatten out (Fig.5F) extending in proximodistal direction on the wing surface. About 96 h after pupation, when the wing does not show evidence of pigment deposition, immature scales predominate on the wing surface (Fig.5G). The immature scales (Fig.5G) can be distinguished from the mature ones (Fig.5H) since they collapse after the critical point, while the mature ones remain intact.

In late *Pre-ommochrome* stage, approximately 120 h, the forewing red-fated scales (Fig.2B, 6A) and the hindwing yellow-fated scales (Fig.2C, 6B) become mature compared to the black and silvery/brownish-fated scales. In *Ommochrome Only* stage (Fig.2D-F), approximately 124 h after pupation the silvery/brownish-fated scales remain immature. On the dorsal surface of hindwing (Fig.7), the acute scales, which are of type I, like white and yellow scales, are immature. The maturation, as well as the pigmentation of the scales from the silvery/brownish surfaces occurs together with the black scales in the *Melanin* stages.

Nijhout (1980) proposed two models for the development of the color patterns in butterfly wings. Both assume that the substrates for pigment synthesis circulate in the hemolymph and are produced in sequence. The model I assumes that all enzymes are present in all scales, and the maturity of the scales determines the definition of color, since it may allow or not access of a certain substrate to a certain enzyme. In model II, the substrates for pigment synthesis have free access to all scales, independent of being mature or not, but a scale fated to show a given color has its own enzymes and can use only certain substrates.

The first model is supported by Koch *et al.* (2000) and ffrench-Constant (2012) for *Papilio glaucus*, in which the pigments vary progressively during development, according to the biosynthetic pathways, and are deposited in the scales that are at an advanced stage of maturation. In this case, the rate of scale maturation is determinant for the development of the color pattern.

Gilbert *et al.* (1988) supported the second model for the development of color patterns in *Heliconius.* To explain the developmental mechanisms responsible for the correlation between ultrastructure and pigmentation, they proposed a genetic switch mechanism coordinated by two "selector genes", M and X. These genes supposedly regulate the morphological decisions and the pigmentation pathways simultaneously. For type I scales, a null state was proposed that develops when none of the selector genes is activated in the scale precursor cells. If only gene M is activated, type II scales develop. If M and X are simultaneously activated, type III scales develop. In this model, gene X can be expressed only in cells that express gene M. Further, they assumed that for *Heliconius* any pleiotropic effect of the genes involved in the pigmentation pathways on ultrastructural development does not occur through pigment, its precursors or substrates. Probably the products of the selector genes act as activators for genes involved in scale ultrastructure and pigmentation.

Janssen *et al.* (2001) analyzed how closely connected are the developmental processes responsible for the pigmentation and microstructure in the scales of *H. melpomene*. Ectopic changes were induced in the black and red-fated scales, that is, the black-fated scales were induced to turn red and vice versa, through microcauterizations on the wings at the beginning of pupal stage. These authors observed that the color change was accompanied by a change in microstructure, suggesting a strong association between the development of both traits.

One novel finding from this study concerns the ultrastructure of scales from the silvery/brownish surfaces. Because these scales are pigmented with melanin, our initial hypothesis was that ultrastructure would be of a single type. The finding that the scales belonging to the silvery/brownish surfaces show three/two types suggests that in those surfaces there is no correlation between pigmentation and ultrastructure, as different ultrastructural types were found there. This finding came as a surprise, since the types I and III by Gilbert *et al.* (1988) are correlated, respectively, to the pathways for 3-OHK (or absence of pigment) and dihydroxanthommatine pigments.

In *H. erato phyllis*, the maturation of type I-scales do not show relationship with the time of 3-OHK deposition in the yellow scales. On the other hand, the maturation timing also do not show relationship with the scale ultrastructure, given that scales ultrastructurally similar become mature in different times, as in the case of type I and III scales from the silvery/brownish *vs.* yellow and red areas. By this, we mean that the pigmentation pathways of scales have a more predominant influence on the scale maturation than the ultrastructure pathways. Possibly the biosynthetic pathways of pigments are pleiotropically associated with scale maturation.

The fact that the red-fated scales become mature before the pigmentation, in *Pre-ommochrome* stage, reveals that the pigment deposition is not the responsible for the stiffness of the scales. Probably the early events in the pigment synthesis are implicated in sclerotization of scales. This reinforces the particular way by which the yellow bar develops, both from the biochemical (non *in situ* synthesis of 3-OHK) and heterochronic (early maturation of the scales compared to the late deposition of pigment) standpoint. It should be stressed that the yellow color plays an important role in *Heliconius* mimicry (Gilbert, 2003), as well as for the evolution of courtship behavior (Klein e Araújo, 2010).

The analysis of *H. erato phyllis* scale morphogenesis, as well as the scales ultrastructure and maturation timing, including the scales from the silvery/brownish

surfaces provided new findings into the developmental architecture of color pattern in *Heliconius*, beyond that for the aposematic colors. Furthermore, the present study could help future molecular approaches seeking to understand the evolution of butterfly color pattern.

Acknowledgements

We thank to our colleagues of the Ecological Genetics Laboratory for their help in collecting butterflies and daily feeding the caterpillars. Thanks are also due to two anonymous reviewers for their excellent suggestions. Scanning electron microscopy was performed at the Electronic Microscopy Center from the Federal University of Rio Grande do Sul, Porto Alegre, Brazil. Thanks are also due to the Conselho Nacional de Desenvolvimento Científico e Tecnológico, CNPq, for financial support and for a doctoral scholarship to the first author.

References

Beldade, P. and Brakefield, P.M., 2002. The genetics and evo–devo of butterfly wing patterns. Nature Reviews 3, 442-452.

Benson, W.W., 1972. Natural selection for Müllerian mimicry in *Heliconius erato* in Costa Rica. Science 76, 936-939.

Brown Jr., K.S., 1979. Ecologia geográfica e evolução nas florestas neotropicais. PhD dissertation. Universidade Estadual de Campinas, Campinas.

Crane, J., 1955. Imaginal behavior of a Trinidad butterfly, *Heliconius erato hydara* Hewitson, with a special reference to the social use of color. Zoologica 40, 167-196.

Ferguson, L.C and Jiggins, C.D., 2009. Shared and divergent expression domains on mimetic *Heliconius* wings. Evolution and Development 11, 408-512.

ffrench-Constant, R.H., 2012. Butterfly wing colours and patterning by numbers. Heredity 108, 1-2.

Ghiradella, H., 1984. Structure of iridescent lepidopteran scales: variations on several themes. Annals of the Entomological Society of America 77, 637-645.

Gilbert, L.E., Forrest, H.S., Schultz, T.D. and Harvey, D.J., 1988. Correlations of ultrastructure and pigmentation suggest how genes control development of wing scales of *Heliconius* butterflies. Journal of Research on the Lepidoptera 26, 141-160.

Gilbert, L.E., 2003. Adaptive novelty through introgression in *Heliconius* wing patterns: evidence for a shared genetic “toolbox” from synthetic hybrid zones and a theory of diversification. In: Boggs, C.L., Watt, W.B. and Ehrlich, P.R. (Eds.), Butterflies: ecology and evolution taking flight. The University of Chicago Press, Chicago, pp. 281-318.

Hines, H.M., Papa, R., Ruiz, M., Papanicolaou, A., Wang, C., Nijhout, H.F., McMillan, W.O. and Reed, R.D., 2012. Transcriptome analysis reveals novel patterning and pigmentation genes underlying *Heliconius* butterfly wing pattern variation. BMC Genomics 13: 288.

Honda, H., Tanemura, M. and Yoshida, A., 2000. Differentiation of wing epidermal scale cells in a butterfly under the lateral inhibition model – appearance of large cells in a polygonal pattern. Acta Biotheoretica 48, 121-136.

Janssen, J.M., Monteiro, A. and Brakefield, P., 2001. Correlations between scale structure and pigmentation in butterflies wings. Evolution and Development 3, 415-423.

Jiggins, C.D., Naisbit, R.E., Coe, R.L. and Mallet, J., 2001. Reproductive isolation caused by colour pattern mimicry. Nature 411, 302-305.

Jiggins, C.D., Mavarez, J., Beltrán, M., McMillan, W.O., Johnston, J.S. and Bermingham, E., 2005. A genetic linkage map of the mimetic butterfly *Heliconius melpomene*. Genetics 171, 557–570.

Joron, M., Jiggins, C.D., Papanicolaou, A. and McMillan, W.O., 2006. *Heliconius* wing patterns: an evo-devo model for understanding phenotypic diversity. Heredity 97, 157–167.

Kapan, D.D., 2001. Three-butterfly system provides a field test of Müllerian mimicry. Nature 409, 338-340.

Kapan, D.D. *et al.*, 2006. Localization of Müllerian mimicry genes on a dense linkage map of *Heliconius erato*. Genetics 173, 735–757.

Klein, A.L. and Araújo, A.M., 2010. Courtship behavior of *Heliconius erato phyllis* (Lepidoptera, Nymphalidae) towards virgin and mated females: conflict between attraction and repulsion signals? Journal of Ethology 28, 409–420.

Koch, P.B., Lorenz, U., Brakefield, P.M. and ffrench-Constant, R.H., 2000. Butterfly wing pattern mutants: developmental heterochrony and co-ordinately regulated phenotypes. Development Genes and Evolution 210, 536-544.

Langham, G.M., 2004. Specialized avian predators repeatedly attack novel color morphs of *Heliconius* butterflies. Evolution 58, 2783-2787.

Mallet, J. and Barton, N.H., 1989. Strong natural selection in a warning colour hybrid zone. Evolution 43, 421-431.

McMillan, W.O., Monteiro, A. and Kapan, D.D., 2002. Development and evolution on the wing. Trends in Ecology and Evolution 17, 125-133.

Monteiro, A., Glaser, G., Stockslager, S., Glansdorp, N. and Ramos, D., 2006. Comparative insights into questions of lepidopteran wing pattern homology. BMC Developmental Biology 6, 1 -13.

Naisbit, R.E., Jiggins, C.D. and Mallet, J., 2003. Mimicry: developmental genes that contribute to speciation. Evolution & Development 5, 269–280.

Nardi, J.B. and Magee-Adams, S.M., 1986. Formation of scale spacing patterns in a moth wing. I. Epithelial feet may mediate cell rearrangement. Developmental Biology 116, 278-290.

Nijhout, H.F., 1980. Ontogeny of the color pattern on the wings of *Precis coenia* (Lepidoptera: Nymphalidae). Developmental Biology 80, 275-288.

Nijhout, H.F., 1991. The development and evolution of butterfly wing patterns. Smithsonian Institution Press, Washington.

Papa, R., Morrison, C.M., Walters, J.M., Counterman, B.A., Chen, R., Halder, G., Ferguson, L., Chamberlain, N., ffrench-Constant, R., Kapan, D.D., Jiggins, C.D., Reed, R.D. and McMillan, W.O., 2008. Highly conserved gene order and numerous novel repetitive elements in genomic regions linked to wing pattern variation in *Heliconius* butterflies. BMC Genomics 9, 345–360.

Prum, R.O., Quinn, T. and Torres, R.H., 2005. Anatomically diverse butterfly scales all produce structural colours by coherent scattering. The Journal of Experimental Biology 209, 748-765.

Reed, R.D., 2004. Evidence for Notch-mediated lateral inhibition in organizing butterfly wing scales. Development Genes and Evolution 214, 43-46.

Reed, R.D., Mcmillan, W.O. and Nagy, L.M., 2008. Gene expression underlying adaptive variation in *Heliconius* wing patterns: non-modular regulation of overlapping *cinnabar* and *vermilion* prepatterns. Proceedings of The Royal Society B 275, 37–45.

Reed e*t al.*, 2011. *optix* drives the repeated convergent evolution of butterfly wing pattern mimicry. Science 333, 1137-1141.

Smith, K.K., 2003. Time's arrow: heterochrony and the evolution of development. International Journal of Developmental Biology 47, 613-621.

Yoshida, A. and Aoki, K., 1989. Scale arrangement pattern in a lepidopteran wing. 1. periodic cellular pattern in the pupal wing of *Pieris rapae.* Development Growth and Differentiation 31, 601-609.

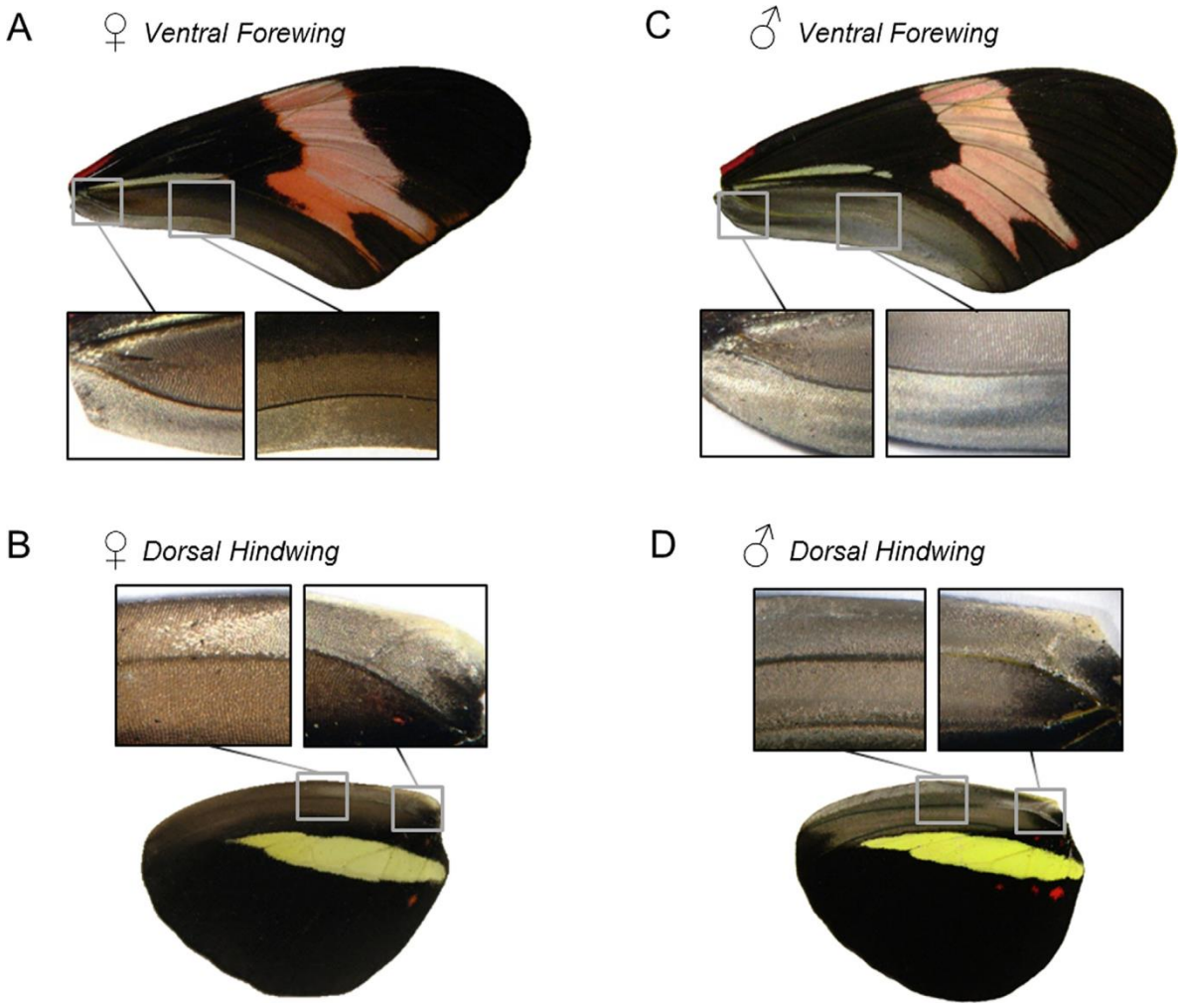

Fig. 1. Silvery/brownish surfaces on the wings of *H. erato phyllis*. In females, the silvery surface on the ventral forewing (A) is located at the inferior limit of the proximal area (left zoom area) and extends halfway the distal margin (right zoom area), where the surface is progressively becoming brownish. On the dorsal hindwing (B) the silvery surface is located on the superior limit of the proximal area (right zoom area) and extends halfway the distal margin (left zoom area). In males the silvery surface is uniformly distributed at the inferior area of the forewing (C, details in zoom areas), as well as at the superior area of the hindwing (D, details in zoom areas). The left fore and hindwings of the female and male were removed from the same individuals.

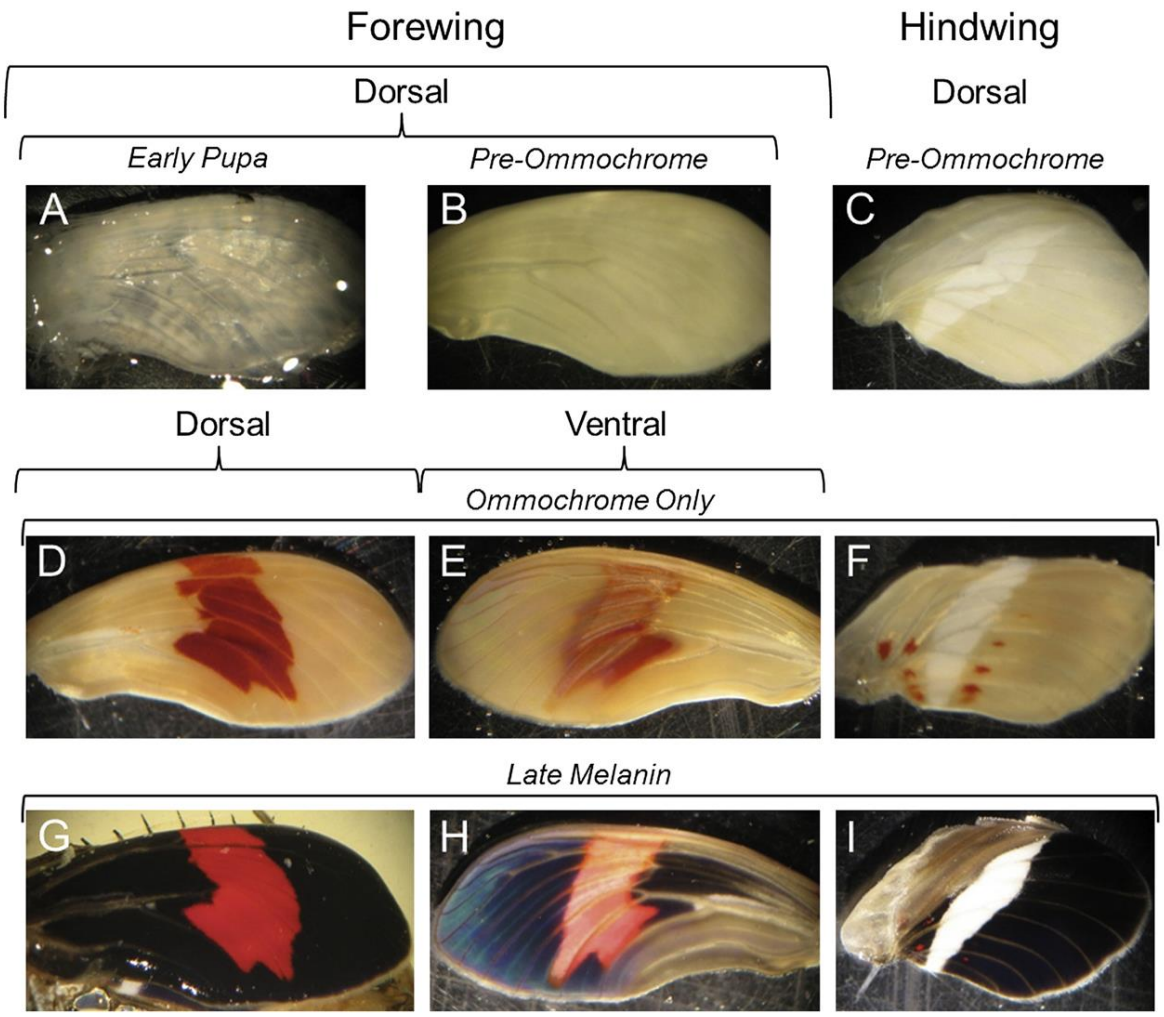

Fig. 2. Ontogeny of the color pattern in *H. erato phyllis* wings. First row: In (A) *Early Pupa* stage, the wing shows a semitransparent tissue. In early *Pre-ommochrome* stage, the wing has an opaque cream color and do not show pigmentation (not shown). In late *Pre-ommochrome* stage, the (B) red-fated scales on the dorsal forewing appear slightly clearer than the opaque cream color, while (C) the yellow-fated scales on the hindwing become white. Second row: In *Ommochrome Only* stage, red-fated scales go on progressively darkening from orange (not shown) to (D) red; on the ventral surface of this wing, (E) the red scales are less intense. (F) In hindwing, the yellow-fated scales remain unpigmented. Third row: In the *Melanin* stages, (G) black scales become pigmented, as well as the scales on the silvery/brownish surfaces (only silvery surfaces of males are shown) at the (H) ventral forewing and (I) dorsal hindwing. The pigmentation of the yellow-fated scales occurs within a few hours before adult emergence. From second to third row, each column shows the respective ontogenetic development.

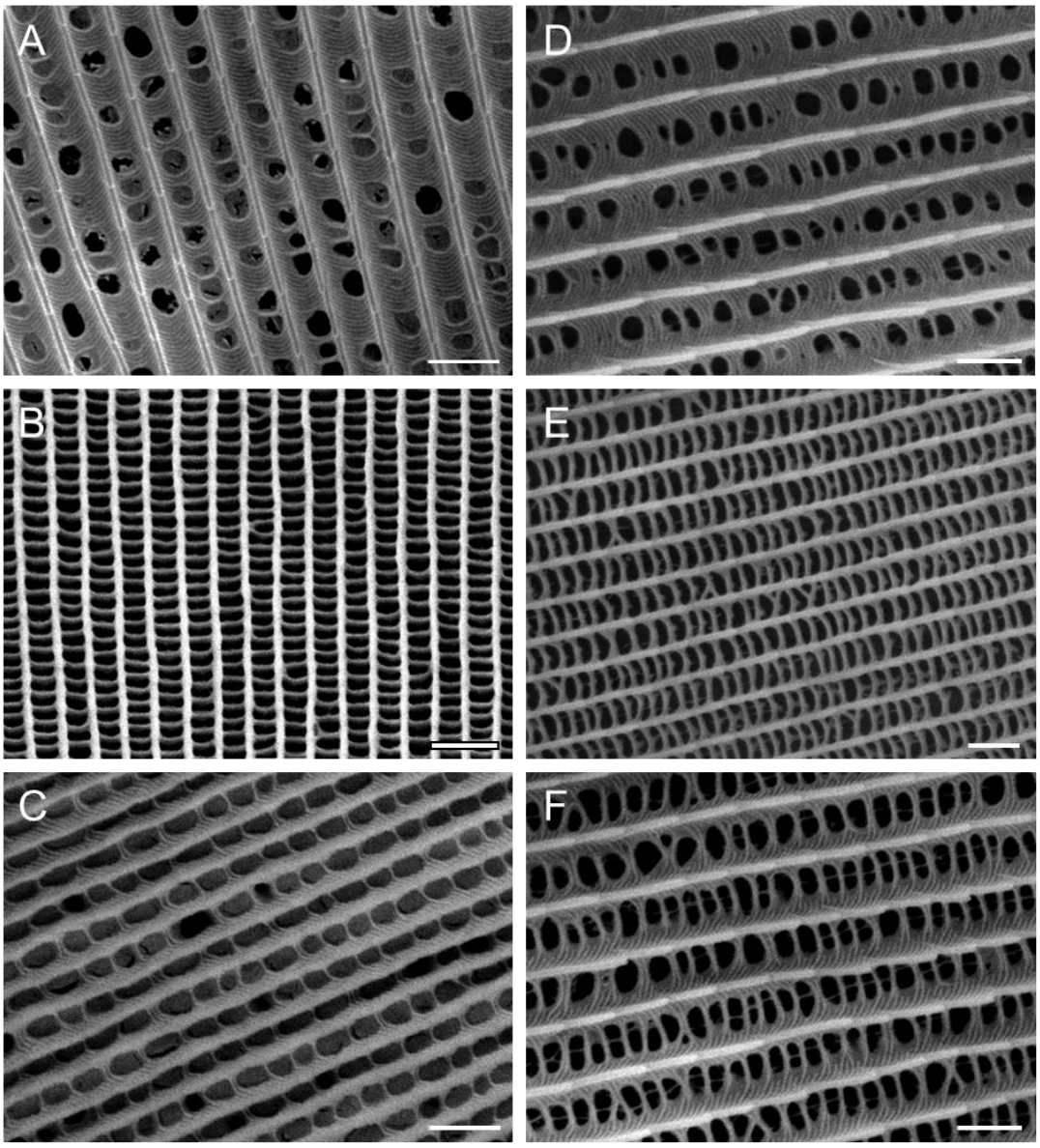
A
D
B
E
C
F

Fig. 3. Ultrastructure of the scales in *H. erato phyllis* male wings. Upper surface of a (A) yellow scale - type I, (B) black scale - type II and (C) red scale - type III. (D-F) Upper surface of the scales situated on the male silvery surface, matched to types I, II, and III-scales. Note the microstructural similarity between: (A) *vs.* (D), (B) *vs.* (E) and (C) *vs.* (F). (D) In a scale similar to type I, between the longitudinal ridges, there is an obverse membrane permeated with windows of different sizes. In the scale lumen, there are trabeculae supporting the obverse membrane. (E) In a scale similar to type II occurs ladder-like crossribs, which are narrower than the longitudinal ridges and are supported by trabeculae. (F) In a scale similar to type III there is an obverse membrane retained immediately adjacent to longitudinal ridges and the crossribs are supported by trabeculae. Bars = 2 µm.

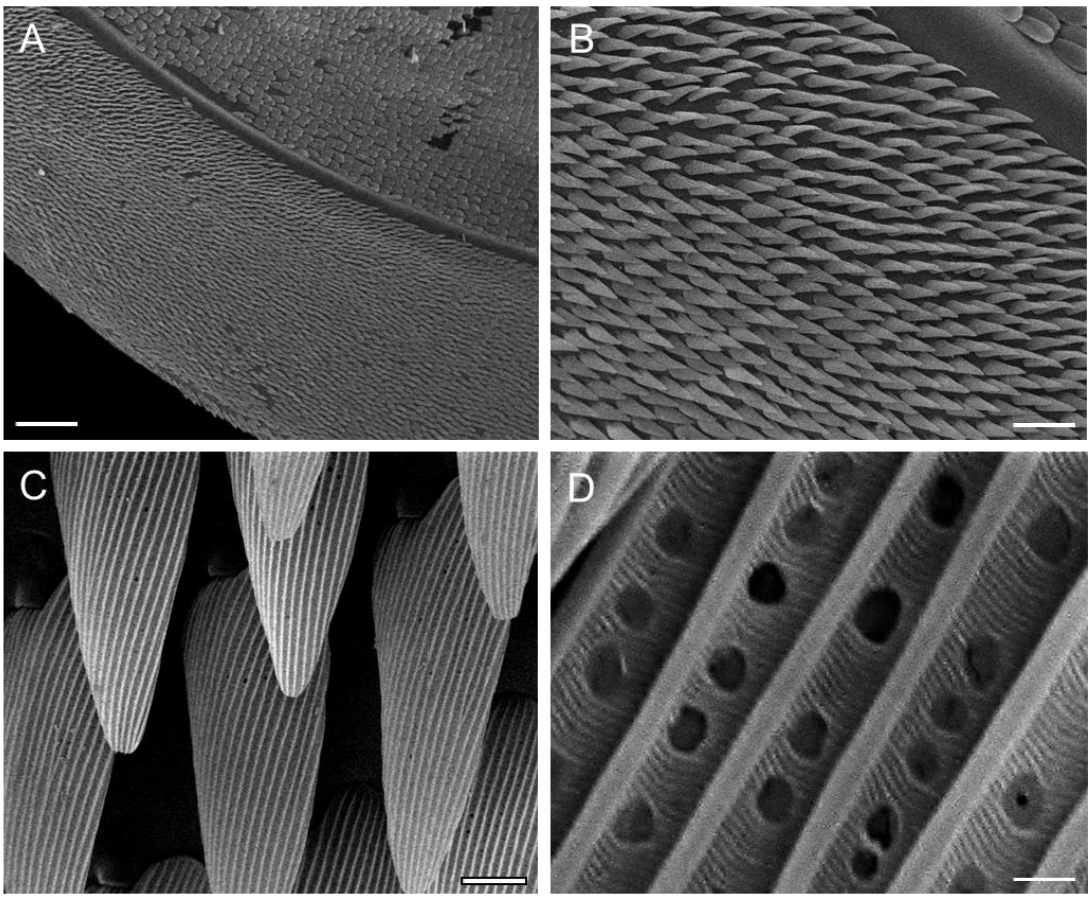

Fig. 4. Acute scales located on the (A) inferior limit of the silvery surface in *H. erato phyllis* adult forewing. (B-C) The shape of the acute scales and (D) the ultrastructure of an acute scale, characterized by the presence of an obverse membrane permeated with windows. Note the similarity with the type I-scales, shown in Fig.2A, D. Bars = 500 µm, 100 µm, 10 µm, 1 µm, respectively.

Table 1. Comparative description of the scale types of *H. erato phyllis.*

Color / wing region	Scale type	Obverse membrane	Crossribs	Trabeculae
Yellow	I	Present between the longitudinal ridges. Windows of different sizes occur, especially in the central region of the scales.	Absent.	Not seen below the obverse membrane.
Black	II	Absent.	Present. Ladder-like alignment. They are narrower than the longitudinal ridges.	Present below the crossribs.
Red	III	Present immediately adjacent to longitudinal ridges and over each crossrib.	Present. They are thicker and show a more angular aspect than the type II crossribs.	Not seen below the crossribs.
Silvery both in males and females (region of the acute scales)	I	Equal to type I	Equal to type I	Equal to type I
Silvery only in males	I	Equal to type I	Equal to type I	Present below the obverse membrane.
Silvery only in males and brownish in females	II	Equal to type II	Equal to type II	Equal to type II
	III	Equal to type III	Equal to type III	Present below the crossribs.

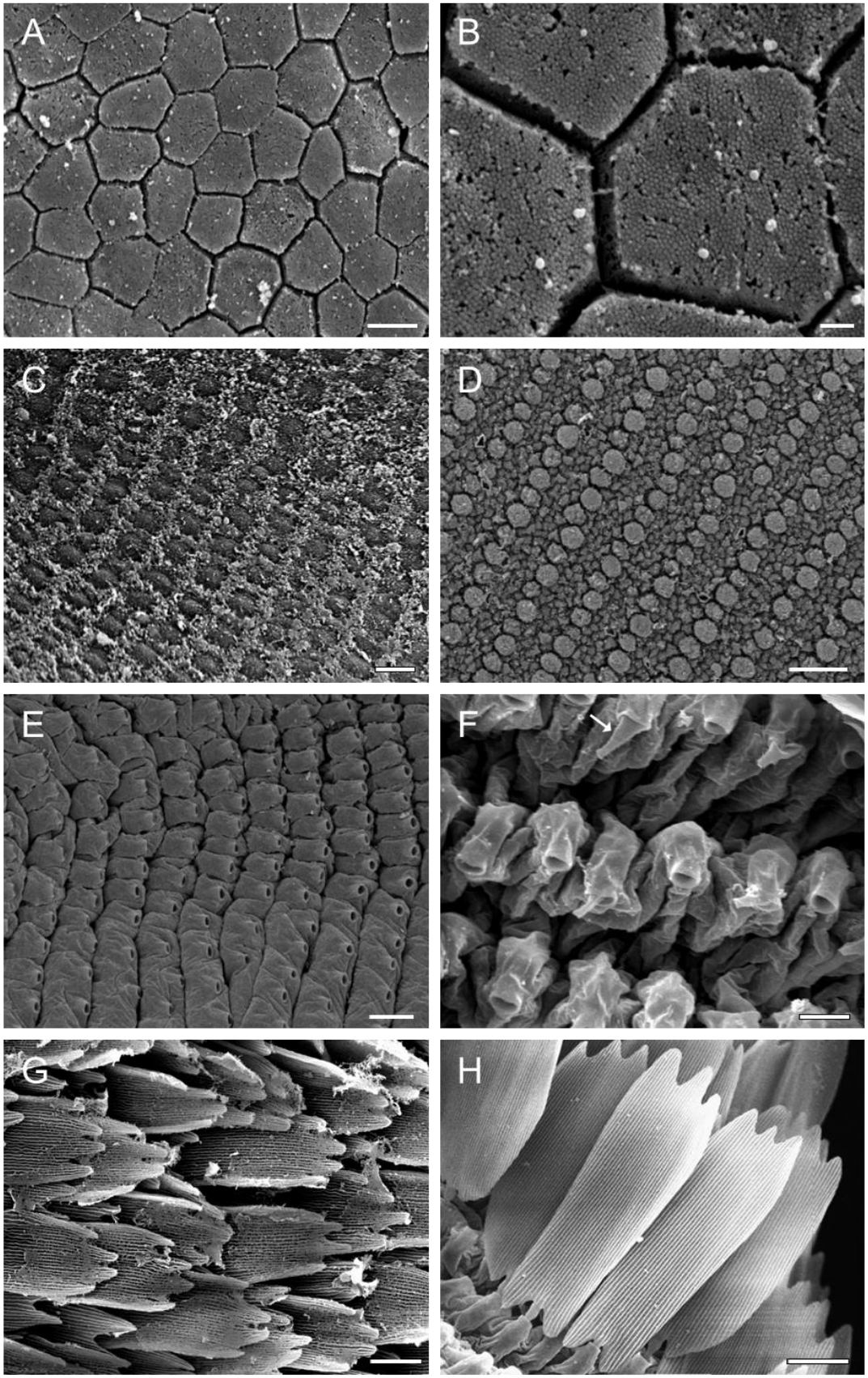
A
B
C
D
E
F
G
H

Fig. 5. Morphogenesis of *H. erato phyllis* scales throughout the pupal development. (A) In *Early Pupa* stage, the wing surface shows a polygonal pattern, consisting of undifferentiated epithelial cells, whose (B) apical surfaces are full of microvillosities. (C) The scale precursor cells begin the differentiation becoming circular and bigger than the general epithelial cells. The differentiation occurs in parallel lines. (D) In early *Pre-ommochrome* stage, the scale precursor cells, arranged in parallel lines, become higher than the general epithelial cells. (E) The sockets arise oriented in the proximodistal direction. (F) Finger-like processes (arrow) are asynchronically projected from the sockets and soon flatten out, originating the (G) scales that are progressively sclerotized. (H) Mature scales. Bars = 5 µm, 1 µm, 20 µm, 20 µm, 20 µm, 10 µm, 20 µm, 20 µm, respectively.

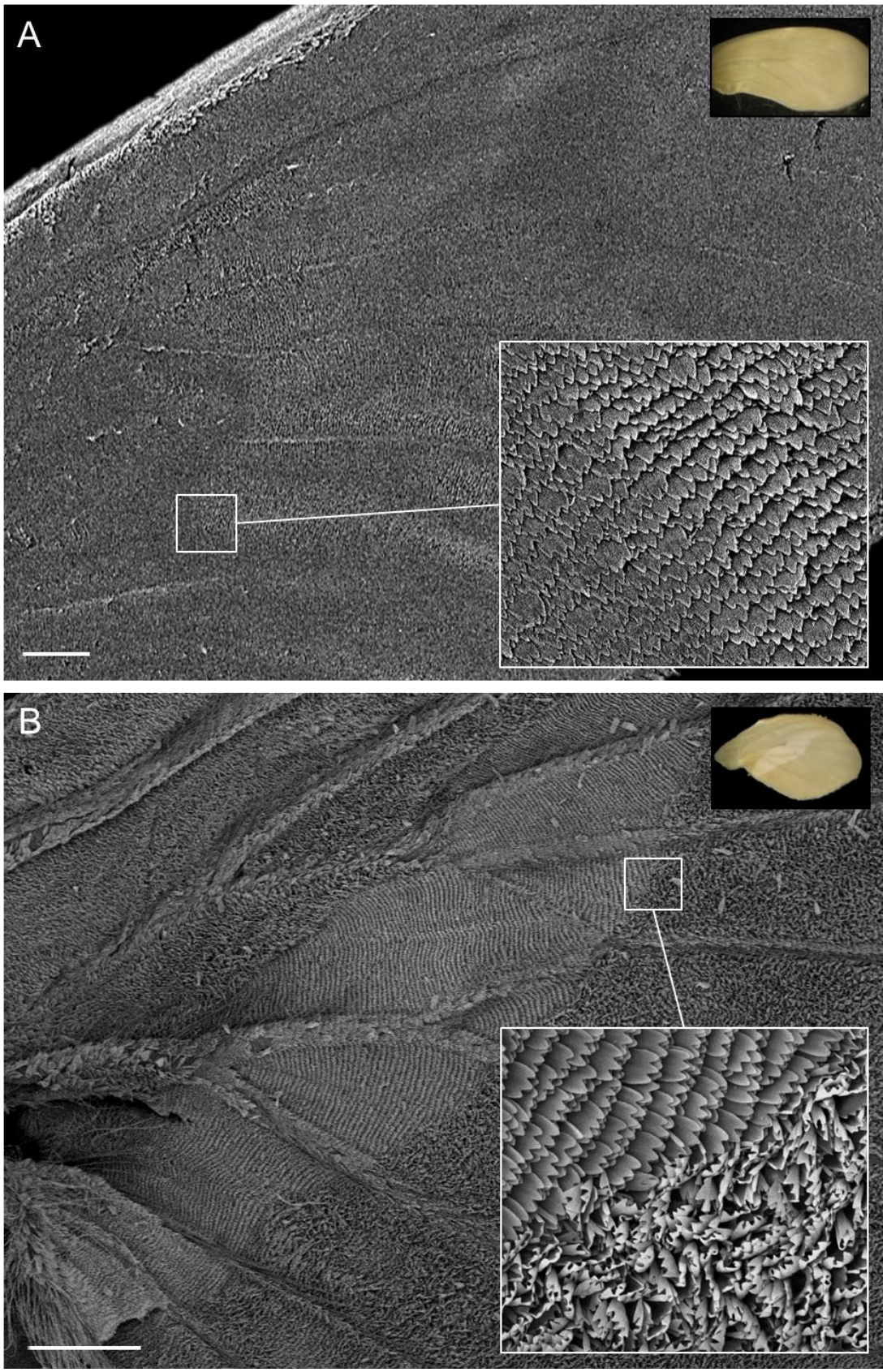
A
B

Fig. 6. Dorsal surface of *H. erato phyllis* fore and hindwing in late *Pre-ommochrome* stage (details in color). (A) In the forewing, the red-fated scales are mature in relation to the black-fated scales. Note the red patch delimitation. Zoom area: Boundary area between red-fated scales, on the right, and black-fated, on the left. (B) In the hindwing, the yellow-fated scales are mature in relation to the black-fated scales. Note the yellow bar delimitation. Zoom area: Boundary area between the yellow-fated scales, on the left, and the black-fated scales, on the right.

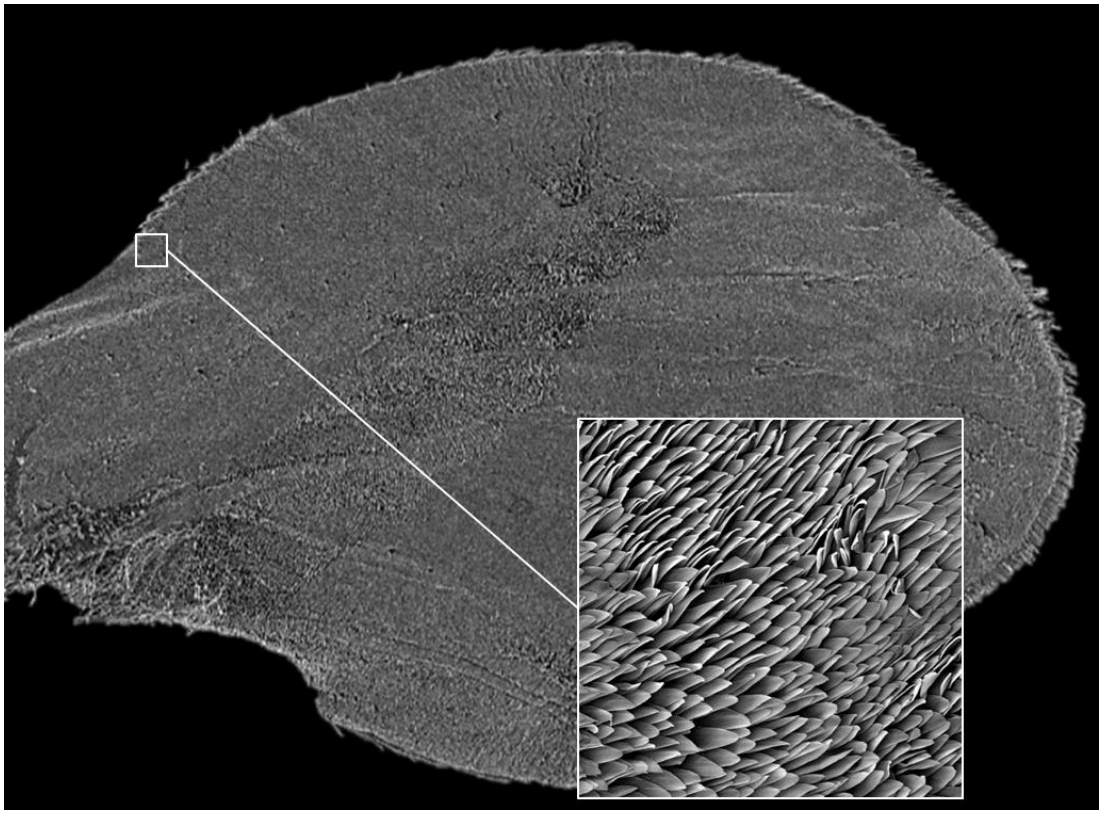

Fig. 7. Dorsal hindwing of *H. erato phyllis* in *Ommochrome Only* stage. Note in the superior area (the place of the silvery-fated scales), the absence of mature scales comparatively to the yellow-fated scales which are mature, as shown in figure 5B. Zoom area: Immature acute silvery-fated scales.

CAPÍTULO 4

The fifth-instar wing disc of *Heliconius erato phyllis* (Lepidoptera: Nymphalidae): New findings into the developmental architecture of the *Heliconius* wings

Ana Carolina Bahi Aymone[1], Nívia Lothhammer[2], Vera Lúcia da Silva Valente[1,3], Aldo Mellender de Araújo[1,3]

[1] Post-Graduate Program of Genetics and Molecular Biology, Federal University of Rio Grande do Sul, Porto Alegre, Brazil. Av. Bento Gonçalves 9500, C.P. 15053, 91501-970, Porto Alegre, RS.

[2] Department of Morphological Sciences, Federal University of Rio Grande do Sul, Porto Alegre, Brazil. St. Sarmento Leite, 500, 90050-170, Porto Alegre, RS.

[3] Department of Genetics, Federal University of Rio Grande do Sul, Porto Alegre, Brazil. Av. Bento Gonçalves 9500, C.P. 15053, 91501-970, Porto Alegre, RS.

Manuscrito em preparação para ser submetido à revista ***Evolution & Development***

Abstract

Although the color prepatterning in *Heliconius* wings is being studied by molecular approaches, the ultrastructural basis that explains how the wings develop is still unclear. Here we analyzed by electron microscopy the fifth-instar wing disc of *Heliconius erato phyllis*. The regions comprising the wing primordium, the peripheral tissue, and the peripodial membrane were described. The wing primordium showed two columnar epithelial monolayers (dorsal and ventral) with microvilli in their apical surfaces. The cytoplasm of the columnar cells showed a large amount of rough endoplasmic reticulum, suggesting intense protein synthesis activity, which possibly is involved in cell prepatterning and differentiation. From the basal regions of the dorsal and ventral epithelia, translumenal processes are extended; this suggests that the differentiation of the scale precursor cells starts before pupation. The peripheral tissue showed little cellular organization, and many vesicles were observed being released from this tissue into the peripodial cavity; possibly, the vesicles are involved in the apoptotic process of the peripheral tissue. The peripodial membrane showed a squamous epithelium, which showed microvilli only near to the peripheral tissue, suggesting that the peripodial epithelium could be involved in the absorption of apoptotic residuals. The ultrastructure of the larval wing disc of *H. erato phyllis* provided a glimpse into the mechanisms involved in the *Heliconius* wing development, as well as in the evolution of butterfly wings.

Introduction

The development of the *Heliconius* wings is an emergent model for studying the genetic control of the intraspecific divergence and interspecific convergence of color patterns (Joron et al. 2006). In *Heliconius* larvae, a pair of meso- and meta-thoracic imaginal discs located on either side of the larvae gives rise to the corresponding fore- and hindwings of the adults. The genetic control of color prepatterning, as well as the prototype of the vein pattern, are already established in the larval wing discs (Reed and Serfas 2004; Martin et al. 2012).

While molecular studies have been performed on the color prepatterning and subsequent scale pigmentation in *Heliconius* (e.g., Reed et al. 2008; Ferguson and Jiggins 2009; Reed et al. 2011; Hill et al. 2012; Hines et al. 2012; Martin et al. 2012), little is known about the histological basis of this process. Aymone et al. (2013) studied the *Heliconius erato phyllis* pupal wing morphogenesis, at ultrastructural level, providing a structural glimpse into the developmental architecture of color pattern in *Heliconius*. However, the ultrastructure of the *Heliconius* larval wing discs is unknown in the literature.

The lepidopteran wing discs arise as epithelial sacs, which are attached to the surface by a thin pedicel and held in position by tracheal connectives (Fig.1A). The wing discs remain relatively small until the fifth (and final) larval instar, at which time they start growing rapidly as tracheae ingress from the base of the discs, between the epithelial layers, to form the wing vein precursors (Nijhout 1991; Fig.1). The proximal-distal and dorsal-ventral spatial relationships are retained throughout development and correspond to the spatial pattern of the adult wings (Nijhout 1991). However, in *Drosophila*, a classical model in evo-devo, the presumptive dorsal and ventral surfaces of the larval wing discs are adjacent to one another, such that the axis specification occurs in an epithelial monolayer (Fristrom et al. 1993; Nardi 1994). During pupation, this monolayer everts,

folding back on itself to form a bilayer which then represents the dorsal and ventral surfaces of the adult wing. This movement involves coordinated cell reorientations, cell shape changes, cell adhesion and cell–cell signaling modifications (Pastor-Pareja et al. 2004).

The bud-like mode of the lepidopteran wing development is probably ancestral in holometabolous insects, as it resembles the development of larval wing primordium in coleopterans and hymenopterans (Quennedey and Quennedey 1999; Abouheif and Wray 2002; Sameshima et al. 2004; Tomoyasu et al. 2005). However, there is one feature that is possibly unique to Lepidoptera, namely, the differentiation and eventual degradation of the ‘‘peripheral tissue’’ (Fig.1) around the developing wing margin (Dohrmann and Nijhout 1988; Kodama et al. 1995). In early fifth-instar wing discs, before tracheal ingression, a border lacuna forms roughly parallel to the margin of the wing primordium. Tracheae invade this lacuna late in fifth-instar larval development (Miner et al. 2000); and after pupation, the peripheral tissue between the border lacuna and the edge of the pupal wing epithelium undergoes apoptosis (Kodama et al. 1995). The peripheral tissue is considered an evolutionary novelty in lepidopteran wing development, as it permitted a decoupling of wing margin and dorsoventral boundary determination. This decoupling, in turn, may have been responsible for the rapid and radical butterfly wing shape diversification, as it released the wing margin from various constraints of larval and pupal wing development (Mcdonald et al. 2010). Thus, the wing margin is flanked by two relatively independent boundaries and presents a useful case study for how novel developmental boundaries originate and facilitate subsequent morphological diversification.

Beyond these boundaries, there is another boundary whose functional connection (or disconnection?) is unknown in lepidopteran wing disc development, namely, the limit between the disc proper and the peripodial membrane. The peripodial membrane surrounds the wing disc, and binds to the outer epithelium (the same which originates the

wing disc proper) of the larva (Nijhout 1991). Studies in *Drosophila* have demonstrated that during development, peripodial cells signal to disc cells via microtubule-based apical extensions, and contribute to growth control and pattern formation in the wing and eye primordia (Cho et al. 2000; Gibson and Schubiger 2000, 2001). These findings challenged the traditional view of *Drosophila* discs as monolayers and provided foundational evidence for peripodial cell function in *Drosophila* appendage development.

In order to gain a better understanding of the *Heliconius* wing disc specification, we analyzed by electron microscopy the ultrastructure of the fifth-instar wing disc of *Heliconius erato phyllis*; and, specifically, the peripodial membrane/wing primordium and peripodial membrane/peripheral tissue boundaries. Does the peripodial membrane contribute for the *Heliconius* wing development?

Materials and Methods

Egg-laying butterflies were captured in natural populations around the city of Porto Alegre (30º01'59"S, 51º13'48"W), State of Rio Grande do Sul, Southern Brazil, and transferred to open air insectaries at the Genetics Department of the Federal University of Rio Grande do Sul. Each unit of the insectaries measured 2 x 3 x 3 m with seminatural conditions and with hostplants (*Passiflora misera*, mainly). Butterflies were fed daily with a mixture of honey: water: pollen that was substituted every morning. After oviposition, eggs were collected and brought to the laboratory, where they were transferred to Petri dishes with humid filter paper, controlled temperature and photophase (25 ± 1ºC; 14 h/light/day).

For light microscopy, fifth-instar larvae were fixed in Bouin's solution and washed in 70% ethanol. The wing discs were removed from larvae and dehydrated in ethanol series, diaphanized, embedded in resin, sectioned (3 µm), and stained with toluidine blue.

For scanning electron microscopy, the larvae were fixed in glutaraldehyde. The wing discs were removed, washed in PBS buffer, dehydrated in a ketonic series, submitted to a critical point dryer (BALTEC®CPD-030), mounted on metal stubs with double-sided carbon tape, metalized with an approximately 15 nm gold layer (BAL-TEC ®SCD-050), and observed under a scanning electron microscope (JEOL®JSM-6060), at 10 kV.

For transmission electron microscope, the larvae were fixed in Karnowisky, postfixed in osmium tetroxide 2%, washed in PBS buffer, dehydrated in a ketonic series, embedded and included in resin (EMBED Epon 812). Ultramicrotomy was performed in LEICA®ULTRACUT UC7 ultramicrotome, with 100 nm sections, which were deposited on copper grids (200 mesh), contrasted with uranyl acetate and lead citrate, and observed under a transmission electron microscope (JEM®1200EXII).

To facilitate the description of the tissue boundaries, we mean that wing disc is equal to wing primordium more peripheral tissue; and, in relation to the peripodial membrane, the wing primordium and peripheral tissue correspond to the ‘wing disc proper’.

Results

In early fifth-instar, a larger trachea, next to the wing disc, branches off originating multiple tracheoles (Fig.2A). Initially, the tracheoles show a chaotic aspect, as they form a tangly near the basis of the wing disc (Fig.2A, C). The branched tracheae invade the basis of the wing disc at the ventral region (Fig.2C, D), and ingress into the vein lacunae preformed into the wing primordium, between the dorsal and ventral epithelial layers (Fig.2B). The peripodial membrane surrounds the wing disc proper (Fig.2C).

The wing disc surface is demarcated by the bordering lacuna which delimits the wing primordium and the peripheral tissue (Fig.2E). The vein lacunae form grooves on the

surface of the wing primordium (Fig.2E), and flow into the bordering lacuna. At this stage, the wing primordium and the peripheral tissue occupies, each one, approximately half of the wing disc. The distal extremity of the peripheral tissue is more angular, and the distance between the bordering lacuna and the peripheral tissue is larger at the imaginary central line of the proximodistal axis (Fig.2E). As the hours go by, the tracheoles are progressively oriented into the wing primordium, such that they show different angles of orientation (Fig.2F, G).

In the middle fifth-instar, the wing primordium grows considerably, and now occupies more than half of the wing disc (Fig.2H). The peripheral tissue, in turn, reduces proportionally, now occupying a narrow margin around the wing primordium. The angular aspect of the peripheral tissue is attenuated, such that the relative distances between the bordering lacuna and peripheral tissue, around the wing primordium, become less discrepant (Fig.2H) compared to the early fifth-instar (Fig.2E), wherein the peripheral tissue is more prominent at the imaginary central line of the proximodistal axis.

Histologically, in transversal sections, the wing primordium is formed by two columnar epithelial monolayers. In each monolayer, the cytoplasm zones occupy mostly the apical region of the columnar cells (Fig.3A, B), while the nuclei occupy mostly the intermediate and basal regions (Fig.3D). The apical surface of the wing primordium shows microvilli directed to the apical surface of the peripodial membrane (Fig.3A, B). The columnar epithelial cells are connected by tight junctions (Fig.3C). The apical region of the columnar cells is full of rough endoplasmic reticulum (Fig.3C), while the intermediated and basal regions show large amount of mitochondria (Fig.3E, F). In the intermediate and basal regions, the nuclei occupy many levels along the apical-basal axis (Fig.3D), and due to this, the epithelia of the wing primordium appear pseudostratified. From the basal regions of the dorsal and ventral epithelia, thin basal processes are extended into the disc lumen (Fig.3G, H); and, at the interface situated in the middle of the disc lumen, the

extremities of the basal ends from the dorsal and ventral epithelia merge (Fig.3J). A large extracellular space separates the basal surfaces of both monolayers. Phagocytes are eventually found dispersed within the disc lumen (Fig.3I).

As for the peripheral tissue, it shows little cellular organization, and, unlike the wing columnar epithelium, it does not show microvilli (Fig.4A, B). The surface of the peripheral tissue is irregular, and many vesicles are released from the apical surfaces of the peripheral tissue into the peripodial cavity (Fig.4A, C, D).

The peripodial epithelium shows squamous cells (Fig.4A). The cytoplasm of the peripodial cells occupy large areas which extend laterally; the nuclei occupy different areas within the cells (Fig.3A; 4A). The cuticle is immediately above the peripodial membrane (Fig.4A), and in some areas between the cuticle and peripodial epithelia, many vesicles are present (Fig.4E). Near to the peripheral tissue, the apical surface of the peripodial epithelia shows microvilli, which are directed to the peripheral tissue (Fig.4E, F).

Discussion

The microscopic analysis of the fifth-instar wing disc of *H. erato phyllis* provided an ultrastructural glimpse on the different tissues involved in the wing development. The wing disc of *H. erato phyllis* shows ultrastructurally different tissues, which in turn are involved with different roles throughout development.

As for the wing primordium, a remarkable feature, which was observed in transversal sections of the wing disc, corresponds to the extension of long basal processes from the dorsal and ventral epithelial layers, forming translumenal extensions which merge at the middle of the lumen. Although a large extracellular space separates the basal surfaces of both monolayers, only a small portion of the basal processes maintain the junctional continuity of the two monolayers. The phagocytes observed into the

lumen disc show morphological similarity with the phagocytes observed in the haemolymph of *Bombyx mori* (Wago 1991).

In *M. sexta* pupal wing development, basal processes stretched from the epithelial layers were observed (Nardi and Ujhelyi 2001) in the same way as in *H. erato phyllis* larval wing discs. In *M. sexta* pupal wing development, the basal processes are involved in transformations of the epithelial layers. After the dorsal and ventral basal processes meet at the middle of the lumen, they become united by specialized junctions to form an epithelial bilayer; but soon, they shorten. This cellular arrangement is ephemeral, and the space separating the two monolayers widens again. These transformations in epithelial morphology change the spatial relationship of the two monolayers during *M. sexta* wing development. Nardi and Ujhelyi (2001) stress that these epithelial transformations are probably unique to invertebrates and may also represent transformations which are unique to epithelia of insect wings. Among the insects, however, cellular bilayers are the exception rather than the rule. It is interesting to note that, in *M. sexta* pupal wings, the scale precursor cells do not extend basal processes; the basal processes are extended only by the general epithelia cells. Thus, we can say that in *H. erato phyllis*, the scale precursor cells begin the differentiation already in the larval discs, as well as the pattern formation and arrangement of the wing bilayer initiate before pupation. The basal processes are important for understanding the transformations involved in the pattern formation of the butterfly wings. For the first time, the basal processes are documented in the fifth-instar wing disc of a lepidopteran species. It is noteworthy that, in *Heliconius*, changes in the relative position of the scale precursor cells fated to different colors are key for the intraspecific divergence and interspecific convergence of color patterns.

The reduction of the peripheral tissue, while the wing primordium grows, is consistent with the fact that the peripheral tissue undergoes apoptosis during the wing development (Dohrmann and Nijhout 1988; Kodama et al. 1995; Mcdonald et al. 2010).

Further, the vesicles released from the apical surfaces of the peripheral tissue possibly are due to the apoptotic process. Kodama *et al.* (1995) showed that the peripheral tissue in *Pieris rapae* pupae releases vesicles near to the periphery of the wing disc, during the apoptosis. Mcdonald et al. (2010) showed that strong Cut expression occurs in the peripheral tissue in the early and late fifth-instar butterfly wing discs. Cut is a transcription factor implicated in cell-type specification in numerous tissues (Nepveu 2001). Mcdonald et al. (2010) speculate that Cut may play some role in activating programmed cell death in this context, and infer that the association between Cut expression and wing disc margin apoptosis is a novel feature of lepidopteran development.

As for the peripodial epithelium, we observed that the apical surface shows microvilli only near the peripheral tissue; while near the columnar epithelium, the peripodial cells does not show microvilli. This suggests that, possibly, the peripodial epithelium is specified for different functions in different regions around the wing disc proper. As the peripheral tissue undergoes apoptosis throughout development (Kodama et al. 1995; Mcdonald et al. 2010), possibly the peripodial epithelium can be involved in the absorption of apoptotic residuals from the peripheral tissue.

Nardi et al. (1987) studied, at the level of transmission electron microscopy, the contraction-eversion functionality of the peripodial epithelium in the larval wing discs of *Manduca sexta*. This role also is present in the appendage primordia of other holometabolous groups, such as *Drosophila* (Gibson and Schubiger 2000). Recent studies in *Drosophila* suggest that varied signals traversing between peripodial membrane and disc proper help in growth control and pattern formation in the imaginal discs (Cho et al. 2000; Gibson and Schubiger 2001; Gibson et al. 2002; Pallavi and Shashidhara 2003, 2005). These studies suggest a functional role for peripodial cells in disc patterning apart from their role in providing mechanical support during disc eversion. Gibson and Schubiger (2000) demonstrated that during *Drosophila* development, peripodial cells form

microtubule-based translumenal extensions, which transverse the acellular space and terminate on the apical surface of developing disc columnar cells. The authors speculated that the evolutionary transition from evaginated buds to invaginated sacs, in insects, placed new demands on disc development while simultaneously creating the structural possibility for novel interactions between peripodial and columnar cells.

In *Drosophila*, the imaginal discs form early (during embryogenesis) and grow rapidly throughout larval development (Gibson and Schubiger 2000). In *M. sexta*, the peripodial-less eye primordium, however, does not initiate proliferative growth until after the last larval instar (Champlin and Truman 1998; Friedrich and Benzer 2000). In *H. erato phyllis*, the wing discs are the only adult primordia which form by epithelial invagination; the other appendages are evaginated during the embryogenesis, but do not correspond to the obvious morphology of the adults (unpublished data), e.g. the adult eye is quite different from the stemmata of the larvae. This suggests that the development of imaginal discs by epithelial invagination might somehow account for the relatively early and aggressive developmental profile observed in *Drosophila* imaginal discs (Held 2002).

In *H. erato phyllis*, the cytoplasm of the wing primordium cells showed large amount of rough endoplasmic reticulum in their apical regions; this suggests intense protein synthesis activity, which possibly is involved in cell prepatterning and differentiation. In butterflies, the genetic prepatterning of the cell differentiation is specified already in the larval wing discs (Carroll 1994; McMillan et al. 2002; Reed and Serfas 2004). Martin et al. (2012) showed that the genetic variation linked to a Wnt-family signaling molecule is responsible for the diversification of complex wing patterns in *Heliconius*. In the larval wing discs of seven *Heliconius* species, the *WntA* mRNA expression prefigured the black patterns of the adult wings. Thus, spatial shifts of morphogen sources may be a key mechanism for generating phenotypic novelty. Further, tissue ultrastructure modifications may reveal how phenotypic novelties could be

developed, since morphological constraints at tissue level are determinant factors for the evolvability degree of a population (Brakefield, 2006; Hendrikse et al., 2007).

The ultrastructural study of the fifth-instar wing disc in *H. erato phyllis* provided new findings into the developmental architecture of the *Heliconius* wing. Furthermore, this study could help cell mapping throughout the development of the *Heliconius* wing patterning. We hope this would be an encouraging field for further inquiry.

Acknowledgements

We thank to our colleagues of the Ecological Genetics Laboratory for their help in collecting butterflies and daily feeding the caterpillars. Electron microscopy were performed at the Electronic Microscopy Center from the Federal University of Rio Grande do Sul, Porto Alegre, Brazil. Thanks are also due to the Conselho Nacional de Desenvolvimento Científico e Tecnológico, CNPq, for financial support and for a doctoral scholarship to the first author.

References

Abouheif, E., and Wray, G. A. 2002. Evolution of the gene network underlying wing polyphenism in ants. Science 297: 249–252.

Aymone, A. C. B., Valente, V. L. S., and Araújo, A. M. 2013. Ultrastructure and morphogenesis of the wing scales in *Heliconius erato phyllis* (Lepidoptera: Nymphalidae): What silvery/brownish surfaces can tell us about the development of color patterning? Arthropod Structure and Development 42: 349-359.

Brakefield, P. M. 2006. Evo-devo and constraints on selection. Trends in Ecology and Evolution 21: 362-368.

Carroll, S. B., Gates, J., Keys, D. N., Paddock, S. W., Panganiban, G. E., Selegue, J. E., and Williams, J. A. 1994. Pattern formation and eyespot determination in butterfly wings. Science 265: 109–114.

Champlin, D. T., and Truman, J. W. 1998. Ecdysteroids govern two phases of eye development during metamorphosis of the moth *Manduca sexta*. Development 125: 2009-2018.

Cho, K.-O., Chern, J., Izaddoost, S., and Choi, K.-W. 2000. Novel signaling from the peripodial membrane is essential for eye disc patterning in *Drosophila*. Cell 103: 331-342.

Dohrmann, C. E., and Nijhout, H. F. 1988. Development of the wing margin in *Precis coenia* (Lepidoptera: Nymphalidae). Journal of Research on Lepidoptera 27: 151–159.

Ferguson, L.C., and Jiggins, C.D. 2009. Shared and divergent expression domains on mimetic *Heliconius* wings. Evolution and Development 11: 408-512.

Friedrich, M., Benzer, S. 2000. Divergent *decapentaplegic* expression patterns in compound eye development and the evolution of insect metamorphosis. Journal of Experimental Zoology 288: 39-55.

Fristrom, D., and Fristrom, J. W. 1993. The metamorphic development of the adult epidermis. In M. Bate and A. Martinez-Arias (eds.) The Development of *Drosophila melanogaster*. Cold Spring Harbor Press, New York, pp. 843–897.

Gibson, M., and Schubiger, G. S. 2000. Peripodial cells regulate proliferation and patterning of *Drosophila* imaginal discs. Cell 103: 343–350.

Gibson, M. C., and Schubiger, G. 2001. *Drosophila* peripodial cells, more than meets the eye? BioEssays 23: 691-697.

Gibson, M. C., Lehman, D. A., and Schubiger, G. 2002. Lumenal transmission of *decapentaplegic* in *Drosophila* imaginal discs. Developmental Cell 3: 451-460.

Held, L. I, Jr. 2002. *Imaginal Discs: The Genetic and Cellular Logic of Pattern Formation*. Cambridge University Press, New York.

Hendrikse, J. L., Parsons, T. E., and Hallgrímsson, B. 2007. Evolvability as the proper focus of evolutionary developmental biology. Evolution & Development 9: 393-401.

Hill, R. I., Gilbert, L. E., and Kronforst, M. R. 2012. Cryptic genetic and wing pattern diversity in a mimetic *Heliconius* butterfly. Molecular Ecology 22: 2760-2770.

Hines, H. M., Papa, R., Ruiz, M., Papanicolaou, A., Wang, C., Nijhout, H. F., McMillan, W. O., and Reed, R. D. 2012. Transcriptome analysis reveals novel patterning and pigmentation genes underlying *Heliconius* butterfly wing pattern variation. BMC Genomics 13: 288.

Joron, M., Jiggins, C. D., Papanicolaou, A., and McMillan, W. O. 2006. *Heliconius* wing patterns: an evo-devo model for understanding phenotypic diversity. Heredity 97: 157-167.

Kodama, R., Yoshida, A., and Mitsui, T. 1995. Programmed cell-death at the periphery of the pupal wing of the butterfly *Pieris rapae*. Roux's archives of developmental biology 204: 418–426.

Martin, A., Papa, R., Nadeau, N. J., Hill, R. I., Counterman, B. A., Halder, G., Jiggins, C. D., Kronforst, M. R., Long, A. D., McMillan, W. O., and Reed, R. D. 2012. Diversification of complex butterfly wing patterns by repeated regulatory evolution of a *Wnt* ligand. Proceedings of the National Academy of Sciences 109: 12632-12637.

Mcdonald, W. P., Martin, A., and Reed, R. D. 2010. Butterfly wings shaped by a molecular cookie cutter: evolutionary radiation of lepidopteran wing shapes associated with a derived Cut/wingless wing margin boundary system. Evolution and Development 12: 296-304.

McMillan, W. O., Monteiro, A., and Kapan, D. D. 2002. Development and evolution on the wing. Trends in Ecology and Evolution 17: 125-133.

Miner, A. L., Rosenberg, A. J., and Nijhout, H. F. 2000. Control of growth and differentiation of the wing imaginal disk of *Precis coenia* (Lepidoptera: Nymphalidae). Journal of Insect Physiology 46: 251–258.

Nardi, J. B., Norby, S. W., and Magee-Adams, S. M. 1987. Cellular events within peripodial epithelia that accompany evagination of *Manduca* wing discs: conversion of cuboidal epithelia to columnar epithelia. Developmental Biology 119: 20–26.

Nardi, J. B. 1994. Rearrangement of epithelial cell types in an insect wing monolayer is accompanied by differential expression of a cell surface protein. Developmental Dynamics 199: 315-325.

Nardi, J. B., and Ujhelyi, E. 2001. Transformations of epithelial monolayers during wing development of *Manduca sexta*. Arthropod Structure and Development 30: 145-157.

Nepveu, A. 2001. Role of the multifunctional CDP/Cut/Cux homeodomain transcription factor in regulating differentiation, cell growth and development. Gene 270: 1–15.

Nijhout, H.F. 1991. *The Development and Evolution of Butterfly Wing Patterns.* Smithsonian Institution Press, Washington.

Pallavi, S. K. and Shashidhara, L. S. 2003. Egfr/Ras pathway mediates interactions between peripodial and disc proper cells in *Drosophila* wing discs. Development 130: 4931-4941.

Pallavi, S. K., and Shashidhara, L. S. 2005. Signaling interactions between squamous and columnar epithelia of the *Drosophila* wing disc. Journal of Cell Science 118: 3363-3370.

Pastor-Pareja, J. C., Grawe, F., Martin-Blanco, E., and García-Bellido, A. 2004. Invasive cell behavior during *Drosophila* imaginal disc eversion is mediated by the JNK signaling cascade. Developmental Cell 7: 387–399.

Quennedey, A., and Quennedey, B. 1999. Development of the wing discs of *Zophobas atratus* under natural and experimental conditions: occurrence of a gradual larval–

pupal commitment in the epidermis of tenebrionid beetles. Cell and Tissue Research 296: 619–634.

Reed, R. D., and Serfas, M. S. 2004. Butterfly wing pattern evolution is associated with changes in a Notch/Distal-less temporal pattern formation process. Current Biology 14: 1159–1166.

Reed, R. D., McMillan, W. O., and Nagy, L. M. 2008. Gene expression underlying adaptive variation in *Heliconius* wing patterns: non-modular regulation of overlapping *cinnabar* and *vermilion* prepatterns. Proceedings of the Royal Society B 275: 37-45.

Reed, R. D., Papa, R., Martin, A., Hines, H. M., Counterman B. A., Pardo-Díaz, C., Jiggins, C. D., Chamberlain, N. L., Kronforst, M. R., Chen, R., Halder, G., Nijhout, H. F., and McMillan, W. O. 2011. *optix* drives the repeated convergent evolution of butterfly wing pattern mimicry. Science 333: 1137–1141.

Sameshima, S. Y., Miura, T., and Matsumoto, T. 2004. Wing disc development during caste differentiation in the ant *Pheidole megacephala* (Hymenoptera: Formicidae). Evolution and Development 6: 336–341.

Tomoyasu, Y., Wheeler, S. R., and Denell, R. E. 2005. Ultrabithorax is required for membranous wing identity in the beetle *Tribolium castaneum*. Nature 433: 643–647.

Wago, H. 1991. Phagocytic recognition in *Bombyx mori*. In: A. P. Gupta (ed.) Immunology of Insects and Other Arthropods. C.R.C. Press, Florida, pp. 215-235.

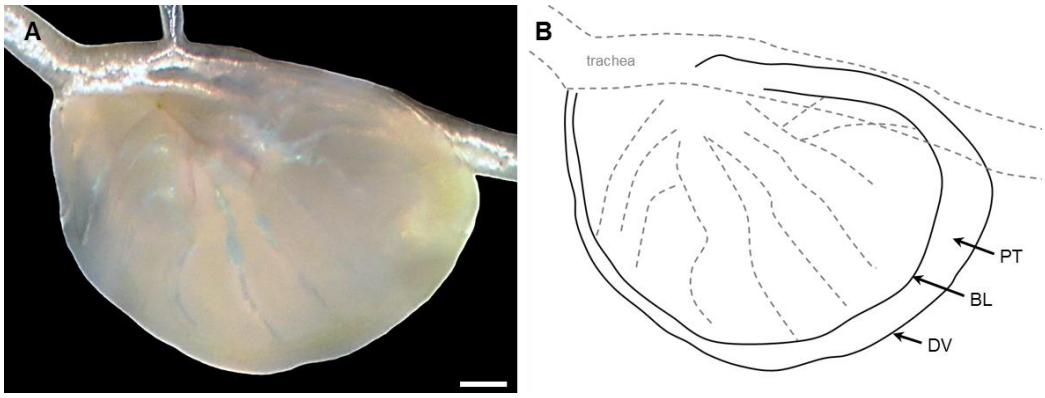

Fig. 1. Fifth-instar larval wing disc of *H. erato phyllis*. (A) The wing disc from a vivisectioned larva. The disc surface shows a cream color, while the branched veins into the disc show a lighter color. (B) A cartoon of the wing disc showing the border lacuna (BL), the peripheral tissue (PT), and the dorsoventral boundary (DV). Bar = 200 µm.

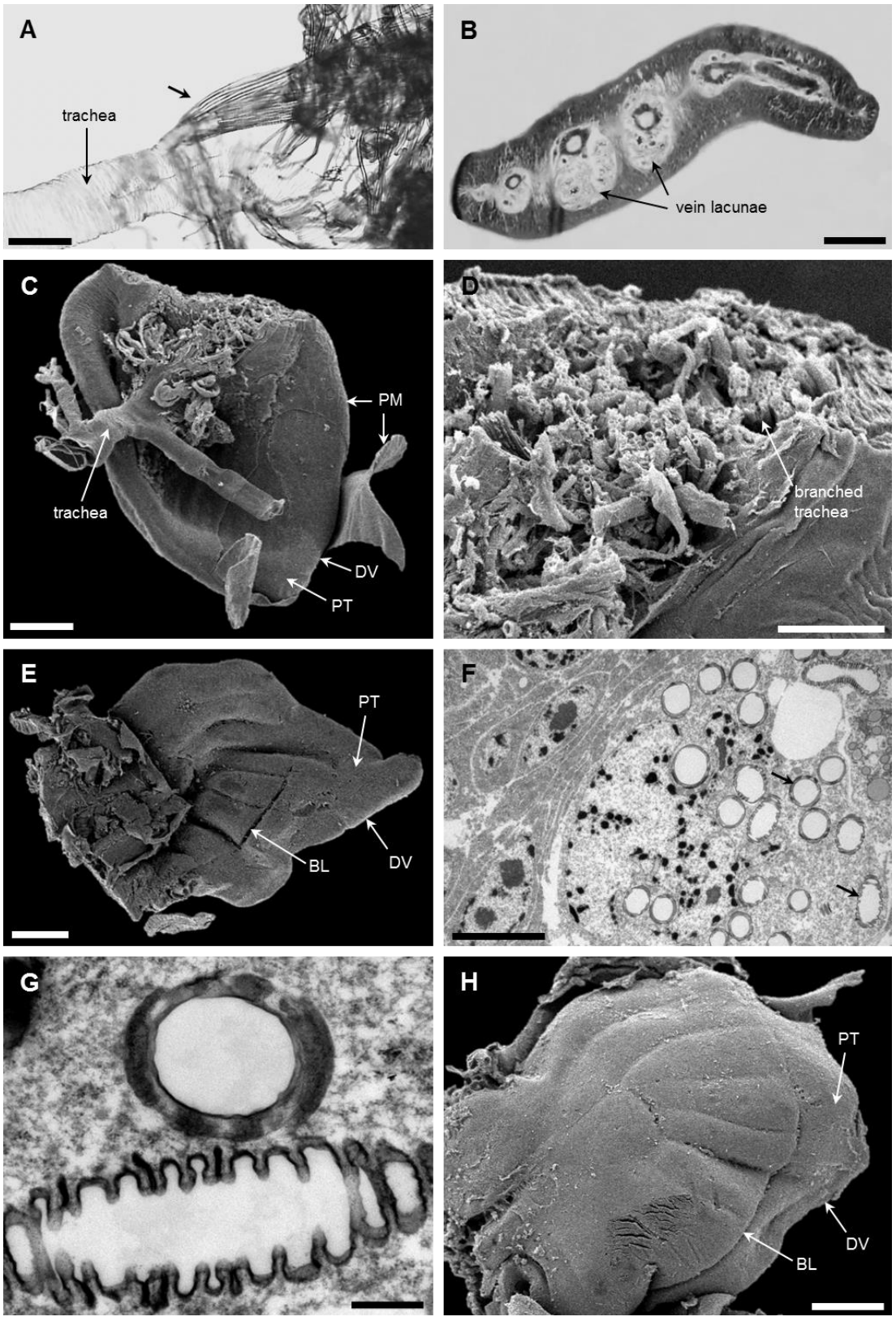
A
trachea
B
vein lacunae
C
PM
trachea
DV
PT
D
branched
trachea
E
PT
BL
DV
F
G
H
PT
DV
BL

Fig. 2. The vein pattern formation in the larval wing discs of *H. erato phyllis*. (A) Early fifth-instar; note the tracheal proliferation (black arrow) which originates the wing veins. (B) Transversal section of a wing disc showing the lacunae (light circles) between the epithelial layers, where the tracheae ingress to form the wing vein precursors. (C) Ventral region of the wing disc, showing the large tracheal cluster and ingression into the wing disc; (D) Zoom area of some tracheae transversely sectioned. (E) Dorsal view of the wing disc showing the grooves which correspond to the early vein pattern, as well as the border lacunae and the large peripheral tissue. (F) Transversal section showing the dorsal epithelial tissue (at left) and a lacuna full of tracheae (black arrows). (G) Detail of two tracheae, transversally and longitudinally sectioned, respectively. (H) Middle fifth-instar; note the growth of the wing primordium, the extension of the vein grooves and the reduction of the peripheral tissue, relative to the early stage at (E). (A, B) Light microscopy; (C, D, E, H) Scanning electron microscopy; (F, G) Transmission electron microscopy. BL = bordering lacuna; DV = dorsoventral boundary; PM = peripodial membrane; PT = peripheral tissue. Bars = 50 µm, 200 µm, 100 µm, 50 µm, 200 µm, 5 µm, 0.5 µm, 200 µm, respectively.

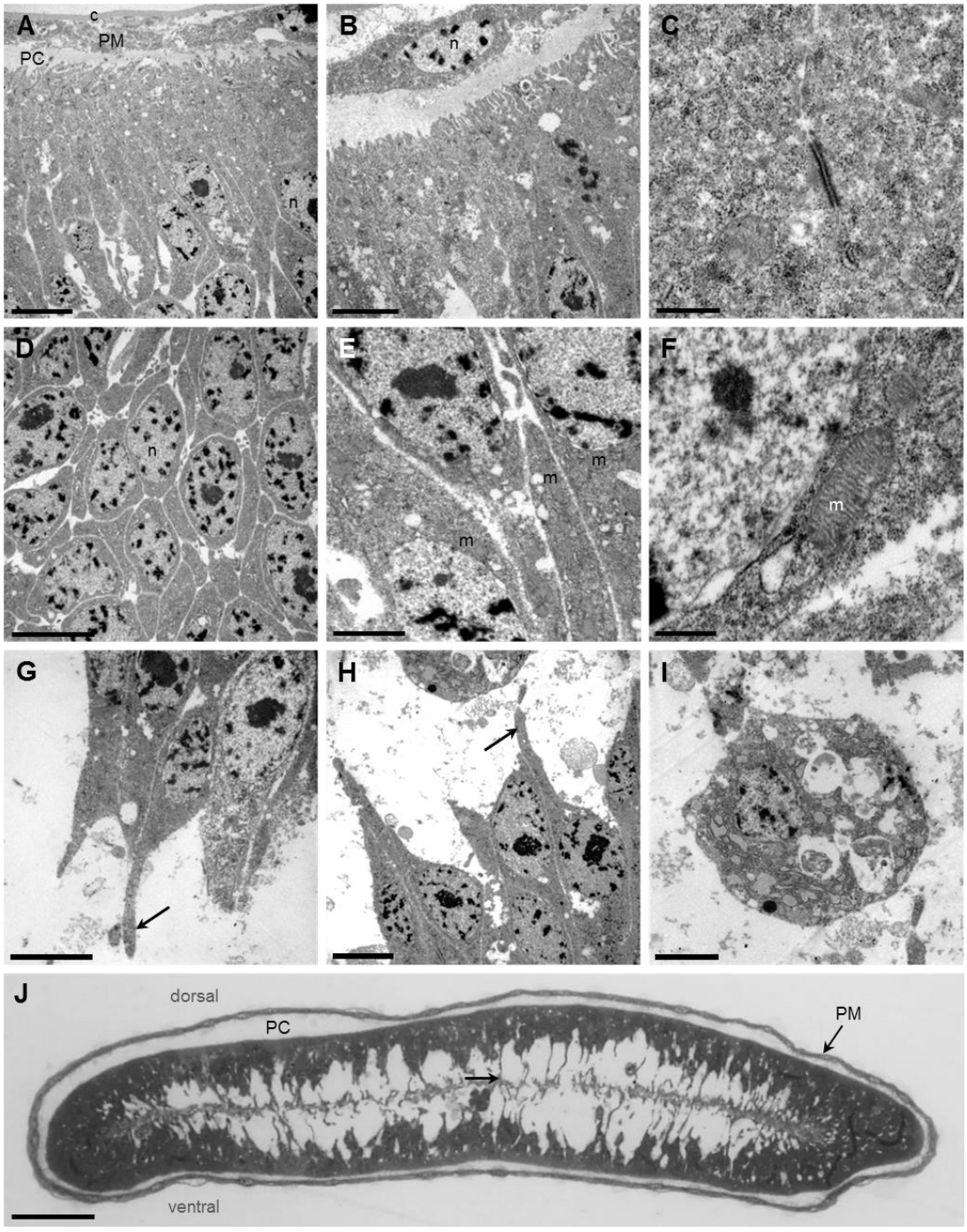
A
c
PM
PC
n
B
n
C
D
n
E
m
m
m
F
m
G
H
I
J
dorsal
PC
PM
ventral

Fig. 3. Epithelial tissue of the larval wing disc in *H. erato phyllis*, visualized by transmission electron microscopy. (A) Dorsal surface of the wing disc showing, in the top, the cuticle; below, the peripodial membrane, the peripodial cavity, and the columnar epithelium of the wing primordium; note the large amount of cytoplasm in the apical region of the wing primordium cells. (B) In the top, a nucleus of a peripodial cell; below, note the microvilli in the apical surface of the columnar epithelium. (C) Tight junction between the columnar cells, which are full of rough endoplasmic reticulum. (D) Intermediate region of the columnar cells showing the nuclei occupying many levels along the apical-basal axis. (E) Detail of the epithelial cells showing many mitochondria near to the nuclei. (F) Mitochondrion beside a nucleus. (G) Basal processes (black arrow) being extended from the dorsal epithelium, in direction to (H) the ventral epithelium, which in turn also extends process (black arrow) in direction to the dorsal epithelium. After extension of the basal processes, their extremities fuse at the middle of the lumen. (I) In the lumen disc, a phagocyte full of phagocytic vacuoles. (J) Transversal section of the wing disc showing the basal processes, from both monolayers, fused at the middle interface of the lumen. C = cuticle; M = mitochondrion; N = nuclei; PC = peripodial cavity; PM = peripodial membrane. Bars = 5 µm, 5 µm, 0.5 µm, 5 µm, 2 µm, 0.5 µm, 5 µm, 5 µm, 2 µm, 100 µm, respectively.

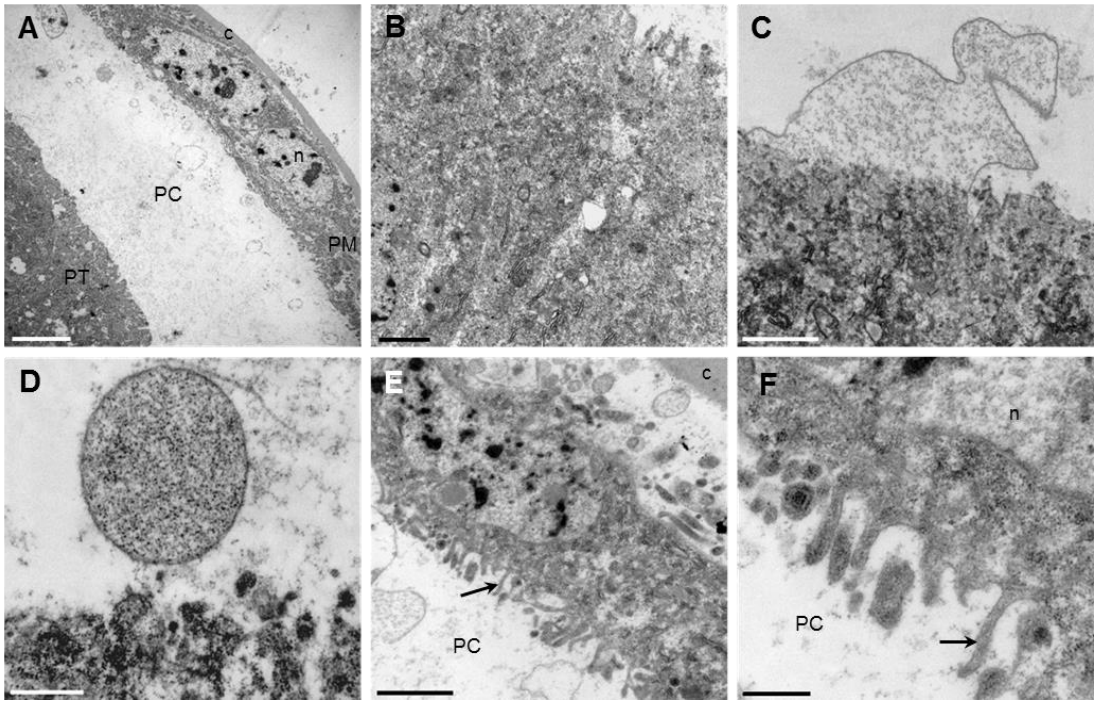

Fig. 4. The interface between the peripodial membrane and the peripheral tissue of the wing discs in *H. erato phyllis*, visualized by transmission electron microscopy. (A) The peripheral tissue, on the left, surrounded by the peripodial cavity and membrane. (B) Detail of the peripheral tissue showing little cellular organization. (C) Vesicle being released from the peripheral tissue into the peripodial cavity; and (D) a free vesicle in the peripodial cavity. (E) The peripodial membrane and the microvilli (black arrow) on the apical surface; (F) Zoom area showing the microvilli. C = cuticle; N = nuclei; PC = peripodial cavity; PT = peripheral tissue. Bars = 5 µm, 1 µm, 2 µm, 0.5 µm, 2 µm, 0.5 µm, respectively.

CAPÍTULO 5

Discussão geral

Nesta tese foram abordados alguns aspectos ultraestruturais do desenvolvimento de *Heliconius erato phyllis*.

Capítulo 1

Nosso primeiro objetivo foi analisar a embriogênese, cujo padrão de desenvolvimento foi consistente com a embriogênese de banda-longa. Foram analisados o modo de formação da banda germinal e membranas extraembrionárias, o padrão de segmentação, e eventos pós-segmentação, como o desenvolvimento da cápsula cefálica e apêndices torácicos e abdominais. O padrão de banda-longa é considerado o mais derivado dentre os insetos, em comparação aos padrões de banda-intermediária e -curta, os quais são encontrados nas linhagens mais ancestrais de insetos, p.ex. Orthoptera (Davis & Patel, 2002).

Embora a classificação baseada nos tipos de banda germinal seja útil para entender a embriogênese de insetos dentro de uma perspectiva macroevolutiva, ela é insuficiente pra abranger a ampla diversidade nos modos de segmentação. A região posterior de embriões de banda-curta, -intermediária e -longa é certamente uma região que contribuiu para a divergência morfológica em insetos. Compreender como as transições de banda-curta à -longa foram progressivamente geradas é um desafio, a ser considerado tanto por abordagens moleculares, morfológicas e ecológicas. De fato, as diferenças entre os modos de segmentação podem ser vistas como consequência de mudanças heterocrônicas ao longo do eixo anteroposterior dos embriões.

Uma possível explicação para a evolução do padrão de banda-longa diz respeito à origem das células *nurse*, as quais contribuem para uma distribuição espacial

amplamente polarizada de morfógenos maternos. Essa novidade evolutiva pode ter sido um importante requisito para a aceleração no tempo de desenvolvimento; se não, diretamente um produto de sua seleção. Uma observação importante, relativa aos padrões de banda germinal, corresponde ao fato de que apenas Holometabola apresenta embriões de banda-longa; enquanto Hemimetabola apresenta apenas embriões de banda-curta e -intermediária. Embriões de banda-longa são encontrados em múltiplos clados dentro de Holometabola, e isso sugere que ou a embriogênese de banda-longa tem sido secundariamente perdida em ordens que apresentam mais de um tipo de banda germinal (p.ex., Lepidoptera e Coleoptera), ou ela evoluiu mais de uma vez.

Embora os padrões de segmentação sejam variáveis dentro de Insecta, os eventos embrionários que ocorrem antes e depois da fase de segmentação apresentam ampla divergência morfológica, sendo por isso a banda germinal considerada o estágio filotípico dos insetos (Sander, 1984). Estudos moleculares recentes corroboram que a banda germinal de *Drosophila* é marcada pela mínima divergência na expressão gênica, comparativamente aos eventos anteriores e posteriores (Kalinka et al., 2010). Extrapolando aos vertebrados, Domazet-Loso & Tautz (2010) estabeleceram um índice filoestratigráfico com base no transcriptoma estágio-específico de *zebrafish*, onde o estágio filotípico apresentou o transcriptoma mais ancestral, enquanto nos estágios anteriores e posteriores o transcriptoma mostrou-se mais derivado. Esses resultados reforçam a noção de que os padrões de expressão de genes responsáveis pela formação de planos corporais básicos, uma vez estabelecidos, permanecem rigidamente conservados por fortes restrições desenvolvimentais. O funil da ampulheta embrionária, portanto, corresponde a um substrato evolutivo estável a partir do qual os organismos podem explorar novas direções morfogenéticas.

O estudo do desenvolvimento embrionário de *H. erato phyllis* trouxe à lista de lepidópteros um exemplo de padrão de banda-longa. Cabe ressaltar que de todos os

lepidópteros cuja segmentação foi estudada, *H. erato phyllis* corresponde à espécie mais derivada, o que sustenta a tendência evolutiva dos padrões de banda germinal em Lepidoptera.

Capítulo 2

Aqui analisamos a ultraestrutura das escamas de *H. erato phyllis*, incluindo as escamas das regiões prateadas/marrons de machos/fêmeas, as quais até então não haviam sido descritas na literatura. O resultado dessa análise foi inesperado, uma vez que foram encontrados três/dois diferentes tipos ultraestruturais em escamas que apresentam a mesma cor (prateada/marrom) - correspondentes ao mesmo pigmento (melanina); enquanto a literatura em *Heliconius* assume uma correlação restrita entre pigmentação e ultraestrutura (Gilbert et al., 1988; Janssen et al., 2001).

Gilbert et al. (1988) propuseram um modelo genético para o desenvolvimento da coloração em *Heliconius* com base em um mecanismo “interruptor” coordenado por dois genes seletores, M e X. Esses genes seriam responsáveis por regular simultaneamente a microestrutura e a pigmentação das escamas. Para o desenvolvimento de escamas de tipo I (brancas ou amarelas), nenhum dos genes é ativado nas células precursoras das escamas. Se apenas o gene M é ativado, escamas de tipo II (pretas) se desenvolvem; se M e X são ativados, escamas de tipo III (vermelhas) se desenvolvem. Nesse modelo, o gene X apenas pode ser expresso em células que expressam o gene M. Foi também assumido que qualquer efeito pleiotrópico dos genes responsáveis pela pigmentação sobre o desenvolvimento microestrutural não se dá através do pigmento em si, seus precursores ou substratos; provavelmente, os produtos dos genes seletores seriam ativadores de genes envolvidos na microestrutura e na pigmentação das escamas.

Janssen et al. (2001) induziram mudanças ectópicas na coloração de escamas destinadas a se tornarem pretas e vermelhas, i.e., escamas destinadas a se tornarem

pretas foram induzidas a se tornarem vermelhas, e vice-versa. Nesse estudo, os autores observaram que mudanças na coloração foram acompanhadas por mudanças correspondentes na microestrutura, sugerindo uma forte associação no desenvolvimento de ambas as características.

A microestrutura das escamas prateadas/marrons, porém, desafia dois paradigmas: primeiro, o de que existe uma correlação restrita entre ultraestrutura e pigmentação; segundo, o modelo dos genes seletores M e X para o desenvolvimento das escamas pretas, vermelhas e amarelas. Embora as escamas das regiões prateadas/marrons não tenham sido incluídas no modelo de Gilbert et al. (1988), o fato de elas apresentarem tipos microestruturais similares às escamas pretas, vermelhas e amarelas, sugere ou que os produtos dos genes M e X podem atuar de forma independente na diferenciação da coloração e da microestrutura, ou que outros genes possam estar envolvidos no desenvolvimento de combinações alternativas entre coloração e microestrutura.

Outro aspecto envolvido na evolução do desenvolvimento de padrões de coloração em borboletas diz respeito ao padrão heterocrônico da maturação e pigmentação das escamas. Nijhout (1980) propôs dois modelos, onde ambos assumem que os substratos para síntese de pigmentos circulam na hemolinfa e são produzidos sequencialmente. O modelo I assume que as enzimas envolvidas nas rotas dos diferentes pigmentos estão presentes em todas as escamas, sendo a taxa de maturação das escamas determinante para pigmentação, uma vez que apenas escamas maduras permitem a consolidação dos pigmentos nas suas superfícies. O segundo modelo é baseado no fato de que os substratos para síntese de pigmentos têm acesso livre a todas as escamas, independente do grau de maturação; porém, escamas destinadas a uma dada cor possuem enzimas específicas aos substratos específicos das diferentes rotas de pigmentação.

O modelo I é consistente com *Papilio glaucus* (Koch et al., 2000; ffrench-Constant, 2012), em que os pigmentos sintetizados, sequencialmente, vão sendo depositados nas escamas que se encontram maduras. Já o desenvolvimento de *Heliconius* é consistente com o modelo II, o qual é independente do grau de maturação das escamas. Em *H. erato phyllis*, um fato que confirma, e ao mesmo tempo intriga, corresponde à maturação "precoce" das escamas destinadas a se tornarem amarelas (Fig.1). O pigmento amarelo (3-OHK) é o último a se depositar nas asas, no entanto, a maturação das escamas destinadas a se tornarem amarelas ocorreu antes de todas as outras. O fato de os pigmentos sintetizados (e depositados) antes (vermelho – dihidroxantomatina e preto - melanina) não se depositarem nas escamas maduras destinadas a se tornarem amarelas sugere que há uma especificidade genética fortemente associada às rotas de pigmentação. Assim, em *H. erato phyllis*, a maturação das escamas é crucial para a pigmentação, porém não suficiente para permitir a deposição de pigmento.

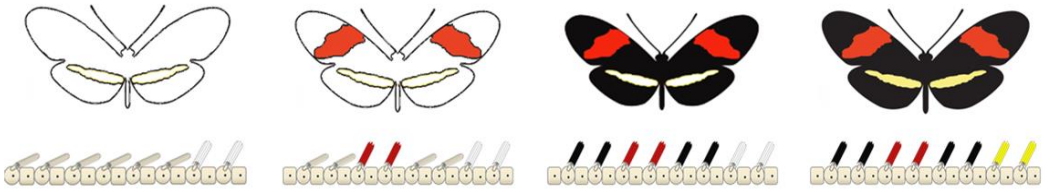

Fig. 1. Ontogenia da pigmentação em *H. erato phyllis*, mostrando a ordem cronológica de deposição dos pigmentos nas escamas.

Do ponto de vista evolutivo, os conceitos de modularidade e integração podem ser aplicados ao desenvolvimento de padrões de coloração em asas de borboletas (Nijhout, 2003). Neste caso, módulos são equivalentes a grupos de escamas de uma mesma cor, p.ex., as manchas das asas anteriores e as barras das asas posteriores em *Heliconius* (Fig.2). Sendo assim, é possível afirmar que em *Heliconius* as enzimas das rotas de pigmentação distribuem-se em módulos não integrados entre si. Contrariamente, na

superfície das asas de *P. glaucus* os módulos são integrados, uma vez que os pigmentos têm acesso livre a todas as células, dependendo apenas do grau de maturação das escamas para nelas se depositarem. Módulos desenvolvimentais e a arquitetura genética que eles determinam são fatores derivados moldados pela seleção natural para o estabelecimento de módulos funcionais (Wagner & Altenberg, 1996); alternativamente, podem ser considerados fatores ancestrais que atuam como restrições ontogenéticas (Raff, 1996; Kirschner & Gerhart, 1998). Cabe aqui ressaltar os fenômenos de divergência intraespecífica e convergência interespecífica em *Heliconius*, em que a evolução da modularidade possivelmente foi um fator chave que contribuiu para a flexibilidade notável nos padrões de coloração em espécies miméticas.

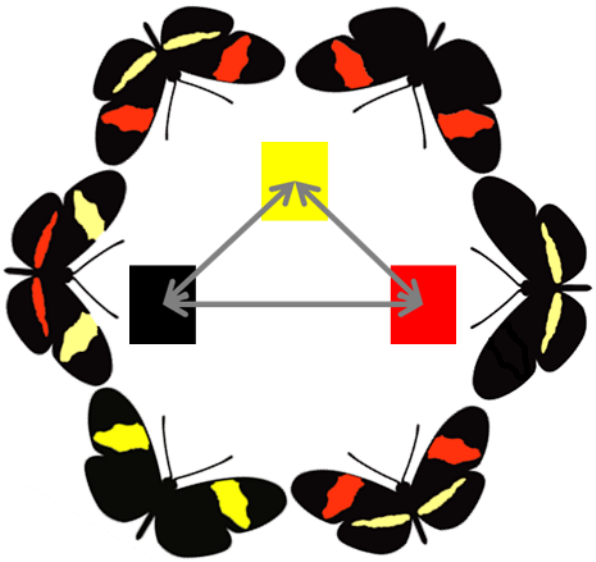

Fig. 2. Módulos desenvolvimentais (grupos monocromáticos de escamas) e a flexibilidade dos padrões de coloração em *Heliconius*. A alteração posicional das escamas amarelas, vermelhas e pretas revela como variações na modularidade e na integração da superfície das asas anteriores e posteriores atuam como mecanismos para propiciar a divergência intraespecífica e a convergência interespecífica nos padrões de coloração.

Capítulo 3

A terceira proposta desta tese foi analisar a ultraestrutura dos discos imaginais das asas em lagartas de quinto instar. Os discos das asas de borboletas possuem origem ectodérmica e são compostos por epitélios diferenciados, responsáveis por diferentes funções ao longo do desenvolvimento (Nijhout, 1991). Em *H. erato phyllis*, o epitélio do primórdio da asa apresentou células colunares com grande quantidade de retículo endoplasmático rugoso, indicando intensa atividade de síntese proteica, possivelmente envolvida nos processos de determinação e diferenciação celular. Estudos moleculares demonstraram que a determinação genética dos padrões de coloração em asas de borboletas ocorre nos discos larvais (Carroll, 1994; McMillan et al., 2002; Reed & Serfas, 2004). Martin et al. (2012) demonstraram que os padrões de expressão de moléculas de mRNA codificadoras de *WntA* - proteína envolvida na sinalização celular - em discos larvais de sete espécies de *Heliconius*, correspondem nos adultos às regiões pretas das asas. Alterações espaciais na expressão de morfógenos são, portanto, mecanismos chave para a geração de novidades fenotípicas. Além disso, modificações ultraestruturais em tecidos revelam “como” novidades fenotípicas podem ser desenvolvidas, uma vez que restrições morfológicas em nível tecidual são fatores determinantes para o grau de evolvabilidade de uma população (Kirschner & Gerhart, 1998; Brakefield, 2006; Hendrikse et al., 2007).

Em discos imaginais de asas de lepidópteros, um dos principais mecanismos ontogenéticos responsáveis pela organização espacial das escamas corresponde ao rearranjo das células precursoras das escamas durante o desenvolvimento (Nijhout, 1991). Nardi & Ujhelyi (2001) observaram que extensões translumenais projetadas de células epiteliais gerais (não precursoras de escamas) desempenham importante papel nos eventos de rearranjo celular nos discos pupais de *Manduca sexta*. Nos discos das asas de *H. erato phyllis*, observamos que extensões translumenais estão presentes já no

estágio larval, isso sugere que a diferenciação das células precursoras das escamas inicia antes do estágio pupal. Ultraestruturalmente, as superfícies apicais das células precursoras das escamas de *H. erato phyllis* se tornam visivelmente diferenciadas no início do estágio pupal (Aymone et al., 2013). Cabe ressaltar que, em *Heliconius*, alterações na posição relativa das células precursoras das escamas destinadas a diferentes cores são de fundamental importância para a divergência intraespecífica e a convergência interespecífica nos padrões de coloração.

Em relação à membrana peripodial, uma importante diferença que observamos foi a presença de microvilosidades em regiões próximas ao tecido periférico, o qual sofre apoptose durante o desenvolvimento. Isso sugere que, possivelmente, o epitélio peripodial absorva resíduos apoptóticos provindos do tecido periférico. Em *Drosophila*, células peripodiais contribuem para o desenvolvimento dos discos imaginais das asas e dos olhos, transferindo morfógenos à superfície apical dos discos, através de extensões apicais microtubulares e translumenais (Gibson & Schubiger, 2000). No entanto, em *H. erato phyllis* (e em outros lepidópteros?), o epitélio peripodial parece contribuir de forma específica à apoptose do tecido periférico. Em Lepidoptera, a única função do epitélio peripodial, conhecida na literatura, corresponde ao seu papel de contração para possibilitar a eversão dos discos imaginais durante a pupação. Para isso, as células peripodias alteram sua forma, tornando-se colunares, o que ocasiona o movimento de contração e evaginação da asa (Nardi et al., 1987).

O fato de em *H. erato phyllis* a membrana peripodial apresentar uma importante função para o desenvolvimento da asa suscita a ideia de que os discos larvais não se desenvolvem unicamente através de eventos subcelulares que ocorrem nas camadas epiteliais que darão origem propriamente à asa. Isso implica que as células peripodiais estão ontogeneticamente integradas aos discos imaginais, sendo mais do que um simples revestimento.

REFERÊNCIAS BIBLIOGRÁFICAS

AYMONE, A.C.B.; V.L.S. VALENTE & A.M. ARAÚJO. 2013. Ultrastructure and morphogenesis of the wing scales in *Heliconius erato phyllis* (Lepidoptera: Nymphalidae): What silvery/brownish surfaces can tell us about the development of color patterning? **Arthropod Structure & Development 42**: 349-359.

BELDADE, P. & P.M. BRAKEFIELD. 2002 The genetics and evo–devo of butterfly wing patterns. **Nature Reviews 3**: 442-452.

BENSON, W.W. 1972. Natural selection for Müllerian mimicry in *Heliconius erato* in Costa Rica. **Science 76**: 936-939.

BRAKEFIELD, P.M. 2006. Evo-devo and constraints on selection. **Trends in Ecology and Evolution 21**: 362-368.

BROWN JR., K.S. 1979. **Ecologia geográfica e evolução nas florestas neotropicais.** PhD dissertation. Universidade Estadual de Campinas, Campinas.

BROWN JR., K.S. 1981. The biology of *Heliconius* and related genera. **Annual Review of Entomology 26**: 427-456.

CARROLL, S.B. 2005. **Endless forms most beautiful: The new science of evo-devo and the making of the animal kingdom.** W.W. Norton & Company, New York. 368p.

CARROLL, S.B. 2008. Evo-devo and an expanding evolutionary synthesis: A genetic theory of morphological evolution. **Cell 134**: 25-36.

CARROLL, S.B.; J.K. GRENIER & S.D. WEATHERBEE. 2005. **From DNA to diversity: Molecular genetics and the evolution of animal design.** Blackwell, Malden. 258p.

DAVIS, G.K. & N.H. PATEL, 2002. Short, long, and beyond: Molecular and embryological approaches to insect segmentation. **Annual Review of Entomology 47**: 669-699.

DOMAZET-LOSO, T. & D. TAUTZ. 2010. A phylogenetically based transcriptome age index mirrors ontogenetic divergence patterns. **Nature 468**: 815-818.

EMSLEY, M. 1963. A morphological study of imagine Heliconiinae (Lep.: Nymphalidae) with a consideration of the evolutionary relationships within the group. **Zoologica 48**: 85-131.

FERGUSON, L.C & C.D. JIGGINS. 2009. Shared and divergent expression domains on mimetic *Heliconius* wings. **Evolution and Development 11**: 408-512.

FFRENCH-CONSTANT, R.H. 2012. Butterfly wing colours and patterning by numbers. **Heredity 108**: 1-2.

FINKBEINER, S.D.; A.D. BRISCOE & R.D. REED. 2012. The benefit of being a social butterfly: communal roosting deters predation. **Proceedings of The Royal Society B 279**: 2769-2776.

GHIRADELLA, H. 1984. Structure of iridescent lepidopteran scales: variations on several themes. **Annals of the Entomological Society of America 77**: 637-645.

GIBSON, M. & G.S. SCHUBIGER. 2000. Peripodial cells regulate proliferation and patterning of *Drosophila* imaginal discs. **Cell 103**: 343–350.

GILBERT, L.E. 1972. Pollen feeding and reproductive biology of *Heliconius* butterflies. **Proceedings of the National Academy of Sciences of USA 69**: 1403-1407.

GILBERT, L.E. 1982. The coevolution of a butterfly and a vine. **Scientific American 247**: 110-121.

GILBERT, L.E. 2003. Adaptive novelty through introgression in *Heliconius* wing patterns: evidence for a shared genetic "toolbox" from synthetic hybrid zones and a theory of diversification, p. 281-318. *In*: BOGGS, C.L.; W.B. WATT & P.R. EHRLICH (Eds.). **Butterflies: ecology and evolution taking flight**. The University of Chicago Press, 739p.

GILBERT, L.E.; H.S. FORREST; T.D. SCHULTZ & D.J. HARVEY. 1988. Correlations of ultrastructure and pigmentation suggest how genes control development of wing scales of *Heliconius* butterflies. **Journal of Research on the Lepidoptera 26**: 141-160.

HENDRIKSE, J.L.; T.E. PARSONS & B. HALLGRÍMSSON. 2007. Evolvability as the proper focus of evolutionary developmental biology. **Evolution & Development 9**: 393-401.

HINES, H.M.; R. PAPA; M. RUIZ; A. PAPANICOLAOU; C. WANG; H.F. NIJHOUT; W.O. MCMILLAN & R.D. REED. 2012. Transcriptome analysis reveals novel patterning and pigmentation genes underlying *Heliconius* butterfly wing pattern variation. **BMC Genomics 13**: 288.

HOLZINGER, H. & R. HOLZINGER. 1994. ***Heliconius* and related genera.** Venette, Sciences Naturelles, 328p.

JANSSEN, J.M.; A. MONTEIRO & P. BRAKEFIELD. 2001. Correlations between scale structure and pigmentation in butterflies wings. **Evolution and Development 3**: 415-423.

JENNER, R.A. & M.A. WILLS. 2007. The choice of model organisms in evo-devo. **Nature Reviews 8**: 311-319.

JIGGINS, C.D.; R.E. NAISBIT; R.L. COE & J. MALLET. 2001. Reproductive isolation caused by colour pattern mimicry. **Nature 411**: 302-305.

JIGGINS, C.D.; J. MAVAREZ; M. BELTRAN; W.O. MCMILLAN; J.S. JOHNSTON & E. BERMINGHAM. 2005. A genetic linkage map of the mimetic butterfly *Heliconius melpomene*. **Genetics 171**: 557–570.

JORON, M.; C.D. JIGGINS; A. PAPANICOLAOU & W.O. MCMILLAN. 2006. *Heliconius* wing patterns: an evo-devo model for understanding phenotypic diversity. **Heredity 97**: 157–167.

KALINKA, A.T.; VARGA, K.M.; GERRARD, D.T.; PREIBISCH, S.; CORCORAN, D.L.; JARRELS, J.; OHLER, U.; BERGMAN, C.M. & TOMANCK, P. 2010. Gene expression divergence recapitulates the developmental hourglass model. **Nature 468**: 811-814.

KALINKA, A.T. & P. TOMANCK. 2012. The evolution of early animal embryos: conservation or divergence? **Cell 27**: 385-393.

KAPAN, D.D. 2001. Three-butterfly system provides a field test of Müllerian mimicry. **Nature 409**: 338-340.

KAPAN, D.D.; N.S. FLANAGAN; A. TOBLER; R. PAPA; R.D. REED; J.A. GONZALEZ; M.R. RESTREPO; L. MARTINEZ; K. MALDONADO; C. RITSCHOFF; D.G. HECKEL & W.O. MCMILLAN. 2006. Localization of Müllerian mimicry genes on a dense linkage map of *Heliconius erato*. **Genetics 173**: 735–757.

KIRSCHNER, M. & J. GERHART. 1998. Evolvability. **Proceedings of the National Academy of Sciences of the United States of America 95**: 8420-8427.

KOCH, P.B.; U. LORENZ; P.M. BRAKEFIELD & R.H. FFRENCH-CONSTANT. 2000. Butterfly wing pattern mutants: developmental heterochrony and co-ordinately regulated phenotypes. **Development Genes and Evolution 210**: 536-544.

KRAFT, R. & H. JÄCKLE. 1994. *Drosophila* mode of metamerization in the embryogenesis of the lepidopteran insect *Manduca sexta*. **Proceedings of the National Academy of Sciences of the USA 91**: 6634–6638.

KRISTENSEN, N.P. 2003. **Lepidoptera, moths and butterflies**. Vol.2: Morphology, Physiology, and Development. Walter de Gruyter, Berlin. 576p.

LANGHAM, G.M. 2004. Specialized avian predators repeatedly attack novel color morphs of *Heliconius* butterflies. **Evolution 58**: 2783-2787.

MALLET, J. & N.H. BARTON. 1989. Strong natural selection in a warning colour hybrid zone. **Evolution 43**: 421-431.

MARTIN, A.; R. PAPA; N.J. NADEAU; R.I. HILL; B.A. COUNTERMAN; G. HALDER; C.D. JIGGINS; M.R. KRONFORST; A.D. LONG; W.O. MCMILLAN & R.D. REED. 2012. Diversification of complex butterfly wing patterns by repeated regulatory evolution of a *Wnt* ligand. **Proceedings of the National Academy of Sciences of the USA 109:** 12632-12637.

MCMILLAN, W.O.; A. MONTEIRO & D.D. KAPAN. 2002. Development and evolution on the wing. **Trends in Ecology & Evolution 17**: 125-133.

MONTEIRO, A.; G. GLASER; S. STOCKSLAGER; N. GLANSDORP & D. RAMOS. 2006. Comparative insights into questions of lepidopteran wing pattern homology. **BMC Developmental Biology 6**: 1 -13.

NAISBIT, R.E.; C.D. JIGGINS & J. MALLET. 2003. Mimicry: Developmental genes that contribute to speciation. **Evolution & Development 5**: 269–280.

NAKAO, H. 2010. Characterization of *Bombyx* embryo segmentation process: expression profiles of engrailed, even-skipped, caudal, and wnt1/wingless homologues. **Journal of Experimental Zoology 314**: 224–231.

NARDI, J. B. & E. UJHELYI. 2001. Transformations of epithelial monolayers during wing development of *Manduca sexta*. **Arthropod Structure & Development 30**: 145-157.

NIJHOUT, H.F. 1980, Ontogeny of the color pattern on the wings of *Precis coenia* (Lepidoptera, Nymphalidae). **Developmental Biology 80**: 275-288.

NIJHOUT, H.F. 1991. **The development and evolution of butterfly wing patterns.** Smithsonian Institution Press, Washington. 297p.

NIJHOUT, H.F. 2003. Development and evolution of adaptive polyphenisms. **Evolution & Development 5**: 9-18.

PAPA, R.; C.M. MORRISON; J.R. WALTERS; B.A. COUNTERMAN; R. CHEN; G. HALDER; L. FERGUSON; N. CHAMBERLAIN; R. FFRENCH-CONSTANT; D.D. KAPAN; C.D. JIGGINS; R.D. REED & W.O. MCMILLAN. 2008. Highly conserved gene order and numerous novel repetitive elements in genomic regions linked to wing pattern variation in *Heliconius* butterflies. **BMC Genomics 9**: 345–360.

PRUD'HOMME, B. & N. GOMPEL, 2010. Genomic hourglass. **Nature 468**: 768-769.

PRUM, R.O.; T. QUINN & R.H. TORRES. 2005. Anatomically diverse butterfly scales all produce structural colours by coherent scattering. **The Journal of Experimental Biology 209**: 748-765.

RAFF, R.A. 1996. **The shape of life: genes, development, and the evolution of animal form**. Univerity of Chicago Press, Chicago. 544p.

REED, R.D. & M.S. SERFAS. 2004. Butterfly wing pattern evolution is associated with changes in a Notch/Distal-less temporal pattern formation process. **Current Biology 14**: 1159–1166.

REED, R.D.; W.O. MCMILLAN & L.M. NAGY. 2008. Gene expression underlying adaptive variation in *Heliconius* wing patterns: non-modular regulation of overlapping cinnabar and vermilion prepatterns**. Proceedings of The Royal Society B 275**: 37–45.

SANDER, K. 1984. Embryonic pattern formation in insects: Basic concepts and their experimental foundations. *In* **Pattern formation: a primer in developmental biology** (Eds. G.M. Malacinski & S.V. Bryant), pp. 245-268. Macmillan, New York. 626p.

SMITH, K.K. 2003. Time's arrow: heterochrony and the evolution of development. **International Journal of Developmental Biology 47**: 613-621.

WAGNER, G.P. & L. ALTENBERG. 1996. Complex adaptations and the evolution of evolvability. **Evolution 50**: 967-976.